12-6-2017

Synthesis of Antimicrobial Polymers to Overcome Antimicrobial Resistance

Md Salauddin Ahmed
Florida International University, mahme010@fiu.edu

DOI: 10.25148/etd.FIDC006577

FLORIDA INTERNATIONAL UNIVERSITY

Miami, Florida

SYNTHESIS OF ANTIMICROBIAL POLYMERS TO OVERCOME ANTIMICROBIAL RESISTANCE

A dissertation submitted in partial fulfillment of the

requirements for the degree of

DOCTOR OF PHILOSOPHY

in

CHEMISTRY

by

Md Salauddin Ahmed

2018

To: Dean Michael R. Heithaus
College of Arts, Sciences and Education

This dissertation, written by Md Salauddin Ahmed and entitled Synthesis of Antimicrobial Polymers to Overcome Antimicrobial Resistance, having been approved in respect to style and intellectual content, is referred to you for judgment.

We have read this dissertation and recommend that it be approved.

_____

Kevin O'Shea

_____

Yukching Tse Dinh

_____

Kalai Mathee

_____

Watson Lees

_____

Joong Ho Moon, Major Professor

Date of Defense: December 6, 2017

The dissertation of Md Salauddin Ahmed is approved.

_____

Dean Michael R. Heithaus
College of Arts, Sciences and Education

_____

Andrés G. Gil
Vice President for Research and Economic Development
and Dean of the University Graduate School

Florida International University, 2018

DEDICATION

To all my friends and family.

ACKNOWLEDGMENTS

First and foremost, I would like to thank my advisor, Dr. Joong Ho Moon, for his endless support and guidance, the occasional push beyond my limits, and his providing me with an excellent environment in which to grow both professionally and personally.

I would like to thank the members of my dissertation committee, Dr. Kevin O'Shea and Dr. Watson Lees, for their help with all sorts of chemistry questions, and Dr. Yukching Tse Dinh and Dr. Kalai Mathee for their outstanding support and help to build up my biochemistry knowledge.

I would like to thank the Chemistry Department for providing me with the opportunity to serve as a teaching assistant for many years, and specifically to Dr. Sandra Stojanovic and Dr. Palmer Graves for their mentorship of my teaching efforts and for the occasional life advice.

My enormous gratitude extends to the past and current members of the Moon Research Group. They have provided me with the friendship and support I could previously only dream of. Dr. Eladio Mendez, thank you for your initial support, which help me to become accustomed to graduate school. Dr. Megan Twomey helped me greatly as well. Dr. Rajesh Kumar helped me to learn basic organic chemistry and technique. I am really grateful to Rajesh because he helped me to overcome initial barriers like the research proposal and original proposal, which were requirements for graduation. Dr. Rajib Chowdhury helped cope with PI and stay in grad school. Prakash Manandhar, my friend and colleague, always stood with me when I was in trouble. I also need to thank Prakash for his excellent works on confocal imaging. Without his support, it would have been very difficult for me to acquire all of the confocal images.

I also like give a big thank you to Dr. Rumum Rohman, who helped me learn how to write a paper and how to make a better presentation. Without his guidance, I might not have managed to write my dissertation. And special thanks for his excellent cooking. I am a big fan of his beef curry.

I would also like to thank Dr. Yong Sim, Hooman Torabi, and Xuerong Li for joining with me in my last year and for their mental support toward my graduation.

A special thanks to Dr. Hoshan Unalla for his collaboration and helping me to get the cellular imaging with gene expression. I would like to thank my friend Rajib Dutta, who taught me about the BEAS 2B cell line along with the primary cell line. Rajib helped me to get the confocal imaging, mRNA study.

I need thank to Mohammad Mamun, who was always kind to me during my studies. Mamun helped me write this dissertation.

Finally, a very special thanks to my family, especially to my parents, who have always stood with me through all sorts of difficulty. My father, Mizanur Rahman, had brain stroke during my final year and lost his movement and voice. My mother, Salma Begum, helped my father to recover from his illness, and most important, she always supports me and tell me to focus on my work. Without their tremendous support, I would not have succeeded.

ABSTRACT OF THE DISSERTATION

SYNTHESIS OF ANTIMICROBIAL POLYMERS TO OVERCOME ANTIMICROBIAL RESISTANCE

by

Md Salauddin Ahmed

Florida International University, 2018

Miami, Florida

Professor Joong Ho Moon, Major Professor

Drug-resistant pathogens are emerging rapidly and thwart the treatment of common bacterial infectious diseases that can lead to death. Many contagious diseases remain difficult to treat because of acquired drug resistance. Compared to small antibiotics, which interrupt the intracellular biochemical processes, antimicrobial polymers with relatively high molecular weights offer a promising strategy to overcome drug resistance by disrupting the physical integrity of the membrane. Because of the unique mechanism, bacteria need a much longer time to develop resistance.

A new class of antimicrobial polymer in which the positive charge and hydrophobic/hydrophilic units are linearly connected in the amidinourea backbone was designed, synthesized, and tested for various bacteria including methicillin-resistant *Staphylococcus aureus* (MRSA). We evaluated the effects of hydrophobicity and polymer molecular weights on antimicrobial activity by measuring minimum inhibitory concentrations (MIC) and hemolytic activities (HC_{50}). Amidinourea antimicrobial polymers exhibit a promising MIC_{90} value (13 μg/mL) with low HC_{50}, resulting in high selectivity (HC_{50}/MIC_{90}) against MRSA.

Many bacteria have developed resistance against Ciprofloxacin. To overcome the antibiotic resistance associated with Ciprofloxacin, we hypothesized that a steady release of Ciprofloxacin at the bacteria membrane can overcome the drug resistance because the local drug concentration can be overwhelmingly high to suppress the drug efflux pump expressed on the membrane. A series of homo and di-block copolymers containing Ciprofloxacin, as the form of prodrugs, was synthesized using ring-opening metathesis polymerization (ROMP), and we evaluated their antimicrobial efficacy. While homo polymers only containing Ciprofloxacin were inactive against almost all bacteria tested, di-block copolymers containing Cipro and triphenylphosphine exhibited some antimicrobial activity against wild type *M. smegmatis*.

Modulation of chemical environments at the positively charged polymeric materials can significantly influence the biophysical properties required for efficient cellular interaction and subsequent entry. Using intrinsic fluorescent conjugated polymers (CPs), we have demonstrated that the modulated guanidine group with various hydrophilic or hydrophobic moieties dramatically changed their cellular behaviors. We prepared a series of modified guanidine-containing CPs and examined their cellular behaviors by using confocal microscopic imaging. Details of the modification chemistry and modification-dependent cellular behaviors and a knockdown of a target protein in primary cells were discussed.

TABLE OF CONTENTS

LIST OF TABLES

LIST OF FIGURES

LIST OF SCHEMES

ABBREVIATIONS AND ACRONYMS

AA	acetic acid
Boc	t-butyl carbamate
CP	conjugated polymer
CPN	conjugated polymer nanoparticle
DCM	dichloromethane
DIPA	*N*, *N*-diisopropylamine
DMF	dimethylformamide
DMSO	dimethylsulfoxide
EtOH	ethanol
FT-IR	Fourier transform infrared spectroscopy
GPC	gel permeation chromatography
HR-MS	high-resolution mass spectrometry
^{i}PrOH	isopropyl alcohol
MeCN	acetonitrile
MeOH	methanol
Mn	number average molecular weight
Mw	weight average molecular weight
m/z	mass-to-charge ratio
NMR	nuclear magnetic resonance
NTA	nanoparticle tracking analysis
OD	optical density

PA	poly(acetylene)
PDI	polydispersity index
$Pd[Cl_2(PPh_3)_2]$	bis(triphenylphosphine)palladium(II) dichloride
PPB	poly(p-phenylenebutadiynylene)
PPE	poly(p-phenyleneethynylene)
PT	poly(thiophene)
PPV	poly(p-phenylenevinylene)
QY	quantum yield
R	substituent
r.t.	room temperature
TEA	triethylamine
TFA	trifluoroacetic acid
THF	tetrahydrofuran
UV-Vis	ultraviolet-visible

CHAPTER I: INTRODUCTION

1.1. General Introduction to Antimicrobial Resistance

Antimicrobial resistance is a worldwide problem for both human and animal health. In 2013, approximately two million people acquired a serious infection, and 23,000 people died as a direct consequence of antibiotic-resistant infection in the United States[1, 2]. The cost of caring for patients with antimicrobial resistance has exceed around $4 billion each year in the United States[1, 2].

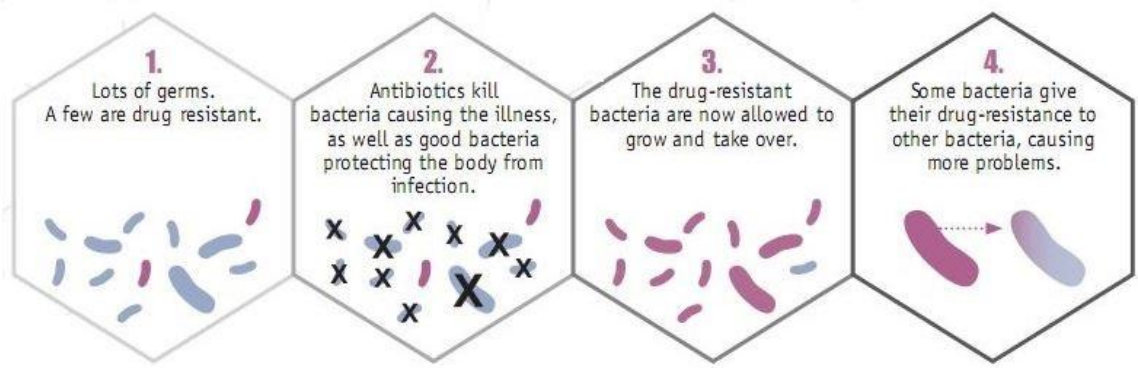

Figure 1.1. Antimicrobial-resistant bacteria sharing their genetic materials with the other bacteria and increasing antibiotic resistance[1].

Several health-related associations, including the World Health Organization (WHO), have declared antimicrobial resistance one of the most dangerous threats to human health[1]. Antimicrobial-resistant bacteria can exchange their DNA with other similar or different types of bacterial species and thus also make them antibiotic resistant, which results in multidrug-resistant bacteria[3] (Figure 1.1). The bacterial resistance appears to be the result of one of the three mechanisms: (1) alteration in the antibiotic enzymatic target, (2) decreased outer membrane permeability, and (3) the development of the efflux mechanism (Figure 1.2)[4, 5]. For example, fluoroquinolone antibiotics such as Ciprofloxacin work against cell membrane synthesis. They primarily inhibit the growth of

bacterial gyrase, an enzyme responsible for DNA repair[1]. The Ciprofloxacin loses its activity because of the bacteria's development of the efflux mechanism.

This dissertation focuses on development of antimicrobial polymers to overcome antimicrobial resistance. More precisely, in Chapter 2 discusses the synthesis of antimicrobial polymers using amidinourea functional group to overcome multidrug resistance, and Chapter 3 presents a synthesis of Cipro-containing antimicrobial polymers in a pro-drug approach to overcome the efflux mechanism associated with Ciprofloxacin. In this introduction, I will provide a general overview of the polymeric approach to overcome antimicrobial resistance.

1.2. Mechanism of Antimicrobial Resistance

It is now of great concern that a number of resistant bacteria are increasing rapidly and are becoming resistant to more than one antibiotic. Bacteria can develop resistance to an existing antimicrobial via several mechanisms (section 1.1).

Figure 1.2. Antimicrobial resistance due to bacterial cell wall. Alteration in the antibiotic enzymatic target, decreased outer membrane permeability and the development of efflux mechanism[4]. (edited)

Among them are the efflux mechanism, which evolve when bacteria prevent antibiotics from entering the cell and immediately kick an antibiotic out of the bacterial cell (Figure

1.2). Development of the efflux mechanism appears to be a result of the loss of antimicrobial concentration at the cell membrane. Each bacterium has a degree of antibiotic tolerance. Above this antibiotic tolerance limit, bacterial growth will be curbed but will not kill the organisms. This is called the minimum inhibitory concentration (MIC)[6]. More generally, bacteria with the efflux mechanism have a higher MIC value than the value should be.

1.3. Overcome Antimicrobial Resistance

To combat pathogenic infections as well as antimicrobial resistance, antimicrobial agents known as antibiotics are widely used[7]. The compounds with the biocidal properties able to inhibit the bacterial growth are called antimicrobial agents. Numerous efforts have been made in the development of antimicrobial agents to kill or suppress the microbial grown to battle emerging pathogenic diseases, but success against infectious diseases remains the same or little improved[8, 9]. Small molecular antimicrobial agents are fulfilling some of those aims, but their use is limited because of cytotoxicity and long-time efficacy[9, 10]. Antimicrobial polymers, first discovered in 1965[11], are promising as agents to kill or suppress bacterial growth. Since then, appreciable developments have been made on antimicrobial polymers.

1.4. Mechanism Action of Antimicrobial Polymers

Bacterial cell walls are structurally different based on their gram strain. Gram-positive bacterial cell walls are composed of teichoic acid molecules, whereas lipopolysaccharides and phospholipids are found in gram-negative bacterial cell membranes. Gram-negative bacteria have an outer membrane composed of a phospholipid bilayer. Most of the functional proteins such as enzymes are enclosed in a cytoplasmic

membrane of gram-negative bacteria. The cytoplasmic membrane controls the transfer of solutes and metabolites to enter the cell cytoplasm[12]. The antimicrobial polymers target the cytoplasmic membrane and are known as membrane-active agents, or antimicrobial polymers, and are composed of hydrophilic-hydrophobic compounds and cationic charge on the side chains. These kinds of structures have surface activity properties and absorption/adsorption ability that can bind with bacterial cells because of the high lipophilicity present in the cytoplasmic membrane. As a result of cytoplasmic membrane disruption, leakage of cytoplasmic contents and cell death occur[13].

1.5. Progress in Antimicrobial Polymer Synthesis

Research on antimicrobial polymers has mainly focused on the development of an easy synthetic method and on improving the antimicrobial properties against resistant pathogens. As compared to small antimicrobial agents, antimicrobial polymers exhibit superior efficacy, minimize environmental problems, and reduce toxicity.

There are several ways to synthesize an ideal antimicrobial polymer. Understanding the bacterial cell wall, outer membrane, and cytoplasmic membrane, a smart design in monomer and polymer has been developed over recent years. Ring-opening metathesis polymerization (ROMP) is one of the useful techniques to synthesize mono and block copolymers. Tew et al. published several articles using ROMP as an efficient method for synthesizing antimicrobial polymers (Figure 1.3. A & B)[14, 15]. Another technique to make antimicrobial polymers is the incorporation of antimicrobial agents into a polymer via a pro-drug approach. In this technique, a well-known antibiotic drug is attached to the monomer by covalent or ester bond formation (Figure 1.3. C) followed by polymerization[16]. Conjugated polymers (CPs) are also used as antimicrobial agents.

Having a proper balance between hydrophobicity and hydrophilicity along with incorporation of positive charge on their side chain, CP-based antimicrobial polymers have been reported to overcome antimicrobial resistance in recent years. In the CP based method, a rigid hydrophobic aromatic backbone provides necessary hydrophobicity while the flexible side chain balances the hydrophilicity (Figure 1.3. D)[17].

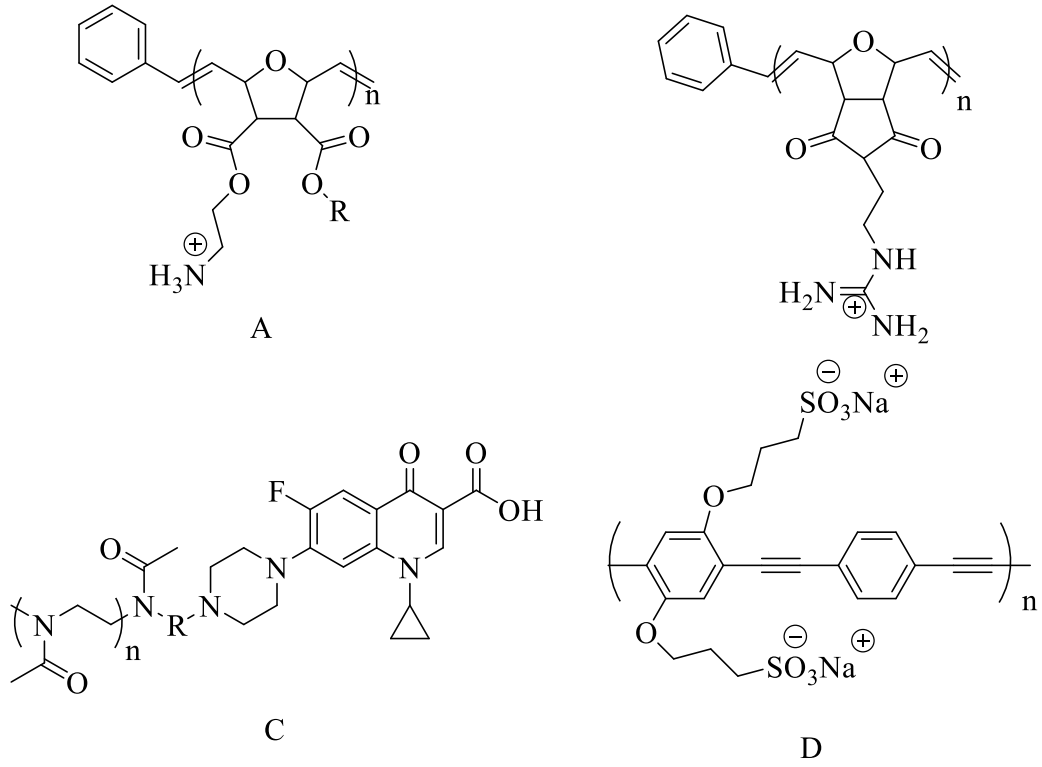

Figure 1.3. Antimicrobial polymer via ring-opening metathesis polymerization (ROMP) (A & B), pro-drug approach of Ciprofloxacin (C) and conjugated antimicrobial polymer (D).

1.6. Design Consideration of Antimicrobial Polymers

Effect of positive charge: The bacterial cell surface is negatively charged, so most of the antimicrobial polymers contain a positive charge on their side chain[18]. Most synthetic antimicrobial polymers target pathogens via cationic interaction. Amine,

guanidine, and quaternary ammonium are the common sources for positively charged antimicrobial polymers[19-24]. Figure 1.4 shows the structures of the positively charged functional groups found in antimicrobial polymers. Among the various sources, protonated primary and tertiary amines of polycarbonates are more active on microbes[25-27]. Unlike low molecular weight, primary amines containing polyacrylate, corresponding quaternary amines do not show antimicrobial activity because of loss of the hydrophobicity required to disrupt the bacterial cell membrane[28, 29]. Compared to quaternary ammonium, protonated secondary amine has higher antimicrobial activity[19, 25]. Therefore, primary and secondary amines may be interacting with the bacterial cell membranes via hydrogen bonding along with cationic interactions to show better antimicrobial activity. At the same time, amines are found to be less toxic to human red blood cells, making them the most functional groups of antimicrobial polymers[21].

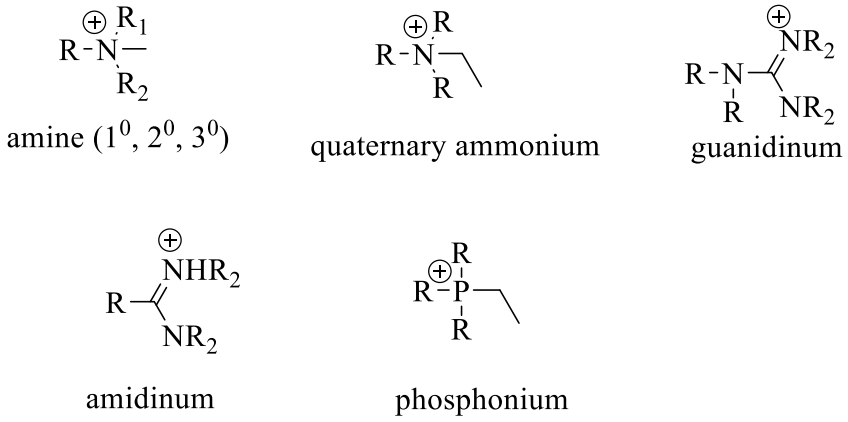

Figure 1.4. Common positively charged functional groups in antimicrobial polymers.

Besides amine and quaternary ammonium, guanidine functional groups possess higher antimicrobial activity on cell membrane of pathogens. Guanidine containing conjugated poly(norbornene) and polyacrylate have excellent antimicrobial activity[15, 30]. Tew et al. reported that incorporation of guanidine moiety in antimicrobial peptides (AMPs)

dramatically increased antimicrobial activity and decreased hemolytic property[15]. Amide bonds in guanidine functional group show strong interaction with the lipid membranes of microbes via hydrogen bonding and thus show higher antimicrobial potency[31].

Effect of hydrophobic-hydrophilic balance: Antimicrobial activity of antimicrobial polymers also depends on a balance between the hydrophobic and hydrophilic natures of synthetic polymers[32]. The bacteria cell membrane is composed of hydrophilic, water-filled porin channels and a hydrophobic lipid bi-layer[33-36]. Hydrophobic antibiotics such as rifampicin and fluoroquinolones cross the cell wall through a diffusion approach[37]. Ikeda et al. reported the highest antimicrobial activity with the longest chain (C_{12}) of poly(trialkylvinyl-benzylammonium chloride)[38]. Recently, Nonaka et al. investigated the length of methacryloyl-ethyl trialkyl phosphonium chlorides on *E. coli* and found antimicrobial activity increased with an increase of the number of hydrophobic units[39, 40].

To increase hydrophobicity, using alkylation and/or copolymerization with hydrophobic units is very common. But excess hydrophobicity also increases the hemolytic activity. To compensate with hemolysis, hydrophilic units are introduced to make a balanced antimicrobial polymer. For example, polyethylene glycol (PEG) has higher antimicrobial properties with higher hemolytic activity. Copolymerization of PEG acrylate with aminohexyl acrylate decreases hemolytic activity, but it also decreases antimicrobial activity[41]. Thus, an optimal balance between hydrophobicity and hydrophilicity is essential for an ideal antimicrobial polymer.

Effect of polymer chain length: The polymer length plays a crucial role in terms of achieving the desired antimicrobial properties. Thus, significant research has been conducted on molecular weight-dependent antimicrobial polymer synthesis. Ikeda et al. synthesized homo and copolymers of polyacrylate and polymethyl acrylates with biguanide groups in the side chain[38, 42]. They reported that the biocidal action of synthesized polymers against *S. aureus* highly depends on the molecular weight. After analyzing various molecular weights, they reported the optimal range of most active antimicrobial polymers as between 5×10^4 and 1.2×10^5 Da. The antimicrobial activity of higher molecular weight polymers, compared to that of lower ones, can be explained by taking into consideration the bacterial cell membrane structure. Bacterial cell walls are negatively charged and susceptible to electrophoresis. Hence, adsorption of higher molecular weight polymers to the negatively charged cell membrane is expected to be greater than that of low molecular weight polymers.

In contrast with those of higher molecular weight, lower molecular weight polymers possess more antimicrobial activity. Tew et al. reported that lower molecular weight polymers showed better biocidal activity than the higher ones[14]. By analyzing different length of oligomers while making antimicrobial peptides (AMPs), Tew et al. reported that a minimum chain length is necessary to obtain any antibacterial activity[14].

1.7. Introduction of Amidinourea Functional Group

Sections 1.1 to 1.6 discussed the definition and mechanism of antimicrobial resistance and a polymeric approach to overcome antimicrobial resistance. As the goal of this dissertation is to discuss the synthesis of polymers to overcome antimicrobial resistance, I will now introduce the actual functional group used in the process.

In Chapter 2, I discussed the synthesis of amidinourea containing antimicrobial polymer and their antimicrobial activities. When Boc guanidine reacts with primary or secondary amine at an elevated temperature, a new functional group emerged called amidinourea[43]. Amidinourea contains features of both guanidine and urea with different physical and chemical properties. Synthesis of an amidinourea functional group can be achieved by modification of guanidine group with a primary or secondary amine. Small molecular amidinoureas and their derivatives have been used in many medicinal chemistry applications, such as in the treatment of irritable bowel syndrome, gastrointestinal, spasmolytic, cardiovascular disorders, and parasitic infections. It also possesses good antimalarial activity and fungicidal properties[44-47]. Because amidinourea-functionalized compounds have been tested for antimalarial and antifungal agents, and plasmodium has a bacteria-like cell surface, it is expected that amidinourea might have some antimicrobial activities. Moreover, polymeric materials are successfully used for overcoming antimicrobial resistance. Hence, amidinourea-containing polymers (polyamidinourea) are expected to have antimicrobial activity on certain bacteria cell surfaces. Antimicrobial activities depend on the proper balance of hydrophobicity and hydrophilicity along with positive charge. The amidinourea functional group containing a new class of polyamidinourea antimicrobial polymers have been designed, synthesized, and tested on several resistant bacterial cell membranes, including multidrug-resistant bacteria (e.g., MRSA).

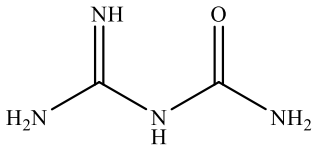

amidinourea

1.8. Cipro-Containing Antimicrobial Polymer via ROMP

Chapter 3 focuses on the synthesis of Cipro-containing antimicrobial polymer via ROMP. As discussed earlier, antimicrobial resistance such as efflux pumping appears because of a low concentration of antibiotics at the bacterial cell membranes. To increase the local concentration of antimicrobial agents, we have polymerized Ciprofloxacin with more hydrophobic monomer to combat the efflux pumping-resistant mechanism. We anticipated that copolymerization of Cipro with more hydrophobic monomer might increase the antibiotic concentration without increasing the drug percentage. In this approach, Cipro-containing homo and di-block copolymers have been designed and synthesized, and their antimicrobial properties are discussed in Chapter 3.

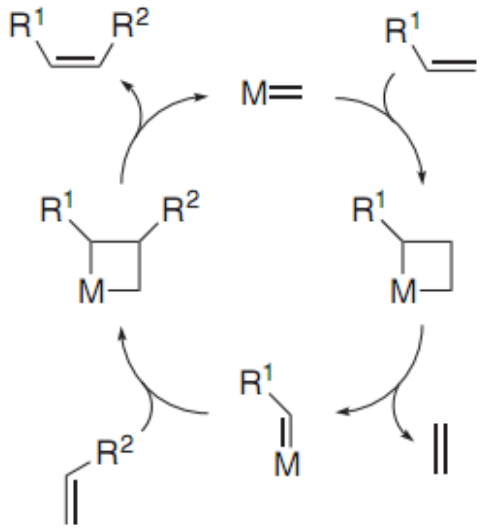

Figure 1.5. Reaction mechanism of ROMP[49].

The ring opening metathesis polymerization (ROMP) reaction is a highly useful technique to synthesize a very narrow and controlled length of polymers[48, 49]. ROMP is a ruthenium catalyst-based ring-opening polymerization technique and generally converts

cyclic olefins into linear polymers. The reaction mechanisms involve the coordination of a cyclic olefin into a ruthenium catalyst complex. Later [2+2] cycloaddition produces a ruthenium-cyclobutane intermediate to form a growing polymer chain[50]. The intermediate then undergoes cycloreversion to form a new metal alkylidene. The intermediate steps are repeated during the propagation stage until the monomer is completely consumed. The ROMP reaction is quenched by an addition of excess ethyl vinyl ether[50].

1.9. Application of Antimicrobial Polymers

Antimicrobial polymers are widely used in the medical, textile, and food industries. Medical or medicinal devices are susceptible to microbial infections. Most are from hospital-acquired infections from medical devices, despite continual improvements in materials and techniques. The copolymer of 4-vinyl-*n*-hexylpyridinum bromide and dimethyl(2-methacryloyloxyethyl) phosphonate helped to reduce biofilm formation and improved the use of medical devices. A significant reduction of several pathogenic infections associated with resistant bacteria such as *Streptococcus sanguinis*, *Escherichia coli*, *Staphylococcus aureus*, and *Staphylococcus epidermidis* have been achieved by coating copolymer on titanium[51].

To overcome catheter-associated infections, a combination of rifampicin, sparfloxacin, and triclosan was developed and a maximum one-month duration of efficacy was achieved. Antimicrobial polymers are a new class of antimicrobial agent with broad spectrum and high antimicrobial activity against a variety of pathogens. Antimicrobial wound-dressing cotton gauze, composed of polycation and polyanion, provide a high antimicrobial effect for *Staphylococcus aureus* and *Klebsiella* pneumonia[51].

Food safety and quality are important for consumer health. Nisin is the only currently approved food preservative because of its low toxicity and antibacterial effectiveness[52]. A great success in packing film has been achieved by incorporation of preservatives into a polyolefin matrix using glycerol mono-oleate as a dispersant[53].

Textiles are another suitable environment for microbial growth because of their optimum conditions of temperature and moisture. Antimicrobials for textiles have attracted numerous attention over the past decades. Eco-friendly antimicrobial textile materials have been prepared by using polypropylene- and corona-modified polypropylene nonwoven material with thymol[54].

1.10. Introduction to CPs

Chapters 2 and 3 discuss and present the synthesis of antimicrobial polymer and its biological assay. Chapter 4 focuses on modification of the guanidine functional group in CPs and their application in cellular imaging and gene or drug delivery. Conjugated polymers (CPs) are widely used in biological applications because of their simple synthetic procedure and easy separation steps. High brightness, excellent photo stability, low cytotoxicity, high quantum yield, and variable surface charges made CP-based drug delivery more advantageous than many other gene carriers[55]. Incorporation of specific recognition elements into CPs adds further ability for targeted recognition and imaging in vitro and in vivo[56].

1.11. Types of Typical CPs and Polymerization Methods

Among several types of CPs, four major CPs with their synthetic schemes are depicted in Figure 1.6. Polythiophenes (PTs) and poly(*p*-phenylenevinylene)s (PPVs) have been widely used in photonic applications. Poly(*p*-phenyleneethynylene)s (PPEs) have

been used for drug or gene delivery applications[57]. The poor solubility and process ability of poly(*p*-phenylenebutadiynylene)s (PPBs) have limited their use in biological applications. Because Chapter 4 mainly focuses on modulation of guanidine functional group in (*p*-phenyleneethynylene) (PPE), I will stick to PPE only. Basically, PPE-conjugated polymers are synthesized following the Sonogashira coupling reaction when a palladium-catalyzed reaction mechanism has been used.

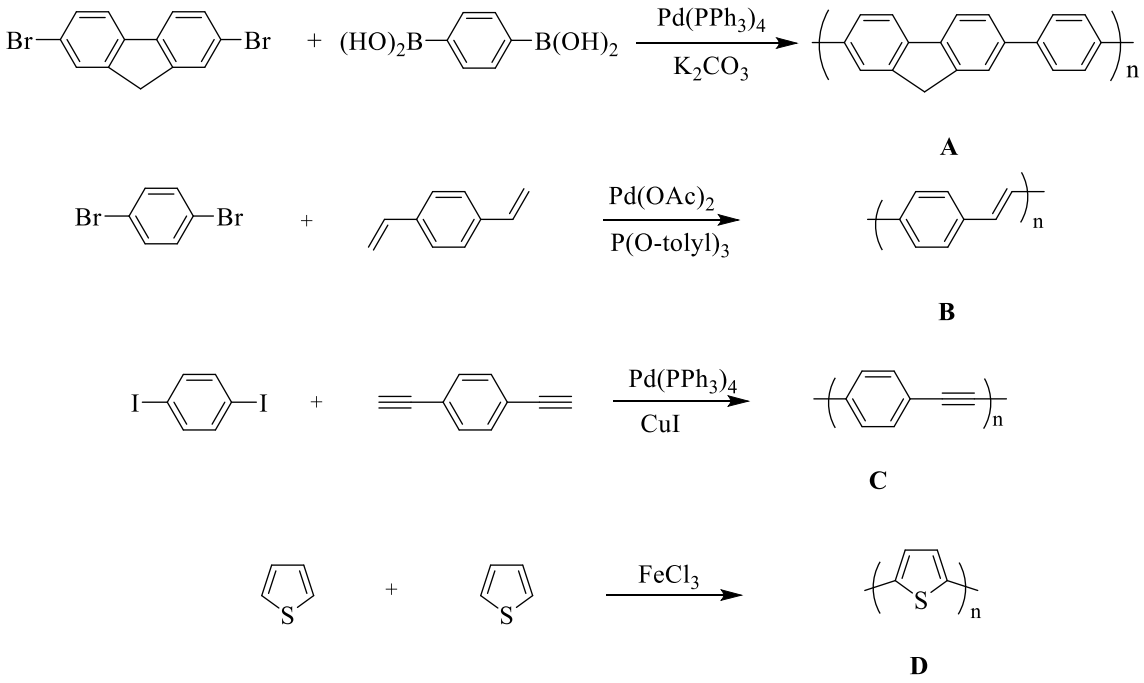

Figure 1.6. Structure of CPs: poly(fluorine) (PF) (A), poly(*p*-phenylenevinylene) (PPV) (B), poly(*p*-phenyleneethynylene) (PPE) (C), and poly(thiophene) (PT) (D)[57-60].

1.12. Guanidine Head Group Modification in CPs

As discussed in section 1.8, Chapter 4 deals with the synthesis and modification of guanidine containing CPs, and their cellular and subcellular behaviors have been studied with gene delivery efficacy.

In Boc-protected guanidine (Boc NHR_1), the amide proton is relatively acidic, which can be deprotonated by a primary or secondary amine to make guanidine-modified compounds. The reaction mechanism involves in situ generation of isocyanate, which can further react with nucleophiles to have the guanidine-modified products. Small molecular guanidine functional group modification has been reported. Kessler et al. modified the guanidine group of the RGD pentapeptide Cilengitide ligand. The authors demonstrated that *N*-methylation, *N*-alkylation, or *N*-acylation of Cilengitide enhanced the binding affinities of the ligands and thus resulted in increased selectivity of Cilengitide ligands[61]. Takemoto et al. used palladium- or iridium-catalyst to modify guanidinum in small molecule in a convenient way[62]. Macrocyclic compounds have also been used in the modification of guanidine moieties, and their applications in the chemical, biological, and medicinal fields have been documented.

Because guanidine moiety is highly charged and its addition in the CPs' side chain triggers cellular entry barriers, we have hypothesized that incorporation of a more hydrophobic and/or hydrophilic group might possess better cellular transfection as well as cellular imaging and gene delivery. To do that, we modified a guanidine group in PPE polymer with more hydrophobic and hydrophilic compounds. Various modified CPs have been prepared, their cellular and sub-cellular localization have been studied, and these are presented in Chapter 4.

1.13. Biological Application of CPs

Guanidine containing CPs show good agreement in terms of CP-based drug delivery vehicles because of their highly positively charged side chain. Moon et al.

synthesized amine containing PPE and demonstrated the delivery of biologically active materials like siRNA into HeLA cells[63].

In addition, positively charged, fluorescent properties of CPs are important in cellular imaging. As anticipated, CP has excellent photostability with low cytotoxicity and enters cytoplasm via endocytosis, which can be monitored by confocal microscopy.

1.14. Summary

This dissertation generally focuses on synthesis of various polymeric materials for antimicrobial resistance or gene or drug delivery. Chapters 2 and 3 discuss the synthesis of antimicrobial polymers. In this project, we demonstrated the synthesis of antimicrobial polyamidinourea with an amidinourea functional group in the polymeric backbone. Chapter 3 discusses the synthetic condition along with antimicrobial assays and their minimum inhibitory concentrations on several resistant bacterial cell walls. Chapter 4 presents the synthesis of guanidine containing PPE polymers and the modification of the guanidine head group with different types of amine and alcohol. Later, the modified polymers were tested for gene delivery and significant protein knockdown was achieved.

1.15. References

1. Frieden, T. (2013). Antibiotic Resistance Threats in the United States. Washington, DC: US Department of Health and Human Services.

2. Beovic, B. (2006). The Issue of Antimicrobial Resistance in Human Medicine. Int J Food Microbiol, 112 (3):280-7. Epub 2006/07/04. doi:10.1016/j.ijfoodmicro.2006.05.001. PubMed PMID: 16815582.

3. Kriti, S. (2012). Fluoroquinolones: Chemistry & Action—A Review. Ind Glob J Pharm Sci, 2:43-53.

4. Kenawy, E.R. (2001). Biologically Active Polymers. IV. Synthesis and Antimicrobial Activity of Polymers Containing 8-hydroxyquinoline Moiety. J Appl Polym Sci, 82:1364-74.

5. Kenawy, el R., Worley S.D., and Broughton R. (2007). The Chemistry and Applications of Antimicrobial Polymers: A State-of-the-Art Review. Biomacromolecules, 8 (5):1359-84. Epub 2007/04/12. doi:10.1021/bm061150q. PubMed PMID: 17425365.

6. Lin, M.Y., Yang, C.H., Huang, K.S. (2014). Biomedical Devices for Pathogen Detection Using Microfluidic Chips. CurrProteom, 11:116-20.

7. Chan, K.S., Lee, M.Y., Yang, C.H., Wang, C. Y., and Lin, Y.S. (2014). Applications of Nanoparticles for Antimicrobial Activity and Drug Delivery. Curr Org Chem, 18:204-15.

8. Huang, K.S., Yang, C.H., Huang, S.L., Chen, C.Y., Lu, Y.Y., and Lin, Y.S. (2016). Recent Advances in Antimicrobial Polymers: A Mini-Review. Int J Mol Sci, 17 (9): Epub 2016/09/23. doi:10.3390/ijms17091578. PubMed PMID: 27657043, PubMed Central PMCID: PMCPMC5037843.

9. Li, G.S., and Appl, J.J. (2000). A Study of Pyridinium-Type Functional Polymers.

IV. Behavioral Features of the Antibacterial Activity of Insoluble Pyridinium-Type Polymers. Polym Sci, 78:676-84.

10. Siedenbiedel, J.C. (2012). Antimicrobial Polymers in Solution and on Surfaces: Overview and Functional Principles. Polymers, 4:46-71.

11. Jain, A., Duvvuri, L.S., Farah, S., Beyth, N., Domb, A.J., and Khan W. (2014). Antimicrobial Polymers. Adv Healthc Mater, 3 (12):1969-85. Epub 2014/11/20. doi:10.1002/adhm.201400418. PubMed PMID: 25408272.

12. Singer, S.J., and Nicolson, G.L. (1972). The Fluid Mosaic Model of the Structure of Cell Membranes. Science, 175 (4023):720-31. Epub 1972/02/18. PubMed PMID: 4333397.

13. Kenawy, E.R., Worley, S.D., and Broughton, R. (1007). The Chemistry and Applications of Antimicrobial Polymers: A State-of-the-Art Review. Biomacromolecules, 8:1359-84.

14. Lienkamp, K., Madkour, A.E., Musante, A., Nelson, C.F., Nusslein, K., and Tew, G.N. (2008). Antimicrobial Polymers Prepared by ROMP with Unprecedented Selectivity: A Molecular Construction Kit Approach. J Am Chem Soc, 130 (30):9836-43. Epub 2008/07/03. doi:10.1021/ja801662y. PubMed PMID: 18593128, PubMed Central PMCID: PMCPMC4106262.

15. Gabriel, G.J., Madkour, A.E., Dabkowski, J.M., Nelson, C.F., Nusslein, K., and Tew, G.N. (2008). Synthetic Mimic of Antimicrobial Peptide with Nonmembrane-Disrupting Antibacterial Properties. Biomacromolecules, 9 (11):2980-3. Epub 2008/10/15. doi:10.1021/bm800855t. PubMed PMID: 18850741, PubMed Central PMCID: PMCPMC2646885.

16. Schmidt, M., Harmuth, S., Barth, E.R., Wurm, E., Fobbe, R., Sickmann, A., et al. (2015). Conjugation of Ciprofloxacin with Poly(2-oxazoline)s and Polyethylene Glycol via End Groups. Bioconjug Chem, 26 (9):1950-62. Epub 2015/08/19. doi:10.1021/acs.bioconjchem.5b00393. PubMed PMID: 26284608.

17. Corbitt, T.S., Sommer, J.R., Chemburu, S., Ogawa, K., Ista, L.K., Lopez, G.P., et al. (2009). Conjugated Polyelectrolyte Capsules: Light-Activated Antimicrobial Micro "Roach Motels." ACS Appl Mater Interfaces, 1 (1):48-52. Epub 2009/01/28. doi:10.1021/am800096q. PubMed PMID: 20355752.

18. Palermo, E.F., and Kuroda, K. (2010). Structural Determinants of Antimicrobial Activity in Polymers Which Mimic Host Defense Peptides. Appl Microbiol Biotechnol, 87 (5):1605-15. Epub 2010/06/22. doi:10.1007/s00253-010-2687-z. PubMed PMID: 20563718.

19. Timofeeva, L., and Kleshcheva, N. (2011). Antimicrobial Polymers: Mechanism of Action, Factors of Activity, and Applications. Appl Microbiol Biotechnol, 89 (3):475-92. Epub 2010/10/19. doi:10.1007/s00253-010-2920-9. PubMed PMID: 20953604.

20. Munoz-Bonilla, A., Cerrada, M., and Fernández-García, M. (2012). Polymeric Materials with Antimicrobial Activity. Prog Polym Sci, 37:281-339.

21. Ganewatta, C.B. (2015). Controlling Macromolecular Structures Towards Effective Antimicrobial Polymers. Polymers, 63:A1-A29.

22. Ganewatta, M.S., Miller, K.P., Singleton, S.P., Mehrpouya-Bahrami, P., Chen, Y.P., Yan, Y., et al. (2015). Antibacterial and Biofilm-Disrupting Coatings from Resin Acid-Derived Materials. Biomacromolecules, 16 (10):3336-44. Epub 2015/09/02. doi:10.1021/acs.biomac.5b01005. PubMed PMID: 26324023.

23. Zheng, Z., Xu, Q., Guo, J., Qin, J., Mao, H., Wang, B., et al. (2016). Structure-Antibacterial Activity Relationships of Imidazolium-Type Ionic Liquid Monomers, Poly(ionic liquids) and Poly(ionic liquid) Membranes: Effect of Alkyl Chain Length and Cations. ACS Appl Mater Interfaces, 8 (20):12684-92. Epub 2016/05/05. doi:10.1021/acsami.6b03391. PubMed PMID: 27145107.

24. Tejero, R., Lopez, D., Lopez-Fabal, F., Gomez-Garces, J.L., and Fernandez-Garcia, M. (2015). High-Efficiency Antimicrobial Thiazolium and Triazolium Side-Chain Polymethacrylates Obtained by Controlled Alkylation of the Corresponding Azole Derivatives. Biomacromolecules, 16 (6):1844-54. Epub 2015/05/07. doi:10.1021/acs.biomac.5b00427. PubMed PMID: 25944495.

25. Timofeeva, L.M., Kleshcheva, N.A., Moroz, A.F., and Didenko, L.V. (2009). Secondary and Tertiary Polydiallylammonium Salts: Novel Polymers with High Antimicrobial Activity. Biomacromolecules, 10 (11):2976-86. Epub 2009/10/03. doi:10.1021/bm900435v. PubMed PMID: 19795886.

26. Palermo, E.F., Sovadinova, I., and Kuroda, K. (2009). Structural Determinants of Antimicrobial Activity and Biocompatibility in Membrane-Disrupting Methacrylamide Random Copolymers. Biomacromolecules, 10 (11):3098-107. Epub 2009/10/07. doi:10.1021/bm900784x. PubMed PMID: 19803480.

27. Palermo, E.F., and Kuroda, K. (2009). Chemical Structure of Cationic Groups in Amphiphilic Polymethacrylates Modulates the Antimicrobial and Hemolytic Activities. Biomacromolecules, 10 (6):1416-28. Epub 2009/04/10. doi:10.1021/bm900044x. PubMed PMID: 19354291.

28. Paslay, L.C., Abel, B.A., Brown, T.D., Koul, V., Choudhary, V., McCormick, C.L., et al. (2012). Antimicrobial Poly(methacrylamide) Derivatives Prepared via Aqueous RAFT Polymerization Exhibit Biocidal Efficiency Dependent upon Cation Structure. Biomacromolecules, 13 (8):2472-82. Epub 2012/06/29. doi:10.1021/bm3007083. PubMed PMID: 22738241.

29. Grace, J.L., Huang, J.X., Cheah, S.E., Truong, N.P., Cooper, M.A., Li. J., et al. (2016). Antibacterial Low Molecular Weight Cationic Polymers: Dissecting the Contribution of Hydrophobicity, Chain Length and Charge to Activity. RSC Adv, 6 (19):15469-77. Epub 2016/03/22. doi:10.1039/C5RA24361K. PubMed PMID: 26998253, PubMed Central PMCID: PMCPMC4792307.

30. Locock, K.E., Michl, T.D., Valentin, J.D., Vasilev, K., Hayball, J.D., Qu, Y., et al. (2013), Guanylated Polymethacrylates: A Class of Potent Antimicrobial Polymers with Low Hemolytic Activity. Biomacromolecules, 14 (11):4021-31. Epub 2013/10/09. doi:10.1021/bm401128r. PubMed PMID: 24099527.

31. Uppu, D.S.S.M., Baul, U., Singh, P., Siersma, T.K., Samaddar, S., Vemparala, S., Hamoen, L.W., Narayana, C., and Haldar, J. (2016), Isosteric Substitution in Cationic-Amphiphilic Polymers Reveals an Important Role for Hydrogen Bonding in Bacterial Membrane Interactions. J Chem Sci, 7:4613-23.

32. Ikeda, T.H.H., Suzuki, K., Yamaguchi, H., and Tazuke, S. (1986), Biologically Active Polycations, 6†. Polymeric Pyridinium Salts with Well-Defined Main Chain Structure. Makromol Chem Phy, 187:333-40.

33. Kumar, A., and Schweizer, H.P. (2005). Bacterial Resistance to Antibiotics: Active Efflux and Reduced Uptake. Adv Dr.ug Deliv Rev, 57 (10):1486-513. Epub 2005/06/09. doi:10.1016/j.addr.2005.04.004. PubMed PMID: 15939505.

34. Berlanga, M., Montero, M.T., Hernandez-Borrell, J., and Vinas, M. (2004). Influence of the Cell Wall on Ciprofloxacin Susceptibility in Selected Wild-Type Gram-negative and Gram-positive Bacteria. Int J Antimicrob Agents, 23 (6):627-30. Epub 2004/06/15. doi:10.1016/j.ijantimicag.2003.12.015. PubMed PMID: 15194135.

35. Marshall, A.J., and Piddock, L.J. (1994). Interaction of Divalent Cations, Quinolones and Bacteria. J Antimicrob Chemother, 34 (4):465-83. Epub 1994/10/01. PubMed PMID: 7868402.

36. Chapman, J.S., and Georgopapadakou, N.H. (1988). Routes of Quinolone Permeation in Escherichia Coli. Antimicrob Agents Chemother, 32 (4):438-42. Epub 1988/04/01. PubMed PMID: 3132091, PubMed Central PMCID: PMCPMC172197.

37. Lambert, P.A. (2002). Cellular Impermeability and Uptake of Biocides and Antibiotics in Gram-positive Bacteria and Mycobacteria. Symp Ser Soc Appl Microbiol, (31):46S-54S. Epub 2002/12/17. PubMed PMID: 12481828.

38. Ikeda, T., Hirayama, H., Yamaguchi, H., Tazuke, S., and Watanabe, M. (1986). Polycationic Biocides with Pendant Active Groups: Molecular Weight Dependence of Antibacterial Activity. Antimicrob Agents Chemother, 30 (1):132-6. Epub 1986/07/01. PubMed PMID: 3092730, PubMed Central PMCID: PMCPMC176450.

39. Nonaka, H., Ise, H., Sugihara, N., Hirose, S., Negishi, N., Kondo, Y., et al. (2003). Development of Highly Functional Long-Term Culture Method of Liver Slice Embedded in Agarose Gel for Bioartificial Liver. Cell Transplant, 12 (5):491-8. Epub 2003/09/05. PubMed PMID: 12953923.

40. Uemura, Y.M.I., Kurihara, S., and Nonaka, T. (1999). Preparation of Resins Having Various Phosphonium Groups and Their Adsorption and Elution Behavior for Anionic Surfactants. J Appl Polym Sci, 72:371-8.

41. Punia, A.M.A., Banerjee, P., and Yang, N. L. (2015). Nonhemolytic and Antibacterial Acrylic Copolymers with Hexamethyleneamine and Poly(ethylene glycol) Side Chains. ACS Macro Lett, 4:426-30.

42. Ikeda, T., Yamaguchi, H, and Tazuke, S. (1984). New Polymeric Biocides: Synthesis and Antibacterial Activities of Polycations with Pendant Biguanide Groups. Antimicrob Agents Chemother, 26 (2):139-44. Epub 1984/08/01. PubMed PMID: 6385836, PubMed Central PMCID: PMCPMC284107.

43. Berlinck, R.G. (1996). Natural Huanidine Derivatives. Nat Prod Rep, 13 (5):377-409. Epub 1996/10/01. PubMed PMID: 8888608.

44. Yelnosky, J., Ghulam, M.N. (1987). US Patent. 4:701-457.

45. Studt, W.L.Z., Dodson, H.K., and Can, S. A. (1986). CA Patent 1. 210-394 A1.

46. Serafin, B., Urbanski, T., and Warhurst, D.C. (1969). Antimalarial Compounds. X. Biguanide and Amidinourea Derivatives of Diphenyl Sulfide, Sulfoxide, and Sulfone. J Med Chem, 12 (2):336-7. Epub 1969/03/01. PubMed PMID: 5783616.

47. Cutler, R.A., and Schalit, S. (1976). US Patent. 3:988-370.

48. Lehman, K. B. (2003). Handbook of Metathesis (ed. Grubbs, R. H.) Ch. 3.9. Wiley-VCH, Weinheim.

49. Grubbs, R.H. (ed.) (2003) Hand book of Metathesis Wiley-VCH, Weinheim.

50. Bielawski, R.H. (2007). Living Ring-Ppening Metathesis Polymerization. Prog Polym Sci, 32:1-29.

51. Fisher, L.E., Hook, A.L., Ashraf, W., Yousef, A., Barrett, D.A., Scurr, D.J., et al. (2015). Biomaterial Modification of Urinary Catheters with Antimicrobials to give Long-Term Broadspectrum Antibiofilm Activity. J Control Release, 202:57-64. Epub 2015/02/03. doi:10.1016/j.jconrel.2015.01.037. PubMed PMID: 25639970.

52. Gharsallaoui, A., Joly, C., Oulahal, N., and Degraeve, P. (2016). Nisin as a Food Preservative: Part 2: Antimicrobial Polymer Materials Containing Nisin. Crit Rev Food Sci Nutr, 56 (8):1275-89. Epub 2015/02/13. doi:10.1080/10408398.2013.763766. PubMed PMID: 25674671.

53. Kuplennik, N.T., Zelas, R., Sadovski, Z.B., Fishman, A., and Narkis, A. (2015). Antimicrobial Packaging Based on Linear Low-Density Polyethylene Compounded with Potassium Sorbate. LWT Food Sci Technol, 62:278-86.

54. Markovic, S., Radeti, M., Jokic, B., and Zizovic, I. (2015). Impregnation of Corona-Modified Polypropylene Non-woven Material with Thymol in Supercritical Carbon Dioxide for Antimicrobial Application. J Supercrit Fluids, 101:215-21.

55. Tuncel, D., and Demir, H.V. (2010). Conjugated Polymer Nanoparticles. Nanoscale, 2 (4):484-94. Epub 2010/07/21. doi:10.1039/b9nr00374f. PubMed PMID: 20644748.

56. Wang, B., Yuan, H., Zhu, C., Yang, Q., Lv, F., Liu, L., et al. (2012). Polymer-Drug Conjugates for Intracellar Molecule-Targeted Photoinduced Inactivation of Protein and Growth Inhibition of Cancer Cells. Sci Rep, 2:766. Epub 2012/10/26. doi:10.1038/srep00766. PubMed PMID: 23097688, PubMed Central PMCID: PMCPMC3479448.

57. Moon, J.H., McDaniel, W., Maclean, P., and Hancock, L.F. (2007). Live-Cell-Permeable Poly(p-phenylene ethynylene). Angew Chem Int Ed Engl, 46 (43):8223-5. Epub 2007/09/25. doi:10.1002/anie.200701991. PubMed PMID: 17886818.

58. Bunz, U.H. (2000). Poly(aryleneethynylene)s: Syntheses, Properties, Structures, and Applications. Chem Rev, 100 (4):1605-44. Epub 2001/12/26. PubMed PMID: 11749277.

59. Liu, B., Wang, S., Bazan, G.C., and Mikhailovsky, A. (2003). Shape-Adaptable Water-Soluble Conjugated Polymers. J Am Chem Soc, 125 (44):13306-7. Epub 2003/10/30. doi:10.1021/ja0365072. PubMed PMID: 14582996.

60. Feng, X., Yang, G., Liu, L., Lv, F., Yang, Q, Wang, S., et al. (2012). A Convenient Preparation of Multi-Spectral Microparticles by Bacteria-Mediated Assemblies of Conjugated Polymer Nanoparticles for Cell Imaging and Barcoding. Adv Mater, 24 (5):637-41. Epub 2011/09/21. doi:10.1002/adma.201102026. PubMed PMID: 21932281.

61. Kapp, T.G., Fottner, M., Maltsev, O.V., and Kessler, H. (2016). Small Cause, Great Impact: Modification of the Guanidine Group in the RGD Motif Controls Integrin Subtype Selectivity. Angew Chem Int Ed Engl, 55 (4):1540-3. Epub 2015/12/15. doi:10.1002/anie.201508713. PubMed PMID: 26663700.

62. Miyabe, H., Yoshida, K., Reddy, V.K., and Takemoto, Y. (2009). Palladium- or Iridium-Catalyzed Allylic Substitution of Guanidines: Convenient and Direct Modification of Guanidines. J Org Chem, 74 (1):305-11. Epub 2008/12/05. doi:10.1021/jo802271d. PubMed PMID: 19053613.

63. Moon, J.H., Mendez, E., Kim, Y., and Kaur, A. (2011). Conjugated Polymer Nanoparticles for Small Interfering RNA Delivery. Chem Commun (Camb), 47 (29):8370-2. Epub 2011/06/23. doi:10.1039/c1cc10991j. PubMed PMID: 21695337.

CHAPTER II:

SYNTHESIS OF ANTIMICROBIAL POLY(GUANYLUREA)S

Reproduced in part with permission from Bioconjugate Chemistry 2018

DOI: 10.1021/acs.bioconjchem.8b00057. Published online: Mar 12, 2018.

Md Salauddin Ahmed,† Thirunavukkarasu Annamalai,† Xuerong Li,† Ahmed Seddeck,† Peng Teng,‡ Yuk-Ching Tse-Dinh,† and Joong Ho Moon*†

†Department of Chemistry and Biochemistry, Biomolecular Sciences Institute, Florida International University, 11200 SW 8th St., Miami, FL 33199, USA

‡Department of Chemistry, University of South Florida, 4202 East Fowler Avenue, Tampa, Florida 33620, United States

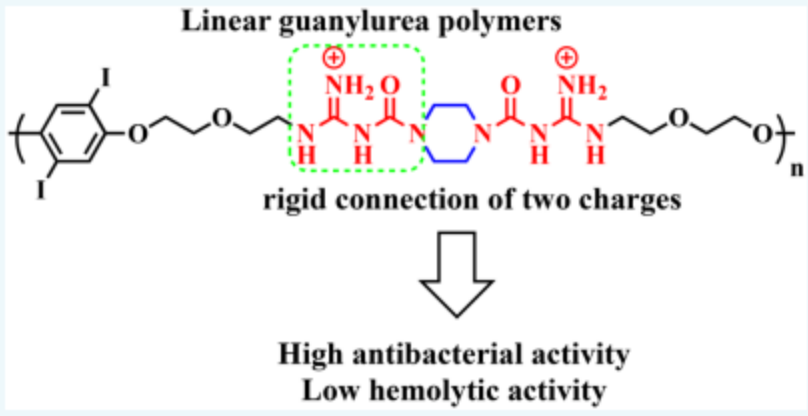

2.1. Abstract

Drug-resistant pathogens are emerging rapidly and thwart the treatment of common bacterial infectious diseases that can lead to prolonged illness, disability, and death. Regardless of the considerable developments made in antimicrobial drugs, many contagious diseases remain difficult to treat because of acquired drug resistance. Compared to small antibiotics, which interrupt the intracellular biochemical processes, antimicrobial polymers with relatively high molecular weights offer a promising strategy to overcome drug resistance by disrupting the physical integrity of the membrane. Because of the unique mechanism, bacteria need a much longer time to develop resistance. A new class of antimicrobial polymers is based on an amidinourea functional group, in which the charges in the backbone have been designed, synthesized, and tested using bacteria, including methicillin-resistant *Staphylococcus aureus* (MRSA). We evaluated the effects of hydrophobicity and polymer molecular weights on antimicrobial activity by measuring MIC_{90} (minimum inhibitory concentration) and HC_{50} (hemolysis assay). Amidinourea antimicrobial polymers exhibit a promising MIC value (13 μg/mL) with selectivity of 30 (HC_{50}/MIC_{90}) against MRSA, supporting the concept that the novel functional group has unique antimicrobial activity. In this research, we discussed a synthetic approach to make a unique functional antimicrobial polymer and discussed several factors that influence antimicrobial activity, such as positive charge, hydrophobicity-hydrophilicity balance, size, and chain length.

2.2. Introduction

Microorganisms are primarily responsible for infectious disease, which may come from resistant bacteria[1]. Infectious diseases kill more people than any other single cause and becoming a great concern in various fields concerning the infectious qualities of medical devices, drugs, and hospitals surfaces[2, 3]. In most cases, infections countered with antimicrobial agents are vulnerable to their action[4, 5]. Bacteria can be resistant to an antimicrobial agent either by development of the efflux mechanism or alteration in the antibiotic enzymatic target. The worst-case scenario is that resistant bacteria can share their DNA with other kinds of microbes and make them antimicrobial resistant as well, which results multidrug-resistant evolution[6-10].

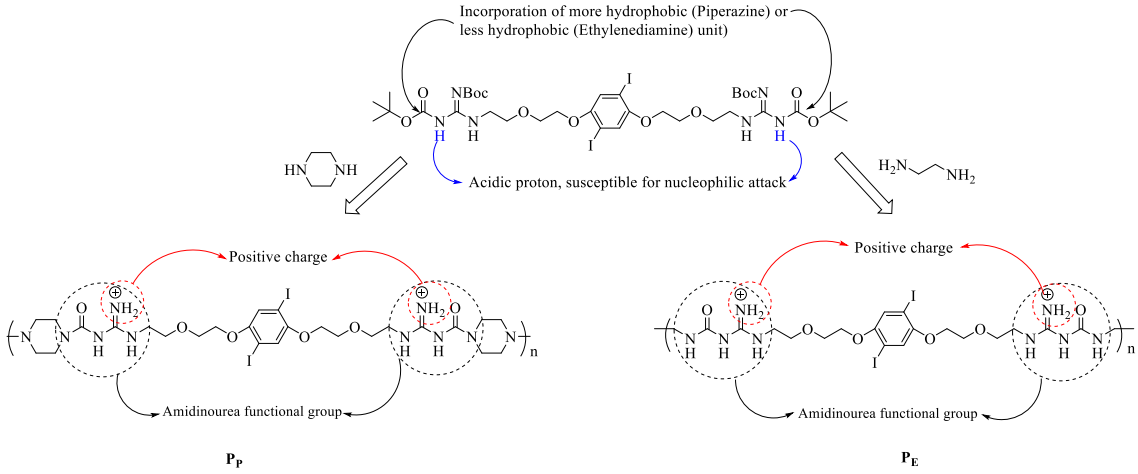

Figure 2.1. Schematic representation of polyamidinourea antimicrobial polymer

Small molecular antibiotics have been widely used as antimicrobial agents, disinfectants, and antiseptics; but bacteria can easily mutate the specific targets of small molecules and result in the formation of drug-resistant microorganism strains. Additionally, the competency of small molecular antibiotics is poor for long-term

safety[11]. Therefore, polymeric materials with antimicrobial properties offer good chances for increasing efficacy[12, 13] because polymeric materials are less toxic, more efficient and selective, and prolong the lifetime of the antimicrobial agents[14-16]. Antimicrobial polymers can slow or inhibit the progress of drug-resistant microorganism strains because of their distinctive antimicrobial mechanism[17, 18]. Antimicrobial polymers are composed of hydrophilic and hydrophobic compounds with cationic charges on the side chains. These kinds of structures have surface activity properties and absorption/adsorption ability that can bind with bacterial cells because of the high lipophilicity present in the cytoplasmic membrane. As a result of cytoplasmic membrane disruption, leakage of cytoplasmic contents and cell death occurs[13].

Many reports published in the field of polymeric materials with antimicrobial activity include synthetic mimicry of antimicrobial polymers, antimicrobial peptides, and more[14-16, 18]. Despite the fact that numerous efforts have been made in the development of polymeric antimicrobial agents to kill or suppress the microbial grown to battle emerging pathogenic diseases, but success against infectious diseases remains the same or little improved[8, 9]. To combat resistant microorganisms, we have developed a new synthetic approach to synthesize amidinourea containing liner antimicrobial polymer designated as polyamidinourea (Figure 2.1). Amidinourea containing small molecules and their derivatives have often been applied in medicinal chemistry[25, 26] and it also possesses good antimalarial and fungicidal properties[27, 28]. Takeda Chemical Co., Japan, isolated TAN-1057 (structurally related to amidinourea) from bacteria *Flexibacter sp*, which has shown some potential antibacterial activities against methicillin-resistant *Staphylococcus*

aureus[29]. However, the antimicrobial activity of amidinourea in polymer has not yet been explored and no reports have been found on polyamidinourea.

Unlike the conventional antimicrobial polymers, polyamidinourea contain charges in the backbone instead of the side chain (Figure 2.1). Polymers bearing charges on the backbone have been reported maximum selectivity (HC_{50}/MIC_{90}) 20000 for *S. epidermidis*[30]. Moreover, positive charge per every repeating unit, meaning constant positive density, providing ample opportunities to modulate hydrophilicity and hydrophobicity using a variety of primary and, or secondary amines. Also, having novel antimicrobial polymers with unique functional groups will add to the functional group's diversity to make bacteria cells will find it hard to develop resistance.

Motivated by all the work done on antimicrobial polymers, we have developed a new synthetic approach to synthesize amidinourea containing a liner polymer designated as polyamidinourea. Here, we present a convenient synthetic technique to prepare a new class of antimicrobial polymer. After careful study of the bacterial cell wall, cell membrane, and cytoplasmic membrane, we have designed the amidinourea antimicrobial polymer with hydrophobicity-hydrophilicity rightly balanced and sufficient charges on the surface. Two series of polyamidinourea have been prepared using ethylenediamine (P_E) and piperazine (P_P), and their biological assays have been determined evaluating minimum inhibitory concentration (MIC), hemolysis assay (HC_{50}), and membrane disruption mechanism study. The P_E series of polymers were inactive with lower selectivity with all the microbes tested. The P_P series of polymers exhibited quite impressive antimicrobial activities with higher selectivity on *M. smegmatis* (WT), *Shigella flexneri*, *S. aureus* (MRSA), and *S. auresus* (WT). Polymer $P_{P\text{-}8K}$ (P_P series, Mn = 8000) showed a promising MIC value (13 μg/mL)

with a selectivity of 30 against *S. aureus* (MRSA), supporting the concept that the novel functional group has unique antimicrobial activity. Further study on the mechanism of action revealed the bacterial cell membrane-disruption mechanism. To investigate the effect of polymeric chain length on antimicrobial activity, we prepared and tested various lengths polyamidinourea. In this research, we synthesized linear polyamidinourea, and we will discuss their antimicrobial properties, hemolysis activity, and structure-functional activity.

2.3. Result and Discussion

Research design. On the basis of the characteristics of the bacterial cell wall, outer membrane, and cytoplasmic membrane, we designed the major part of the polymer as a cationic hydrophilic-hydrophobic system, a target site for which the cytoplasmic membrane was considered[19]. The aromatic hydrophobic nonpolar unit with the amidinourea cationic charge polymeric structure provides surface-activity properties and adsorption/absorption ability toward the bacterial cells[31]. The high lipophilicity caused adequate damage of the structural system and principle of cell membranes, followed by cell membrane disruption, leakage of cytoplasmic contents, and cell lysis[22, 32]. As discussed earlier, the balance between hydrophobicity and hydrophilicity and the positively charge play important roles in obtaining the desired antimicrobial properties. Hence, the first task was to design an easy and modular synthetic pathway toward the amphiphilic monomer and polymer. The amidinourea functional group has been proposed to make the final antimicrobial polymer necessary to find a suitable synthetic approach toward the making of amidinourea functional polymer (Figure 2.1). There are several methods

available to make the synthesis amidinourea functional compound. The common methods are hydrolysis of biguanides[27], reaction of guanidine with isocyanates[33], hydrolysis of cyanoguanidines, reaction of Acyl-S-Methylisothiourea with amines[34], and reaction of di-Boc-Guanidines with amines. As guanidinium has been used for making an amidinourea functional compound and is a major source of positive charge, we have designed guanidinum containing monomer to fulfil the synthetic target. The balance between hydrophobicity and hydrophilicity is maintained by carefully introducing aromatic and the alkyl chain, respectively. The iodo group is attached to the aromatic ring for further incorporation of hydrophobic/antibacterial unit to make a more active polymer.

Monomer synthesis. The multiple-step approach was taken to obtain the monomer **A** (scheme 2.1). Compound **1** was synthesized according to the literature and reacted with commercially available *N, N'*-Di-Boc-^{1}H pyrazole- 1 -carboxamide using dichloromethane (DCM), acetonitrile (MeCN) and diisopropylethylamine (DIPEA) 7:3.5:1 ratio (v/v). After extraction, the monomer was purified by column chromatography. The final product was a white powder, and the overall yield was ~70%.

Polymer synthesis. To make a series of amidinoure-containing antimicrobial polymers (**P_E** & **P_P**), monomer **A** reacted with ethylenediamine and piperazine, respectively, in the presence of K_2CO_3 and tetrahydrofuran (THF) as a solvent. The monomer ratio, temperature, and concentration of solvents played important roles in achieving the targeted high molecular weight polymers. After screening several ratios, temperatures, and solvent conditions, we found a 1:1.15 ratio of two monomers at 70^0C and 2.60 mg/mL of solvent, as compared with monomer **B**, which provided high molecular weight polymer with a good yield.

Antimicrobial and hemolysis assay. The antimicrobial properties of synthesized polymers, (i.e., their MIC_{90}, value toward the growth of *M. smegmatis* (WT), *Shigella flexneri*, *S. aureus* (MRSA), and *S. aureus* (WT) bacteria, and their HC_{50} toward red blood cells were determined. The MIC_{90} and HC_{50} measurements were carried out by Ahmed and Wenjie in Dr. Tse Dinh lab as collaborators for this project. The biological data obtained for these polymers are included in Table 2.1. The ratio of HC_{50}/MIC_{90} was used to calculate the selectivity. In summary, polymers with diamine series (**$P_{E\text{-}11K}$ & $P_{E\text{-}7K}$**) were inactive or showed little activity **(**Table 2.1**)**, whereas polymers with the piperazine series (**$P_{P\text{-}14K}$ & $P_{P\text{-}8K}$**) showed better antimicrobial activities than the diamine series. More precisely, the piperazine series showed promising antimicrobial activity on *S. aureus* (MRSA) compared with using Ciprofloxacin as a control. Additionally, the antimicrobial activities toward the

Table 2.1. Characterization of antimicrobial polyamidinoureas by biological assay

Polymer	MIC_{90} (μg/mL)[a]				HC_{50} (μg/mL)[b]	Selectivity[c]			
	M. smegmatis (WT)	*Shigella flexneri*	*S. aureus* (MRSA)	*S. aureus* (WT)		*M. smegmatis* (WT)	*Shigella flexneri*	*S. aureus* (MRSA)	*S. aureus* (WT)
$P_{P\text{-}14K}$	6.5	25.5	25.5	13	504	77.5	19.8	19.8	38.8
$P_{P\text{-}8K}$	3.125-6.5	25.5	13	13	394	60.6-126	15.4	30.3	30.3
$P_{P\text{-}3K}$	102	>203	>203	>203	>2000	n.d	n.d	n.d	n.d
$P_{E\text{-}11K}$	25	25-50	99	99	232	4.6-9	6	2.3	2.3
$P_{E\text{-}7K}$	50-99	198	198	198	257	2.6-5	1.3	1.3	1.3
*Control	0.25-0.5	0.006	20	0.8-1.6					

[a] Inhibitory activity toward bacterial growth of *M. smegmatis* (WT), *Shigella flexneri*, *S. aureus* (MRSA) and *S. auresus* (WT). (MIC_{90} = minimum inhibitory concentration preventing 90% bacterial growth), [b] Hemolytic activity toward red blood cells (HC_{50} = concentration lysing 50% of blood cells), [c] ratio between HC_{50}/MIC_{90} value, * Ciprofloxacin was used as a control.

bacteria tested decreased as $\mathbf{P_E}$ polymer length decreased, the opposite behavior observed with the $\mathbf{P_P}$ series of polymers.

These observations can be explained by taking different bacterial membranes into account. The membranes of gram-negative bacteria like *Shigella flexneri* consist mostly of phosphatidylethanolamine and anionically charged phosphatidyglycerol (PG), whereas gram-positive bacteria like *S. aureus* and *M. smegmatis* have membranes that consist mainly of anionically charged PG and cardiolipin[14, 35, 36]. Tew et al. reported that the anionic surface charge, along with hydrophobicity, plays an important role in penetrating the lipid bilayer of the bacterial cell membrane. If the synthesized polymers are attached with highly positive charge and their amphilicity is rightly balanced, they will penetrate the cell wall. Hence, less hydrophobic polymers $\mathbf{P_E}$ were not able to penetrate the hydrophobic core of the lipid bilayer and thus showed less activity on the tested microbe. Hydrophilic polymers may prefer to remain in solution as opposed to being adsorbed to the membrane. However, more hydrophobic polymers $\mathbf{P_P}$ showed strong membrane activity. These observations led to recognizing the maximum activity against *S. aureus* for $\mathbf{P_{P\text{-}14K}}$ & $\mathbf{P_{P\text{-}8K}}$ polymers because it seemed to have the optimal amphilicity to penetrate the bacterial membrane.

The better antimicrobial activity of a lower molecular weight polymer than of the higher one can be addressed by again referring Tew's work [14]. By analyzing different lengths of oligomers while making antimicrobial peptides (AMPs), the Tew group proved that a minimum chain length is necessary to obtain any antibacterial activity. In our work, we observed that $\mathbf{P_{P\text{-}8K}}$ showed better antimicrobial activity against *S. aureus* than $\mathbf{P_{P\text{-}14K}}$.

Gram-positive bacteria like *S. aureus* have a 15-80 nm-thick, negatively charged murein layer around the cell membrane. Complexation of a polyion with a lower charged species is reversible, whereas oppositely charged polyion complexed irreversibly. Thus, assuming that the negatively charged murein layer forms a polyion-polyion complex with the positively charged **P$_{P\text{-}14K}$**, increasing molecular weight (more charges on the polymer surface) makes the dissociation of such a complex more difficult. Thus, the higher molecular weight **P$_{P\text{-}14K}$** gets stuck in the murein layer of gram-positive bacteria before reaching the plasma membrane and thus shows less antimicrobial activity. To prove this statement, we synthesized a low molecular weight polymer (**P$_{P\text{-}3K}$**) and found inactivity on all the microbes tested. Another rationalization can be considered for the higher activity of **P$_{P\text{-}8K}$** over all other polymers because of the lower size of **P$_{P\text{-}8K}$** measured in the phosphate buffer (Table 2.2). The nanoparticle sizes increased with $P_{P\text{-}8K} < P_{P\text{-}14K} < P_{E\text{-}11K} < P_{E\text{-}7K} < P_{P\text{-}3K}$, and antimicrobial activity decreased along with the size increase. This revelation supports our earlier statement that a larger size of polymers might become stuck in the cell wall and result in less or no antimicrobial activity on the cell membrane.

The HC_{50} values toward human red blood cells (RBCs) showed that the piperazine series of polymers (**P$_P$**) are less toxic than the ethylenediamine series of polymers (**P$_E$**). The maximum selectivity of 77.5 was achieved from the polymer **P$_{P\text{-}14K}$**, whereas **P$_{P\text{-}8K}$** produced a range of 60.6-126. **P$_{P\text{-}3K}$** polymer was nontoxic up to 2000 μg/mL. This phenomenon can be explained by analyzing the difference between bacteria and the cell membrane of RBCs. Bacterial membranes are more negatively charged than RBC membranes. Red blood cells (RBCs) are composed of cholesterol and phosphatidylcholine, whereas gram-negative bacteria such as *E. coli* contain mainly phosphatidylethanolamine

and anionically charged phosphatidylglycerol, and gram-positive bacteria such as *S. aureus* consist of anionically charged phosphatidyglycerol and cardiolipin. The higher positively charged polymers can attract the RBCs' membrane more strongly than the less charged polymers. Thus, more positively charged $\mathbf{P_E}$ polymers can lyse the RBCs more than less positively charged $\mathbf{P_P}$ polymers.

Polymer characterization. All Boc-protected polymers are soluble in regular organic solvents like DCM and THF and exhibit high molecular weights and acceptable experimental yields, as listed in Table 2.2. After Boc-deprotection polymer solubility was reduced, polymers were soluble only in DMF and DMSO. The experimental yields were low because of the removal of low-MW fragments during the polymer purification process by precipitation. The proton NMR spectra of all polymers were consistent with their predicted average structure. The analysis of predicted polymer structures examined the ethoxy protons on the side chain of monomer **A** (b ~4.23 ppm) and the guanidinum amide NH protons characteristic of monomer **A** (g ~ 12.20 ppm and f ~ 8.35 ppm, respectively). As compared with monomer **A**, the resultant polymer showed only one Boc peak at 1.45 ppm, which is another confirmation of the final polymer structure. All proton peaks were integrated relative to the ethylene oxide proton peak (b) and were in good agreement with the integration values predicted by theoretical analysis. Figure 2.3 shows an example spectrum of polymer $\mathbf{P_P}$.

2.4. Conclusion

In this study, we investigated several important parameters that influence the antimicrobial and hemolytic activity of polyamidinoureas. We demonstrated that polymer length, charge, size, and ratio of hydrophobicity and hydrophilicity affect antimicrobial

activity. We also demonstrated a noble synthetic approach to make linear antimicrobial polyamidinourea with charges in the backbone. We discussed polymer condition optimization and characterization by screening different solvents, temperatures, and ratios of both monomers. Finally, we studied the antimicrobial assay along with HC_{50} determination. We identified that out of two types of polymers, the piperazine series of polyamidinoureas were more active on bacterial cell membranes and less hemolytic on RBCs than the diamine series of polyamidinourea.

2.5. Outlook

Further study on the structure-function relationship along with the bacteria cell membrane is needed to understand the actual antimicrobial mechanism. This research might open a door for synthesis of antimicrobial polymer using the amidinourea functional group in the backbone. Understanding bacterial cell walls and the membrane disruption mechanism, a smart design in polymer structure might increase its antimicrobial activity and selectivity. At the same time, proper balancing between hydrophobicity and hydrophilicity needs to be considered while synthesizing antimicrobial polymers. Incorporation of fluorescent material might enhance the live monitoring of antimicrobial mechanism inside the bacteria cell membrane.

2.6. Experimental Section

2.6.1. Monomer synthesis

A 100 mL round bottom flask (RBF) filled with compound **1** (1.00 g, 1.87 mmol) (synthesized according to literature procedure[35]) and *N,N'*-Di-Boc-1H-pyrazole-1-carboxamide (1.16 g, 3.73 mmol) under a nitrogen atmosphere. A mixture of acetonitrile and DCM (1:2 v/v, 20.0 mL) was degassed with N_2 flow for 10 min and transferred into

the reaction flask via a cannula. The reaction mixture was allowed to stir at room temperature overnight, and then was quenched with water before the two layers were separated. The aqueous layer was extracted with DCM, and the combined organic layers were washed with brine, filtered, and concentrated *in vacuo*. Column chromatography under 30% of ethyl acetate in hexane yielded monomer **A** as a white powder (1.53 g, 80% yield).

Scheme 2.1. Synthesis of guanidinum-containing aryl halide monomer **A**

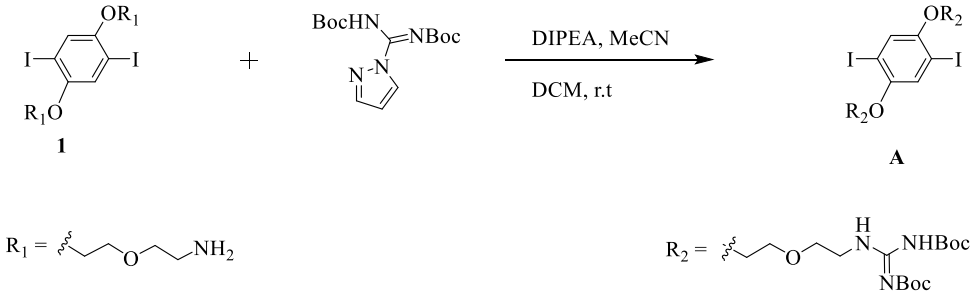

^{1}H NMR (400 MHz, $CDCl_3$, δ): 11.46 (s, 1H), 8.42 (t, *J* = 5.3 Hz. 1H), 7.35 (s, 1H), 4.09 (t, *J* = 4.4 Hz, 2H), 3.49 (t, *J* = 5.2 Hz, 2H), 1.43 (s, 9H), 1.39 (s, 9H). ^{13}C NMR (400 MHz, δ): 163.0, 155.4, 152.5, 152.0, 122.7, 86.8, 82.9, 78.1, 69.7, 68.6, 68.5, 28.0, 27.6. FT-IR (neat): 3329, 2978, 2929, 2851, 1719, 1665, 1639, 1614, 1573, 1516, 1482, 1466, 1406, 1394, 1326, 1276, 1242, 1155, 1125, 1048, 1024 cm^{-1}. HRMS (ESI+, m/z): [M + H^+]. calcd. For $C_{36}H_{58}I_2N_6O_{12}$, 1021.2275; found, 1021.2008.

2.6.2. Synthesis of polyamidinourea (P_E and P_P)

Boc P_E: A Schlenk flask was charged with 20.0 mg (0.02 mmol) of Boc-protected guanidine containing diiodo monomer **A**, 1.35 mg (0.02 mmol) of ethylenediamine, and 0.14 mg of potassium carbonate (0.001 mmol). Then 0.52 mL of anh THF solvent was

added, and the Schlenk flask was degassed for 1 minute. The reaction was then stirred in a pre-set oil bath at 70 ^{0}C for 16 hours under a nitrogen balloon. A viscous polymer solution was filtered through a glass wool pipette to remove K_2CO_3. The polymer was purified by re-precipitating in diethyl ether at first and then re-precipitating in methanol. The final polymer was a white gel (12.9 mg with 65.5% yield).

Scheme 2.2. Synthesis of amidinourea polymer

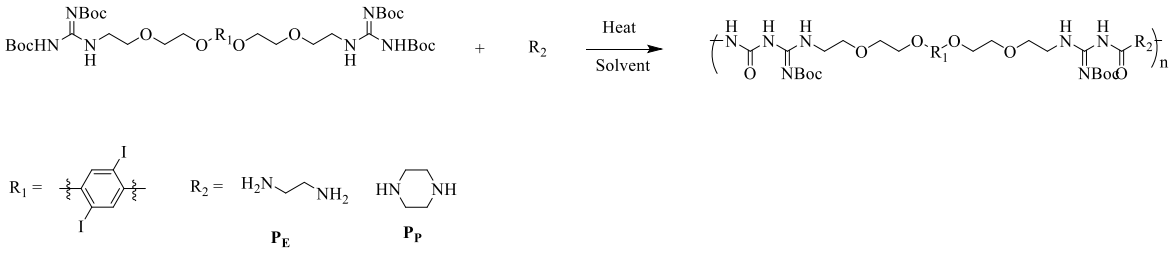

Table 2.2. Properties of polyamidinourea **P$_E$** and **P$_P$**.

Polymer	R_2	n [a]	Mn (g/mol) [b]	PDI [c]	Hydrodynamic diameter, nm [d]	Yield (%) [e]
$P_{E\text{-}11K}$	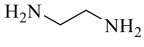	11	11200	1.9	146	65.5
$P_{E\text{-}7K}$	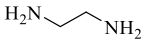	7	7500	1.9	162	65
$P_{P\text{-}14K}$	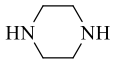	14	14500	1.4	76	62
$P_{P\text{-}8K}$	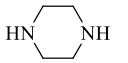	8	8700	1.5	58	60
$P_{P\text{-}3K}$	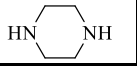	3	3100	2.5	225	65

[a] Degree of polymerization. [b] Determined by gel permeation chromatography in THF. [c] PDI (polydispersity index) = *Mw/Mn*. [d] Hydrodynamic diameter measured in PBS (2.5μM). [e] Percent yield per repeating unit after repeated purification by precipitation.

^{1}H NMR (400 MHz, $CDCl_3$, δ): 12.02 (s, 1H), 8.29 (s, 1H), 7.21 (s, 1H), 5.54 (s, 1H), 4.09 (t, 2H, *J* = 4.04), 3.86 (t, 2H, *J* = 3.79), 3.74 (t, 2H, *J* = 4.80), 3.55 (m, 2H), 3.31 (m, 2H),

1.44 (s, 9H). FT-IR (neat): 3405, 2531.9, 2159.37, 2033.8, 1662.4, 1437.4 cm-1. GPC: Mw = 21400 g/mol, Mn = 11200 g/mol, PDI = 1.90

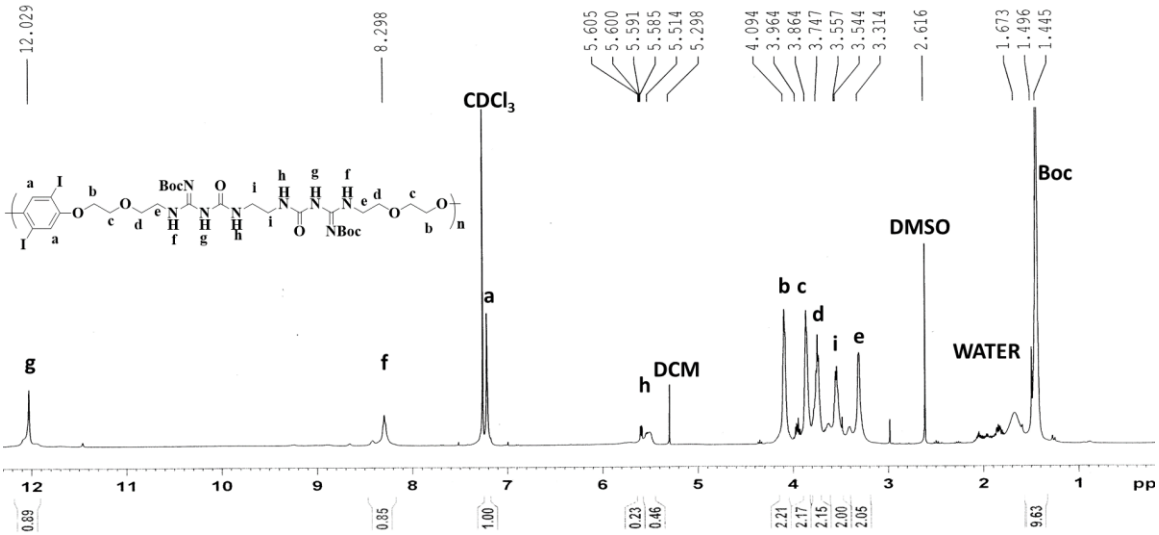

Figure 2.2. ^{1}H NMR of Ethylenediamine polyamidinourea **(P_E).**

Boc P_P: A Schleck flask was charged with 20.0 mg (0.02 mmol) of Boc-protected guanidine containing diiodo monomer **A**, 1.94 mg (0.02 mmol) of piperazine, and 0.14 mg of potassium carbonate (0.001 mmol). Then 0.52 mL (by volume) anh THF solvent was added, and the Schleck flask was degassed for 1 minute. The reaction was then stirred in a pre-set oil bath at 70 ^{0}C for 16 hours under a nitrogen balloon. A viscous polymer solution was filtered through a glass wool pipette to remove K_2CO_3. The polymer was purified by re-precipitating in diethyl ether at first and then re-precipitating in methanol. The final polymer was a white gel (12.5 mg with 62% yield).

^{1}H NMR (400 MHz, $CDCl_3$, δ): 12.20 (s, 1H), 8.35 (t, 0.96H, *J* = 4.80), 7.22 (s, 1H), 4.10 (t, 2H, *J* = 4.55), 3.88 (t, 2H, *J* = 4.55), 3.80 (t, 2H, *J* = 5.05), 3.73 (br s, 2H), 3.61 (q, 2H, *J* = 5.31, *J* = 5.05), 3.53 (br s, 2H), 1.44 (s, 9H). FT-IR (neat): 3280.07, 2938.13, 1668.25,

1534.75, 1483.01, 1448.18, 1346.94 cm-1. GPC: Mw = 27500 g/mol, Mn = 14500, g/mol. PDI = 140.

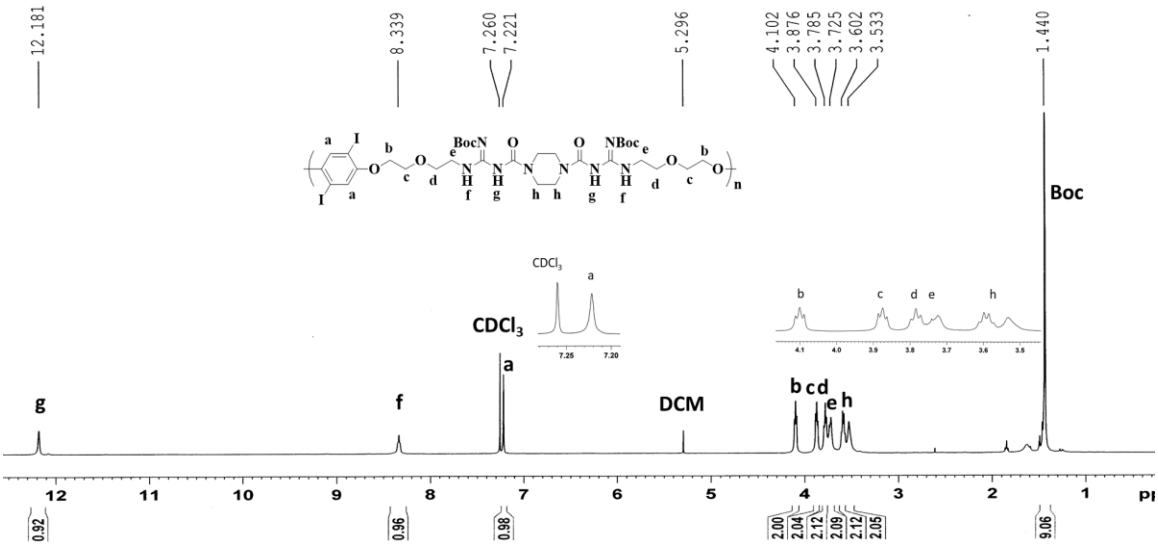

Figure 2.3. ^{1}H NMR of Piperazine polyamidinourea **(P_P).**

2.6.3. Boc deprotection of polyamidinourea

Scheme 2.3. Boc deprotection of polyamidinourea

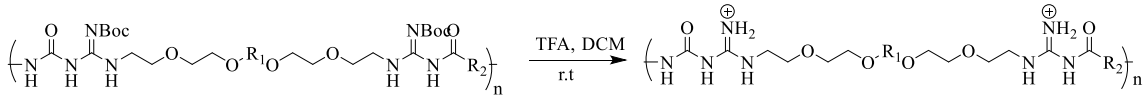

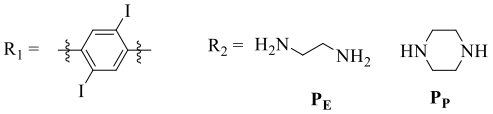

P_E P_P

General procedure for Boc deprotection of polyamidinourea

In a vial, Boc-protected polymer was dissolved in dicholoromethane (DCM) (1.00 mL) and trifluoroacetic acid (TFA) (1.00 mL) and stirred at r.t for 24 hours. Upon precipitation in DCM, we confirmed that the complete Boc deprotection and solvent evaporated in *vacuo*. Trifluoroacetic acid (TFA) was removed by azeotrope distillation and

the deprotected polymer purified by re-precipitating in ethyl acetate (EA) (2x). After drying in a high vacuum, the Boc deprotection was confirmed by ^{1}H NMR.

P_E: Using the general procedure described above, the final deprotected polymer was a white gel (62 % yield).

^{1}H NMR (400 MHz, DMSO-d_6, δ): 10.56 (s, 1H), 9.11 (s, 1H), 8.52 (s, 2H), 7.65 (s, 1H), 7.36 (s, 1H), 4.11 (s, 2H), 3.79 (s, 2H), 3.70 (s, 2H), 3.20 (s, 2H). FT-IR (neat): 3360.36, 2160.37, 1736.79, 1681.18 cm^{-1}

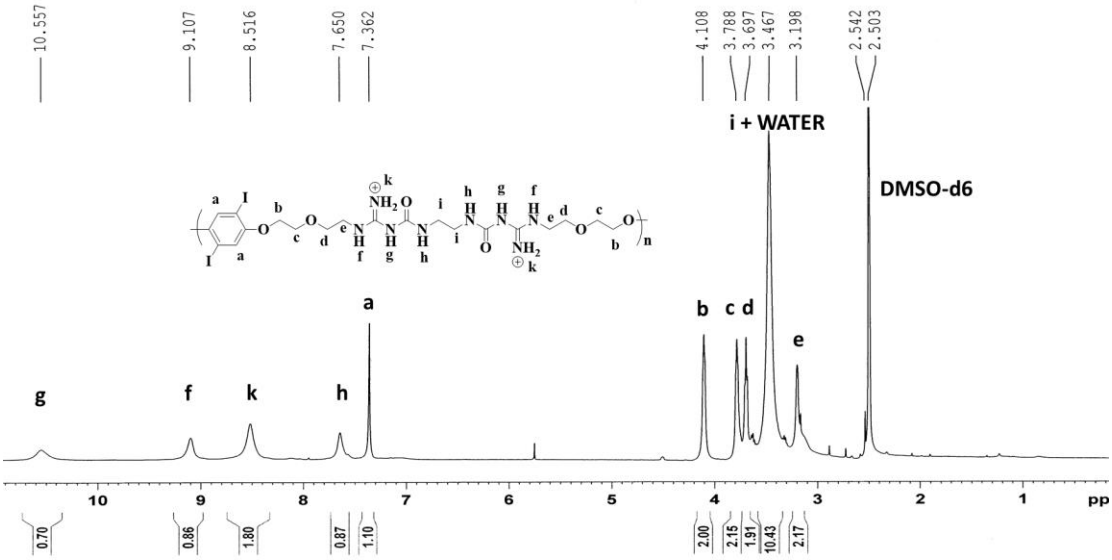

Figure 2.4. ^{1}H NMR of Boc deprotected Ethylenediamine polyamidinourea **(P_E).**

P_P: Using the general procedure above the final deprotected polymer was a white gel (66 % yield).

^{1}H NMR (400 MHz, DMSO-d_6, δ): 10.41 (s, 1H), 9.13 (s, 1H), 8.61 (s, 1H), 7.38 (s, 1H), 4.11 (s, 2H), 3.80 (s, 2H), 3.71 (s, 2H), 3.53 (s, 4H), 3.50 (s, 2H), 3.38 (s, 2H) 7. FT-IR (neat): 3360.36, 2160.37, 1736.79, 1681.18 cm^{-1}

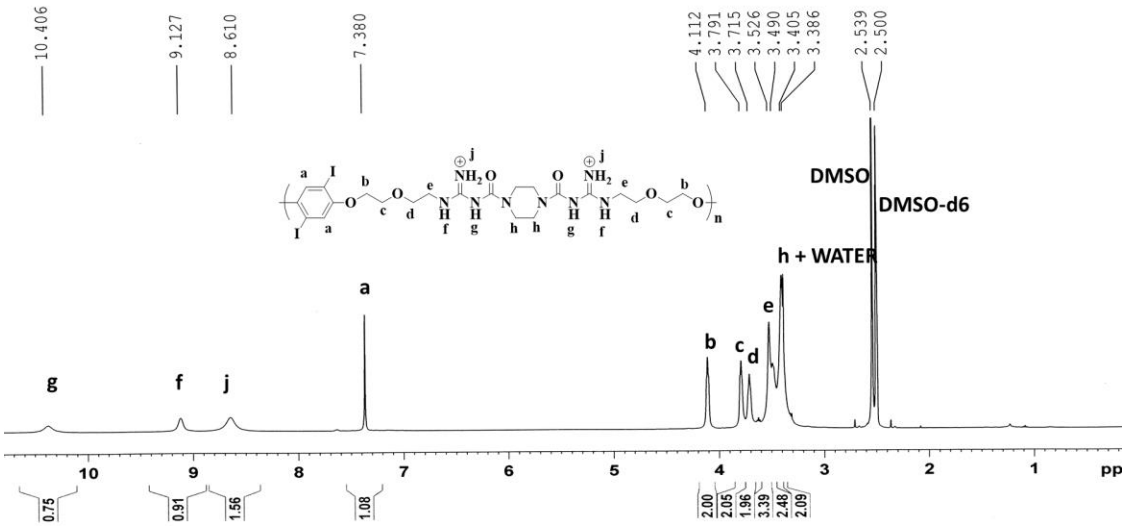

Figure 2.5. ^{1}H NMR of Boc deprotected Piperazine polyamidinourea **(PP).**

2.6.5. Antimicrobial assay

The compounds were dissolved in either DMSO or a buffer to make a stock solution, which was then diluted into 96-well plates and diluted with a Muller Hinton (M-H) medium to a constant volume. *M. smegmatis* (WT), *Shigella flexneri*, *S. aureus* (MRSA), and *S. aureus* (WT) were taken from stock glycerol solutions, diluted into an M-H medium, and grown overnight at 37^0C. Subsamples of these cultures were grown for 3 hours at 37^0C with agitation; the OD_{600} was measured, and then the cells were diluted to 0.001 OD_{600}. The diluted cell solutions (approximately 105 cells/mL) were then added to the 96-well plate. Table 2.1 shows the minimum concentration necessary to inhibit 50% of the cell growth. We determined this by serial dilutions of the abiogenic polymer following standard protocols. All reported values represent a minimum of quadruplicate experiments.

2.6.6. Hemolysis assay procedure

The hemolysis assay was carried out following the literature[36]. Basically, fresh human RBCs purchased from Zenbio, Inc., were used without further processing. The

RBCs were diluted for experimental use to 2% v/v RBCs in TBS and NaCl (TBS, pH 7.4, 0.01 M Tris-HCl, 0.155 M NaCl). The polymer samples were prepared as stock solutions in dimethyl sulfoxide (DMSO) at 8 mg mL^{-1} and diluted with TBS to give a working solution at 8000 µg mL^{-1}. Serial dilutions were made in a 96-well plate (Bio-One, Cellstar, Greiner) so that concentrations were stepwise halved eight times to give a range from 4,000 µg mL^{-1} to 31.25 µg mL^{-1} in 50 µL TBS. 10 µL of a 1 mg mL^{-1} stock solution of the hemolytic compound triton X-100 was added to 40 µL TBS as a positive control, 50 µL TBS as control (blank), and 100 µL TBS as background control. Finally, 50 µL of the 2% RBC solution was added to each well containing a 50 µL sample or a control. The plate was shaken gently for 1 minute then incubated for 1 hour at 37 °C. Thereafter, the plate was centrifuged at 400 g for 5 minutes, subsequent to which 50 µL of the supernatant was pipetted into a new 96-well plate, and the optical density (OD) was measured at 414 nm on a UV-vis plate reader. For statistical analysis, blank OD_{414} values were subtracted from both sample OD_{414} and positive control OD_{414} values. OD_{414} was normalized to 100 % with the lowest OD_{414} assigned to 0% hemolysis, and the triton X-100 positive control assigned to 100% hemolysis. The data were plotted as OD_{414} vs. $\log_{10}$ of the concentration using the graphing software Graphpad Prism. A sigmoidal curve was fitted to the data by the software to yield an HC_{50} value and 95% confidence intervals. The HC_{50} values reported are the average values derived from three replicates of hemolysis experiments, and error bars represent the standard error of the mean (SEM).

2.7. References

1. Chen, S. L. (2000). Recent Advances in Antimicrobial Dendrimers. Adv Mater, 12:843-6.

2. Tashiro, T. (2001). Antibacterial and Bacterium Adsorbing Macromolecules. Macromol Mater Eng, 286.

3. Pascual, A. (2002). Pathogenesis of Catheter-Related Infections: Lessons for New Designs. Clin Microbiol Infect, 8 (5):256-64. Epub 2002/06/06. PubMed PMID: 12047402.

4. Svenson, S., and Tomalia, D.A. (2005). Dendrimers in Biomedical Applications—Reflections on the Field. Adv Dr Drug Deliv Rev, 57 (15):2106-29. Epub 2005/11/25. doi:10.1016/j.addr.2005.09.018. PubMed PMID: 16305813.

5. Hetrick, E.M., and Schoenfisch, M.H. (2006). Reducing Implant-Related Infections: Active Release Strategies. Chem Soc Rev, 35 (9):780-9. Epub 2006/08/29. doi:10.1039/b515219b. PubMed PMID: 16936926.

6. Woo, G.L., Yang, M.L., Yin, H.Q., Jaffer, F., Mittelman, M.W., and Santerre, J.P. (2002). Biological Characterization of a Novel Biodegradable Antimicrobial Polymer Synthesized with Fluoroquinolones. J Biomed Mater Res, 59 (1):35-45. Epub 2001/12/18. PubMed PMID: 11745535.

7. Jiang, S., and LeeWong, A.C., and Denes, F.S. (2004). Plasma-Enhanced Deposition of Silver Nanoparticles onto Polymer and Metal Surfaces for the Generation of Antimicrobial Characteristics. J Appl Polym Sci, 9 (3):1411-22.

8. Hume, E.B., Baveja, J., Muir, B., Schubert, T.L., Kumar, N., Kjelleberg, S., et al. (2004). The Control of Staphylococcus Epidermidis Biofilm Formation and in vivo Infection Rates by Covalently Bound Furanones. Biomaterials, 25 (20):5023-30. Epub 2004/04/28. doi:10.1016/j.biomaterials.2004.01.048. PubMed PMID: 15109864.

9. Baveja, J.K., Li, G., Nordon, R.E., Hume, E.B., Kumar, N., Willcox, M.D., et al. (2004). Biological Performance of a Novel Synthetic Furanone-Based Antimicrobial. Biomaterials, 25 (20):5013-21. Epub 2004/04/28. doi:10.1016/j.biomaterials.2004.02.007. PubMed PMID: 15109863.

10. Acharya, V., Prabha, C.R., and Narayanamurthy, C. (2004). Synthesis of Metal Incorporated Low Molecular Weight Polyurethanes from Novel Aromatic Diols, Their Characterization and Bactericidal Properties. Biomaterials, 25 (19):4555-62. Epub 2004/05/04. doi:10.1016/j.biomaterials.2003.11.044. PubMed PMID: 15120500.

11. Baym, M., Stone, L.K., and Kishony, R. (2016). Multidrug Evolutionary Strategies to Reverse Antibiotic Resistance. Science, 351 (6268):aad3292. Epub 2016/01/02. doi:10.1126/science.aad3292. PubMed PMID: 26722002, PubMed Central PMCID: PMCPMC5496981.

12. Kenawy, el R., Worley, S.D., and Broughton, R. (2007). The Chemistry and Applications of Antimicrobial Polymers: A State-of-the-Art Review. Biomacromolecules, 8 (5):1359-84. Epub 2007/04/12. doi:10.1021/bm061150q. PubMed PMID: 17425365.

13. Kim, J., and Van der Bruggen, B. (2010). The Use of Nanoparticles in Polymeric and Ceramic Membrane Structures: Review of Manufacturing Procedures and Performance Improvement for Water Treatment. Environ Pollut, 158 (7):2335-49. Epub 2010/05/01. doi:10.1016/j.envpol.2010.03.024. PubMed PMID: 20430495.

14. Lienkamp, K., Madkour, A.E., Musante, A., Nelson, C.F., Nusslein, K., and Tew, G.N. (2008). Antimicrobial Polymers Prepared by ROMP with Unprecedented Selectivity: A Molecular Construction Kit Approach. J Am Chem Soc, 130 (30):9836-43. Epub 2008/07/03. doi:10.1021/ja801662y. PubMed PMID: 18593128, PubMed Central PMCID: PMCPMC4106262.

15. Lienkamp, K., Madkour, A.E., Kumar, K.N., Nusslein, K., and Tew, G.N. (2009). Antimicrobial Polymers Prepared by Ring-Opening Metathesis Polymerization: Manipulating Antimicrobial Properties by Organic Counterion and Charge Density Variation. Chemistry, 15 (43):11715-22. Epub 2009/10/03. doi:10.1002/chem.200900606. PubMed PMID: 19798715.

16. Lienkamp, K., Kumar, K.N., Som, A., Nusslein, K., and Tew, G.N. (2009). "Doubly Selective" Antimicrobial Polymers: How Do They Differentiate between Bacteria? Chemistry, 15 (43):11710-4. Epub 2009/10/01. doi:10.1002/chem.200802558. PubMed PMID: 19790208.

17. Zasloff, M. (2002). Antimicrobial Peptides in Health and Disease. N Engl J Med, 347 (15):1199-200. Epub 2002/10/11. doi:10.1056/NEJMe020106. PubMed PMID: 12374882.

18. Zasloff, M. (2002). Antimicrobial Peptides of Multicellular Organisms. Nature, 415 (6870):389-95. Epub 2002/01/25. doi:10.1038/415389a. PubMed PMID: 11807545.

19. Timofeeva, L., and Kleshcheva, N. (2011). Antimicrobial Polymers: Mechanism of Action, Factors of Activity, and Applications. Appl Microbiol Biotechnol, 89 (3):475-92. Epub 2010/10/19. doi:10.1007/s00253-010-2920-9. PubMed PMID: 20953604.

20. Lichter, K.J., and Rubner, M.F. (2009). Design of Antibacterial Surfaces and Interfaces: Polyelectrolyte Multilayers as a Multifunctional Platform. Macromolecules, 42:8573-86.

21. Lichter, J.A., and Rubner, M.F. (2009). Polyelectrolyte Multilayers with Intrinsic Antimicrobial Functionality: The Importance of Mobile Polycations. Langmuir, 25 (13):7686-94. Epub 2009/03/26. doi:10.1021/la900349c. PubMed PMID: 19317389.

22. Vasilev, K., Cook, J., and Griesser H.J. (2009). Antibacterial Surfaces for Biomedical Devices. Expert Rev Med Devices, 6 (5):553-67. Epub 2009/09/16. doi:10.1586/erd.09.36. PubMed PMID: 19751126.

23. Gabriel, G.J., Madkour, A.E., Dabkowski, J.M., Nelson, C.F., Nusslein, K., and Tew, G.N. (2008). Synthetic Mimic of Antimicrobial Peptide with Nonmembrane-Disrupting Antibacterial Properties. Biomacromolecules, 9 (11):2980-3. Epub 2008/10/15. doi:10.1021/bm800855t. PubMed PMID: 18850741, PubMed Central PMCID: PMCPMC2646885.

24. Palermo, E.F., and Kuroda, K. (2010). Structural Determinants of Antimicrobial Activity in Polymers Which Mimic Host Defense Peptides. Appl Microbiol Biotechnol, 87 (5):1605-15. Epub 2010/06/22. doi:10.1007/s00253-010-2687-z. PubMed PMID: 20563718.

25. Yelnosky, J., and Ghulam, M.N. (1987). US Patent, 4:701-457.

26. Studt, H.K., and Dodson, S.A. (1986). Can. CA Patent 1. 1986:210-394 A1.

27. Serafin, B., Urbanski, T., and Warhurst, D.C. (1969). Antimalarial Compounds. X. Biguanide and Amidinourea Derivatives of Diphenyl Sulfide, Sulfoxide, and Sulfone. J Med Chem, 12 (2):336-7. Epub 1969/03/01. PubMed PMID: 5783616.

28. Cutler, R.A., and Schalit, S. (1976). US Patent 3. 1976:988-370.

29. Katayama, N., Fukusumi, S., Funabashi, Y., Iwahi, T., and Ono, H. (1993). TAN-1057 A-D, New Antibiotics with Potent Antibacterial Activity against Methicillin-Resistant Staphylococcus Aureus. Taxonomy, Fermentation and Biological activity. J Antibiot (Tokyo), 46 (4):606-13. Epub 1993/04/01. PubMed PMID: 8501003.

30. Strassburg, A., Kracke, F., Wenners, J., Jemeljanova, A., Kuepper, J., Petersen, H., et al. (2015). Nontoxic, Hydrophilic Cationic Polymers-Identified as Class of Antimicrobial Polymers. Macromol Biosci, 15 (12):1710-23. Epub 2015/08/05. doi:10.1002/mabi.201500207. PubMed PMID: 26240988.

31. Gilbert, P., and Moore, L.E. (2005). Cationic Antiseptics: Diversity of Action under a Common Epithet. J Appl Microbiol, 99 (4):703-15. Epub 2005/09/16. doi:10.1111/j.1365-2672.2005.02664.x. PubMed PMID: 16162221.

32. Som, A., and Tew, G.N. (2008). Influence of Lipid Composition on Membrane Activity of Antimicrobial Phenylene Ethylene Oligomers. J Phys Chem B, 112 (11):3495-502. Epub 2008/02/26. doi:10.1021/jp077487j. PubMed PMID: 18293958, PubMed Central PMCID: PMCPMC3774278.

33. Tilley, H., Levitan, P., and Blount, J.F. (1980). The Synthesis of 3, 5-Diamino-1, 2, 4-Oxadiazoles. Helv Chem Acta, 63:841-59.

34. Yuan, R.M. (1997). Total Synthesis of the Anti Methicillin-Resistant Staphylococcus Aureus Peptide Antibiotics TAN-1057A-D. J Am Chem Soc, 119:11777-84.

35. Drake, M., and Lebl, M.A. (1994). Convenient Preparation of Monosubstituted N,N′-di(Boc)-Protected Guanidines. Synthesis, 6:579-82.

36. Al-Ahmad, A., Laird, D., Zou, P., Tomakidi, P., Steinberg, T., and Lienkamp, K. (2013). Nature-Inspired Antimicrobial Polymers—Assessment of Their Potential for Biomedical Applications. PLoS One, 8 (9):e73812. Epub 2013/09/17. doi:10.1371/journal.pone.0073812. PubMed PMID: 24040079, PubMed Central PMCID: PMCPMC3767731.

CHAPTER III

SYNTHESIS OF POLYMERIC ANTIMICROBIALS TO OVERCOME ANTIBIOTIC RESISTANCE AND INCREASE ANTIMICROBIAL EFFICACY

3.1. Abstract

Antimicrobial resistance is an increasingly serious threat to global public health that requires an immediate global action. The bacterial resistance appears to be the result of decreased outer membrane permeability and the development of the efflux mechanism by resistant bacteria, which seems to be the commonest and most challenging. To overcome antibiotic resistance associated with efflux pumping, we have developed polymeric antimicrobials to increase local antimicrobial concentration at the bacterial cell membrane. We synthesized a series of homo and di-block copolymeric antimicrobials using ring-opening metathesis polymerization (ROMP), and we evaluated their antimicrobial efficacy using various methods, including measuring the minimum inhibitory concentration (MIC). Homo polymer was inactive, but the di-block copolymer exhibited some antimicrobial activity against *M. smegmatis* (WT) (MIC = 2 μg/mL) and *M.s/MtTOP* (overexpression strain) (MIC = 1 μg/mL). We have studied the effect of polymer chain lengths and block ratios along with hydrophobicity on the polymer's antimicrobial activity. Chapter 3 will present the synthesis of homo and block copolymer via ROMP and the characterization and effect of block ratio on antimicrobial activity.

3.2. Introduction

Antimicrobial resistance is of immense concern in human health[1]. Antibiotic resistance occurs when an antibiotic loses its capacity to inhibit bacterial growth. The action of antibiotics like Ciprofloxacin (fluoroquinolones) is to inhibit the growth of bacterial gyrase[1, 2]. Bacterial gyrase is an enzyme responsible for DNA replication, repair, and recombination. The bacteria generate resistance to Cipro by development of the

efflux mechanism[2]. In this resistance mechanism, antibiotics are pumped away before reaching the cytoplasmic membrane.

Overcoming fluoroquinolone-type antibiotic resistance against the efflux mechanism can be achieved by increasing the local concentration of drugs at the bacterial cell membrane[3]. Because of the side effects, toxicity, and more important, chances of killing the bacteria, it is not feasible to increase the number of dosages to increase the antimicrobial concentration[4]. To increase local antimicrobial concentration to overcome efflux resistance, we have come up with a polymeric approach in which Cipro-containing monomer is attached with a positively charged hydrophobic monomer. We anticipated that the positively charged hydrophobic units would enhance ionic interaction with the negatively charged lipid bilayer in the bacterial cell membrane and thus increase the local concentration of Cipro. In Chapter 2, we discussed and exhibited the value of polymeric materials as an antimicrobial agent. We also demonstrated how antimicrobial polymers are combatting pathogenic bacteria and showed improved efficacy.

The research goal is to synthesize a polymeric antimicrobial to overcome antibiotic resistance associated with the efflux mechanism as well as to increase the antimicrobial efficacy by increasing the local antimicrobial concentration at the cell membrane without further dosing. We chose to employ Ciprofloxacin, a second-generation fluoroquinolone antibiotic. Fluoroquinolones are a class of antibiotics used against a variety of infections including urinary tract infections (UTIs), gastrointestinal infections, respiratory tract infections (RTIs), and abdominal infections[1].

We synthesized a series of positively charged Cipro-containing antimicrobial homo polymer and Cipro-TPP (triphenylphosphine)-containing hydrophobic antimicrobial di-

block copolymer using ROMP, which is a ruthenium catalyzed-based living polymerization technique where the polymer chain length can be controlled[5, 6]. Charge and hydrophobicity of the synthesized polymer were controlled by varying the TPP unit.

We tested the final polymers with resistant bacteria cell walls and determined their antimicrobial properties, such as the minimum inhibitory concentration (MIC) value. The Cipro-containing homo polymer was inactive against almost all the microbes tested, but di-block copolymers exhibited some antimicrobial activity against *M. smegmatis* (WT) (MIC = 2 μg/mL) and *M.s/MtTOP* (overexpression strain) (MIC = 1 μg/mL). In this Chapter 3, we describe the synthesis of Cipro-containing homo and di-block copolymer using ROMP along with its biological properties. We will also discuss the effect of block ratio and hydrophobicity on antimicrobial activity.

3.3. Result and Discussion

The antimicrobial must penetrate the bacterial cell wall in order to suppress the bacterial cell growth[7]. It can enter the bacterial cell wall via a hydrophilic pathway through the water-filled porin channels and by a hydrophobic pathway through the lipid bi-layer [2-4, 8]. Carefully studying bacterial cell walls and cytoplasmic membranes, we have designed and synthesized a rightly balanced hydrophobic-hydrophilic polymer.

Monomer synthesis: To use the ROMP method, we had to combine the Cipro with norbornene. Norbornene and its derivatives are the most frequently used because of their high ROMP activity and easy incorporation of substituents on the ring. The molecule contains a cyclohexene ring with a double bond. The double bond carries the ring strain as well as the reactivity of the norbornene. Scheme 3.1 shows the detailed reaction procedure for the synthesis of the antibiotic-containing monomer. Commercially available

oxonorbornene reacts with 2-(2-aminoethoxy)ethan-1-ol to prepare an alcohol form of oxonorbornene. Hydroxyl derivatives of oxonorbornene are essential to make an ester derivative with a carboxylic group presence in the Ciprofloxacin. The Boc-protected Cipro directly reacts with the norbornene moiety via the Mitsunobu reaction to form the expected drug monomer. To make more hydrophobic polymer, we prepared triphenylphosphine (TPP) containing ROMP monomer. Three aromatic rings in TPP contribute hydrophobicity, and TPP possesses some antimicrobial activity. Similar synthetic procedure has been followed to achieve the final monomer.

Polymer synthesis: Ring opening metathesis polymerization (ROMP) is very sensitive and must be done in an inert environment such as a nitrogen-charged glove box. After following the general procedure, we repeatedly failed to polymerize the monomer **CIP-1** using ROMP. Several well-known procedures[4, 6] from different ROMP reaction pathways were followed with modified conditions depending on structure. Although the reaction was carefully carried out inside the glove box, at the end the polymer was not obtained. Later, we changed reaction conditions to induce the polymer's formation. Following the literature, different solvent conditions with catalyst loading were tried (Table 3.1); however, nothing worked to form the living ROMP polymer. The following table shows the different reaction conditions tried to polymerize the antibiotic monomer. We chose the percentage of solvent and catalyst from the literature, most of which suggested Grubbs' third-generation catalyst for its reactivity and stability[5, 6, 9]. However, repeating the process using the Grubbs' catalyst yielded the same result. Later, we believed that the amine could have interacted negatively with the Grubbs' catalyst's ruthenium center. However, other literature showed that Boc-protected amine does not interact with the

Grubbs' catalyst's center. Monomer **CIP-1** structure is also Boc protected and NMR confirmed.

At this point, we were not able to find any rational data to explain the failure of the ROMP process. Later, we changed the structure of the antibiotic monomer to make it work. At first we thought the hydrophilic ethoxy alkyl chain might interact with Grubbs' catalyst [6]. Then we made a new antibiotic monomer by changing the hydrophilic ethoxy alkyl chain to a more hydrophobic alkyl chain (**CIP-2**). Schemes 3.2 and 3.3 show the modified antibiotic monomer structure, which was confirmed by ^{1}H-NMR, ^{13}C-NMR, and IR. Unfortunately, repeating the ROMP polymerization process using Grubbs' second- and third-generation catalyst did not result in polymerization.

Unfortunately, after repeating every condition under which ROMP was conducted with the previous antibiotic monomer, this monomer also failed to polymerize.

Later, we changed the alkyl length of antibiotic monomer to reduce any interaction between the monomer chain and the ruthenium center of Grubbs' catalyst. Because this was the only option we could change, we decided to make a short-chain antibiotic monomer (**CIP-3**) to avoid any negative effect by the alkyl chain. The ROMP had a result similar to that from earlier antibiotic monomers. We tried all the possible conditions including changing solvent and catalyst ratio. We did the reaction in a Schlenk flask at 40^{0}C to 50^{0}C to see whether temperature could have any influence on polymerization. However, the process failed under all conditions.

With the failure of all previous trials, we changed the polymerization technique. At first, we tried to polymerize the precursor of the **CIP-1** monomer via ROMP and then add Cipro by the post-polymerization method. The first attempt to polymerize the bromine

Table 3.1. List of different solvent and catalyst condition tried for ROMP

No.	% catalyst[a]	% DCM[b]	% Methanol	% THF[c]	GPC[d]
1.	2	100	0	0	1402
2.	1.5	100	0	0	1307
3.	1	100	0	0	1536
4.	1-2	90	10	0	1465
5.	2.5	80	20	0	1203
6.	1.5-2.5	50	0	50	1005
7.	2	50	10	40	1103

[a] Grubb's third-generation catalyst, [b] dichloromethane, [c] tetrahydrofuran, [d] gel permeation chromatography

containing ROMP failed as a result of solubility issue. Finally, we were successful with the polymerization of tosyl containing ROMP was successful and attached Cipro later. Later, we synthesized block copolymers following the same technique and using triphenylphosphine (**TPP**) containing ROMP monomer.

Antimicrobial assay: Antimicrobial study on synthesized Cipro containing homo and di block copolymers has been carried out by Dr. Arasu Annamalai in Dr. Tse Dinh lab as a collaborator for this project and used on several resistant bacterial cell membranes. Table 3.2 shows the minimum inhibitory concentration result. On the basis of the data, Cipro homo polymer was inactive with almost all microbes tested, but **Cipro**-**TPP** di-block copolymers (1:1.3 ratio) exhibited some antimicrobial activities. The inactivity of the Cipro homo polymer can be explained by saying that the positive charge is not enough to increase the local concentration of Cipro. Thus, the **CIP** homo polymer failed to reach the

cytoplasmic membrane and lost its activity. Hydrophobicity is another essential parameter to enhance the bacterial membrane penetration. Thus, the more hydrophobic polymer **CIP-TPP** block copolymer possesses some antimicrobial properties (Table 3.2). The maximum antimicrobial activity recorded on *M.s/MtTOP* (overexpression strain) (1 μg/mL) by the di-block copolymer (**CIP-TPP**). To support this statement, we increased the TPP ratio and synthesized more hydrophobic **CIP-TPP** di-bloc copolymer (1:2 ratio). Unfortunately, this combination did not show any activity against the microbes tested. On the basis of this result, we concluded that there must be an optimum ratio between hydrophobicity and hydrophilicity for better antimicrobial activity. Furthermore, slow kinetics could be another potential issue for inactivity or poor antimicrobial properties of synthesized polymers.

Table 3.2. Minimum inhibitory concentration (MIC) assay

MIC	Compounds (μg/mL)[a]			
Strains	Cipro (control)	CIP homo-polymer	CIP:TPP = 1: 1.3[b]	CIP:TPP = 1:2[b]
M. smegmatis (WT)	0.25	>4.7	2	No activity
M.s/MtTOP(overexpression)	0.25	>2.3	1	
M.s/pknol	0.25	>2.3	1	
E. coli (WT)	0.03	>14	24.75	

[a] inhibitory activity towards bacterial growth of *M. smegmatis* (WT), *M.s/MtTOP* (overexpression), *M.s/pknol* (control vector) and *E. coli* (WT) (MIC_{90} = minimum inhibitory concentration preventing 90% bacterial growth), [b] bl-ock co-polymer

3.4. Conclusion

We have demonstrated the synthesis of Cipro-containing homo and di-block copolymers using ROMP. We also discussed polymerization condition and characterization. Finally, we did antimicrobial assay determining MIC. The MIC values

were showed poor or no activity against the resistant bacteria tested. By analyzing the result, we concluded that a proper balance between hydrophobicity-hydrophilicity along with positive charge might be missing from the polymers we prepared. Another conclusion can be drawn from the inactivity of polymers because of poor pharmacokinetics or slow release to the bacterial membrane. Further study needed to address those problems and to increase the antimicrobial activity of the synthesized polymers.

3.5. Outlook

The goal of this research was to increase local concentration of antimicrobial agents at the bacterial cell wall. We incorporated Cipro and Cipro with triphenylphosphine via ROMP. The Chapter 3 mainly discusses our synthetic approach along with characterization of the monomer, homo, and di block copolymers. Further study was needed to complete this project, including a deep understanding of the bacterial cell wall, cytoplasmic membrane, and outer membrane. We concluded that hydrolysis kinetics might provide the reason behind the inactivity of the polymers by analyzing the release process inside the bacterial cell wall.

3.6. Experimental Section

3.6.1. Monomer synthesis

Scheme 3.1. Synthesis of Cipro containing ROMP monomer (**CIP-1**)

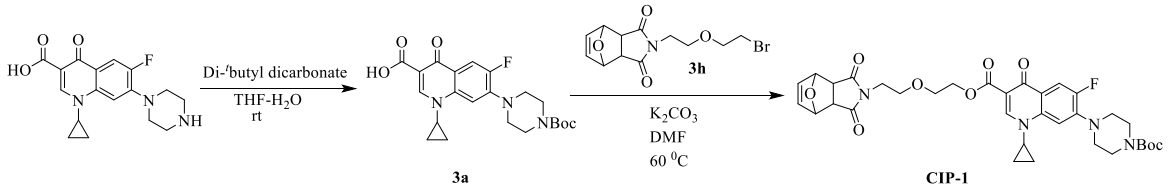

Compound **3a** was synthesized according to the literature[10]. More precisely, in a reaction flask, Ciprofloxacin (1.00 g, 3.02 mmol) was dissolved in water. In another flask, di-butyl

dicarbonate (Boc) (0.70 g, 3.17 mmol) was dissolved in tetrahydrofuran (THF) and added to the reaction flask drop by drop using an addition funnel. The reaction mixture was stirred at r.t. overnight. The solvent was then removed *in vacuo*, and Boc-protected Cipro was dissolved in DCM. The mixture of product was washed with water (3x) and brine (1x). The final white powder product was dried in a high vacuum (0.85 g, 90% yield).

CIP-1: Compound **3a** (2.00 g, 4.63 mmol) and **3h** (2.50 g, 8.11 mmol) and K_2CO_3 (1.90 g, 13.9 mmol) were added into a round-bottom flask (RBF). The solvent DMF was added to the RBF, and the reaction mixture was stirred at 60^0C overnight. The next day, the reaction mixture was quenched in water, and precipitate was collected through vacuum filtration. The final product (precipitate) was dissolved in DCM and washed with water (3x) and brine (1x). After column purification with a 30% EA-Hexane mixture, the final white amorphous product was dried over a high vacuum (2.31 g and 75 % yield).

^{1}H NMR (400 MHz, $CDCl_3$, δ): 8.54 (s, 1H), 8.05 (d, *J* = 13.1 Hz. 1H), 7.29 (s, 1H), 6.49 (s, 2H), 5.25 (s, 2H), 4.41 (t, *J* = 5.1 Hz, 2H), 3.78 (t, *J* = 4.8 Hz, 2H), 3.71 (s, 4H), 3.67 (t, *J* = 5.1 Hz, 4H), 3.42 (m, 1H), 3.22 (t, *J* = 4.8 Hz, 4H), 2.90 (s, 2H), 1.51 (s, 9H), 1.33 (d, J = 6.8 Hz, 2H), 1.17 (m, 2H). ^{13}C NMR (400 MHz, δ): 176.4, 173.1, 165.3, 154.7, 152.2, 148.4, 144.6, 144.5, 138.1, 136.6, 123.4, 123.3, 113.6, 113.4, 110.2, 105.1, 80.9, 80.3, 68.8, 67.2, 63.7, 47.3, 38.3, 34.6, 28.5. FT-IR (neat): 3690.8, 3501.3, 2976.2, 2920.7, 2861.6, 1692.0, 1619.6, 1478.8, 1393.5, 1244.2, 1163.1, 1124.7, 1022.3 cm^{-1}.

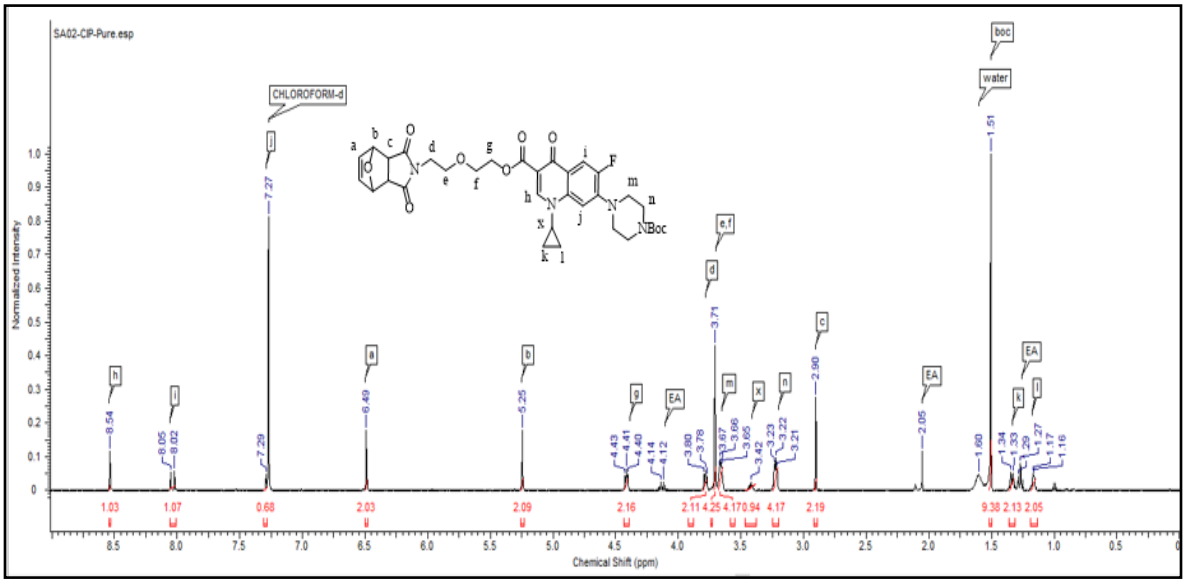

Figure 3.1. ^{1}H NMR of **CIP-1**

Scheme 3.2. Synthesis of Cipro containing hydrophobic ROMP monomer **(CIP-2)**

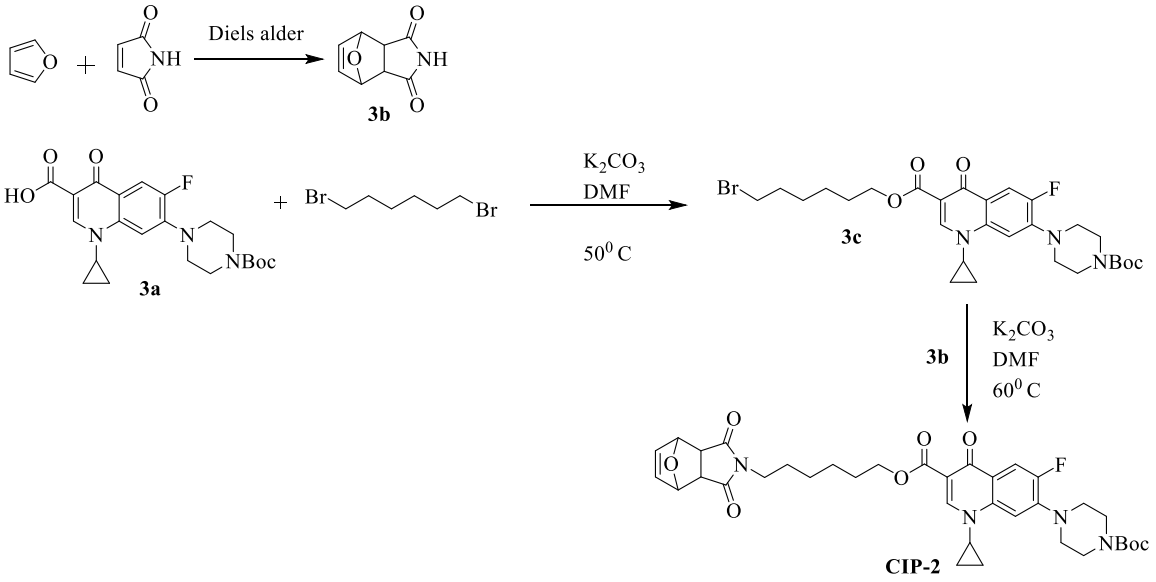

Compound **3b** was synthesized according to the literature[11]. Basically, furan (2.00 g, 29.4 mmol) and 1H-pyrrole-2,5-dione (2.71 g, 27.9 mmol) were dissolved in ethyl acetate and stirred at 90^{0}C overnight. The resulting precipitates were collected by vacuum filtration

and washed with water (3x). The final product was white powder and was dried over high vacuum (4.10 g and 85% yield).

Compound **3c** was synthesized according to the literature procedure[12]. More precisely, compound **3a** (2.00 g, 4.63 mmol), 1,6-dibromohexane (1.13 g, 4.63 mmol), and K_2CO_3 (3.2 g, 23.1 mmol) were dissolved in DMF and stirred at 50^0C overnight. The final white powder product was collected after extraction (DCM, water, and brine) and column purification (30% EA in hexane) (1.54 g and 56% yield).

CIP-2: Monomer **CIP-2** was prepared following the same procedure as **CIP-1**. Basically, compound **3c** (1.20 g, 2.01 mmol), compound **3b** (0.36 g, 2.22 mmol), and K_2CO_3 (1.38 g, 10.0 mmol) were dissolved in DMF and stirred at 60^0C overnight. The final white powder product was collected after extraction and column purification (0.80 g and 53% yield).

^{1}H NMR (400 MHz, $CDCl_3$, δ): 8.52 (s, 1H), 8.05 (d, *J* = 13.1 Hz. 1H), 7.29 (s, 1H), 6.51 (s, 2H), 5.26 (s, 2H), 4.29 (t, *J* = 6.5 Hz, 2H), 3.65 (t, *J* = 4.5 Hz, 2H), 3.49-3.44 (m, 3H), 3.22 (t, *J* = 5.0 Hz, 4H), 2.83 (s, 2H), 1.78-1.73 (m, 4H), 1.59 (m, 2H), 1.50 (s, 9H), 1.48-1.44 (m, 2H), 1.33 (m, 4H), 1.17 (m, 2H). ^{13}C NMR (400 MHz, δ): 176.4, 165.9, 154.7, 148.2, 136.6, 81.0, 80.3, 64.9, 47.5, 38.9, 34.6, 28.7, 28.5, 27.6, 26.4, 25.6. FT-IR (neat): 3615.1, 3516.2, 2973.3, 2934.4, 2863.6, 2827.3, 1699.1, 1682.7, 1610.6, 1503.5, 1474.5, 1426.2, 1400.5, 1333.8, 1247.9, 1211.5, 1167.9, 1127.4, 1080.6 cm^{-1}.

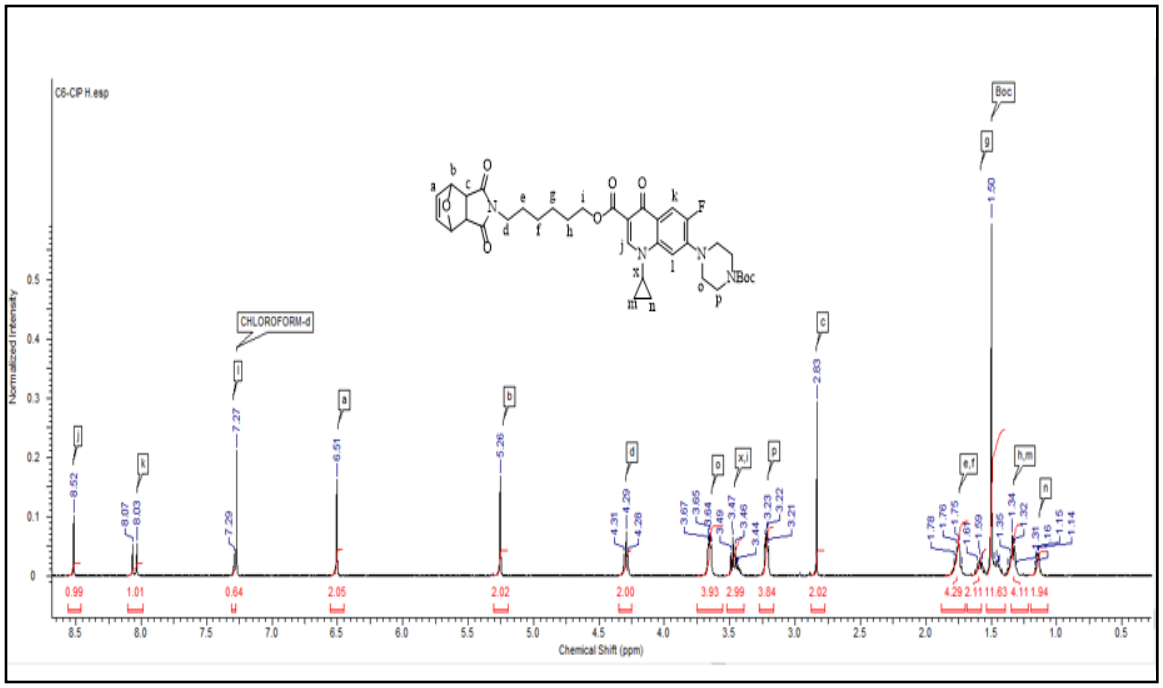

Figure 3.2. ^{1}H NMR of **CIP-2.**

Compound **3d** was synthesized following the same procedure as compound **3c**. Basically, compound **3a** (2.00 g, 4.63 mmol), 1,2-dibromoethane (0.86 g, 4.63 mmol), and K_2CO_3 (3.20 g, 23.1 mmol) were dissolved in DMF and stirred at 50^0C overnight. The final white powder product was collected after extraction and column purification (1.20 g and 50% yield).

CIP-3: Monomer **CIP-3** was prepared following the same procedure as **CIP-1**. Basically, compound **3d** (2.00 g, 3.71 mmol), compound **3b** (0.67 g, 4.10 mmol), and K_2CO_3 (2.60 g, 18.5 mmol) were dissolved in DMF and stirred at 60^0C overnight. The final white powder product was collected after extraction and column purification (1.20 g and 56% yield).

Scheme 3.3. Synthesis of Cipro containing short chain ROMP monomer **(CIP-3)**

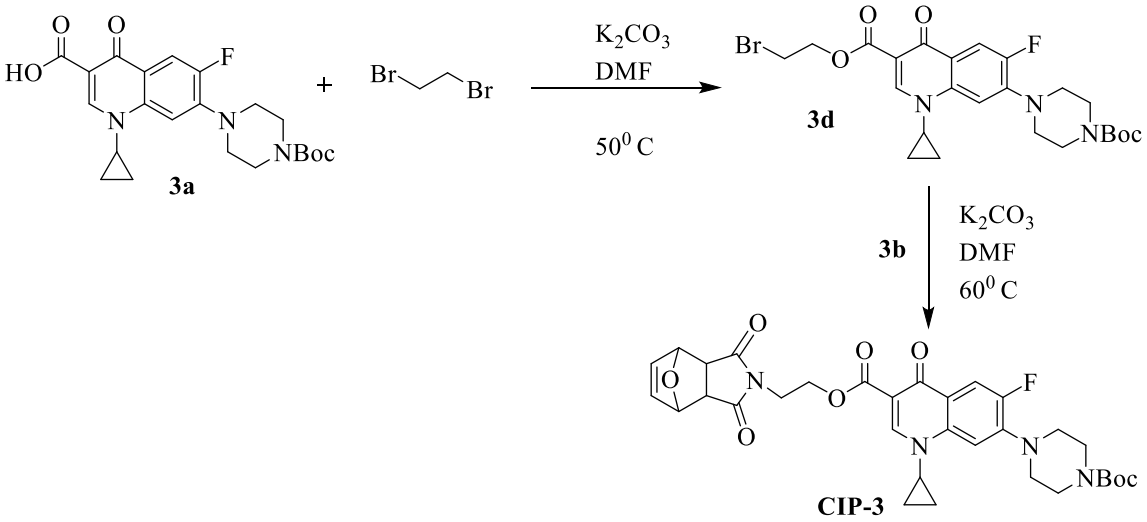

^{1}H NMR (400 MHz, $CDCl_3$, δ): 8.49 (s, 1H), 7.98 (d, *J* = 7.9 Hz. 1H), 7.28 (s, 1H), 6.51 (s, 2H), 5.26 (s, 2H), 4.43 (t, *J* = 5.0 Hz, 2H), 3.87 (t, *J* = 5.3 Hz, 2H), 3.65, 3.65 (t, *J* = 4.5 Hz, 4H), 3.43 (m, 1H), 2.95 (s, 2H), 1.50 (s, 9H), 1.33 (d, *J* = 6.6 Hz, 2H), 1.19 (m, 2H). ^{13}C NMR (400 MHz, δ): 176.2, 164.5, 154.6, 148.4, 144.4, 138.0, 136.5, 113.5, 105.1, 80.8, 80.2, 80.9, 47.6, 37.8, 34.6, 28.4. FT-IR (neat): 3090.8, 3001.3, 2890.6, 2851.3, 1768.7, 1731.2, 1698.1, 1621.9, 1501.5, 1430.5, 1399.5, 1341.7, 1240.7, 1155.8. cm^{-1}.

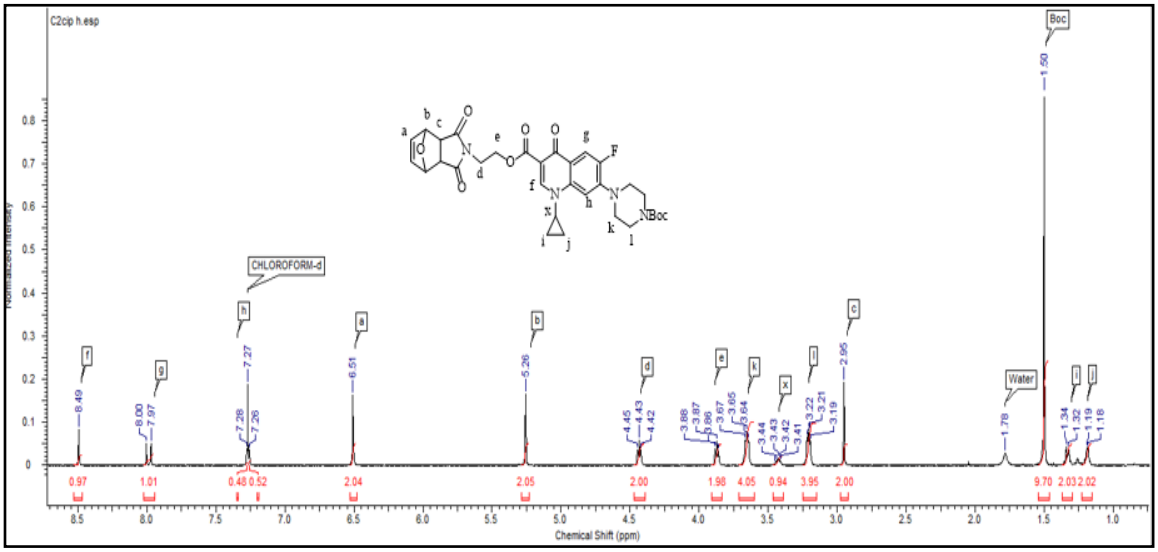

Figure 3.3. ^{1}H NMR of **CIP-3**

Scheme 3.4. Synthesis of tosyl containing ROMP monomer **(3e)**

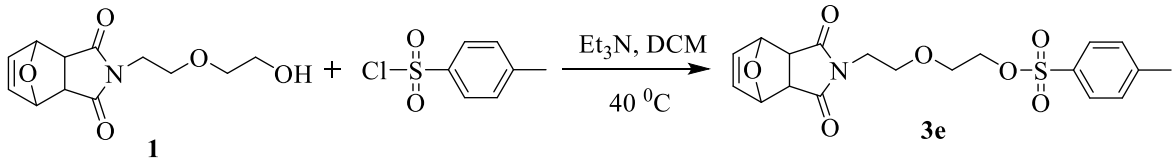

Compound **3e** was synthesized according to the literature[13]. Basically, in an RBF, compound **1** (5.20 g, 20.5 mmol) (Scheme 3.5) and triethylamine (4.18 g, 41.0 mmol) were dissolved in DCM and made a homogenous solution by stirring at r.t. Later, the reaction mixture was cooled to 0^0C using an ice bath. Tosylchloride (4.30 g, 22.5 mmol) was dissolved in DCM and added to the reaction mixture using an addition funnel over an hour. The RBF was left overnight stirred at 40^0C. The product was extracted in ethyl acetate and washed with water (3x) and brine (1x). The final white crystalline product was purified by recrystallization in a THF and diethyl ether mixture (7.00 g, 84% yield).

^{1}H NMR (400 MHz, $CDCl_3$, 25 ^{0}C): δ_h = 7.78 (d, J = 4.06, 2H), 7.30 (d, J = 4.20, 2H), 6.50 (s, 2H), 5.28 (s, 2H), 4.23 (t, *J* = 4.05, 2H), 3.64-3.55 (m, 6H), 2.90 (s, 2H), 2.50 (s, 3H).

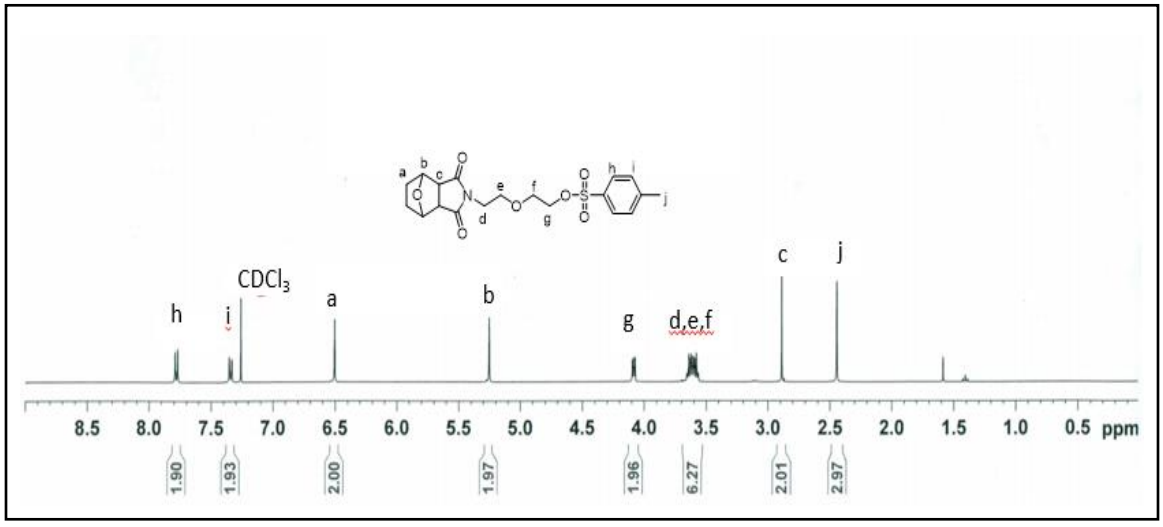

Figure 3.4. ^{1}H NMR of monomer **3e**

Scheme 3.5. Synthetic route to TPP containing monomer **3g**

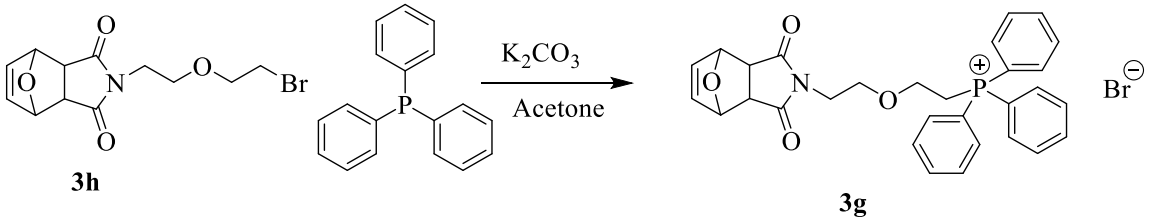

Compound **3g** was synthesized according to the literature[10]. A pressure tube was charged with 2-(2-(2-bromoethoxy)ethyl)-3a,4,7,7a-tetrahydro-1H-4,7-epoxyisoindole-1,3 (2H)-dione (1.33 g, 0.004 mol) and triphenylphosphine (4.41 g, 0.016 mol). A minimum amount of acetone as a solvent was added to the pressure tube to cover both reactants. The reaction vessel was then closed and made airtight using Teflon paper. The reaction vessel was heated at 50^0C for 24 hours. The reaction progress was monitored and confirmed by thin layer chromatography (TLC). The colorless solution was cooled to room temperature, and the viscous reaction mixture was dissolved in a minimum amount of DCM to make a homogenous solution. Upon precipitation in ethyl acetate (EA), unreacted triphenylphosphine was removed by vacuum filtration. The precipitate was washed with EA and dried over high vacuum overnight. An amorphous crystalline final product (0.50g and 20% yield) was confirmed by ^{1}H NMR.

^{1}H NMR (400 MHz, $CDCl_3$, 25 ^{0}C): δ_h = 7.78-7.68 (m, 15H), 6.5 (s, 2H), 5.21 (s, 2H), 4.2 (p, *J* = 5.56 Hz, 2H), 3.92-3.86 (dt, *J* = 5.8 Hz, *J* = 5.5 Hz, 2H), 3.35 (t, *J* = 5.8 Hz, 2H), 3.25 (t, *J* = 5.5 Hz, 2H), 2.89 (s, 2H). ^{13}C NMR (400 MHz, δ): 176.0, 136.5, 134.8, 134.7, 134.0, 133.9, 130.2, 130.1, 119.3, 118.4, 80.9, 67.2, 64.2, 64.1, 47.5, 38.0. FT-IR (neat):

3605.6, 3036.9, 2956.2, 2876.8, 2854.4, 2786.1, 1769.5, 1730.1, 1694.5, 1481.7, 1436.2, 1402.7, 1336.4, 1126.3, 1110.7, 1021.9.

Scheme 3.6. Synthetic route toward precursor compound **3h**

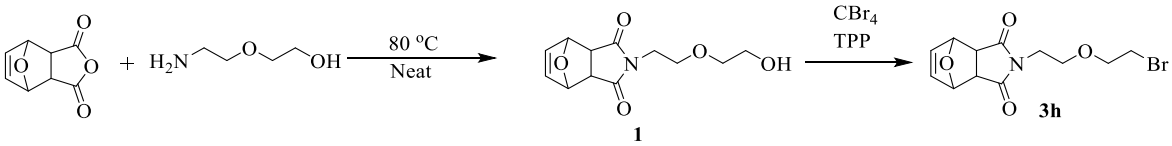

Compound **1** was synthesized according to the literature[10]. An RBF was charged with exo-3,6-epoxy-1,2,3,6-tetrahydrophthalic anhydride (5.00 g, 30.0 mmol) and dissolved in 50.0 mL methanol. The reaction mixture was cooled to 0^0C using ice bath with stirring. 2-(2-aminoethoxy)ethanol (7.50 g, 71.0 mmol) was dissolved in methanol and added into the RBF drop by drop using an additional funnel. The RBF was stirred at 60^0C overnight. The reaction progress was confirmed by TLC, and methanol was removed by rotary evaporator. The colorless, oily liquid was dissolved in ethyl acetate and washed with water (3x) and brine (1x). Ethyl acetate was evaporated, and the liquid product was dried in a high vacuum overnight (5.69 g and 75% yield).

^{1}H NMR (400 MHz, $CDCl_3$, 25 ^{0}C): δ_h = 6.52 (s, 2H), 5.28 (s, 2H), 3.67 (t, *J* = 4.05, 2H), 3.64-3.60 (dt, *J* = 5.05, 4H), 3.59 (t, *J* = 4.07, 2H), 2.88 (s, 2H), 2.50 (br s, 1H)

Compound **3h** was synthesized according to the literature[10]. An RBF was filled with 2-(2-(2-hydroxyethoxy)ethyl)-3a,4,7,7a-tetrahydro-1H-4,7-epoxyisoindole-1,3(2H)-dione (8.00 g, 31.6 mmol) and triphenylphosphine (9.12 g, 34.7 mmol) and dissolved in DCM. The RBF was stirred at r.t. to make a homogeneous solution. In another flask, carbon

tetrabromide (11.5 g, 34.7 mmol) was dissolved in DCM and added to the RBF drop by drop using an additional funnel. The overall reaction mixture was stirred at r.t. for 1 hour, and reaction progress was monitored by TLC. The pure product was obtained by column chromatography (Hx/EA: 8.5/1.5) without further purification. The colorless, viscous product was confirmed by ^{1}H NMR (5.50 g and 55% yield.

^{1}H NMR (400 MHz, $CDCl_3$, 25 ^{0}C): δ_h = 6.44 (s, 2H), 5.18 (s, 2H), 4.02 (t, *J* = 4.1, 2H), 3.67-3.58 (dt, *J* = 5.06, 4H), 3.33 (t, *J* = 4.2, 2H), 2.80 (s, 2H).

3.6.2. Synthesis of Cipro-containing antimicrobial polymer via ROMP

*Polymer **3f,*** tosyl-containing intermediate polymer (**3f**) was synthesized according to the literature[13]. Basically, monomer **3e** (50.0 mg, 0.21 mmol) was charged into a glass vial and put into a nitrogen-charged glove box. The monomer was dissolved in 1.00 mL DCM and stirred to make a clear solution. The DCM was prepared by three freeze-thaw cycles before the reaction occurred. Grubb's third-generation catalyst (1.80 mg, 0.0021 mmol) (1 mmol%) was prepared by dissolving in DCM. The freshly dissolved Grubb's third-generation catalyst was added to the monomer containing a vial in one pot and stirred at r.t. for 1 hour.

Scheme 3.7. Synthesis of Cipro containing homo polymer **(CIP poly)**

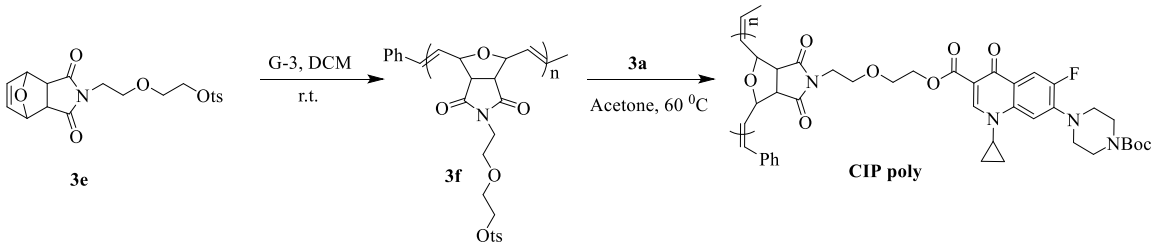

After 1 hour, the reaction mixture was quenched by ethyl vinyl ether. The product was obtained by reprecipitation in ethyl acetate (2x) and diethyl ether (1x) and was dried over a high vacuum. A white fiber-like product was confirmed by ^{1}H NMR (30.1 mg and yield 65%). ^{1}H NMR (400 MHz), $CDCl_3$, δ: 7.82-7.76 (m, 2H), 7.42-7.30 (m, 2H), 6.03 (s, 1H), 5.75 (s, 1H), 5.00 (br s, 1H), 4.42 (br s, 1H), 4.13 (s, 2H), 3.62-3.55 (m, 3H), 3.48-3.35 (m, 2H), 2.5 (s, 3H).

CIP poly: The final Cipro-containing ROMP polymer was synthesized using the post-polymerization technique. The synthetic procedure was the same as for the synthesis of **CIP-1** monomer (Scheme 3.1). More precisely, in a 50 mL RBF, polymer **3f** (55.6 mg, 0.15 mmol), compound **3a** (83.5 mg, 0.19 mmol), and K_2CO_3 (107 mg, 0.77 mmol) were dissolved in acetone and stirred at 60^0C overnight. The reaction mixture was filtered through a glass wool pipette to remove K_2CO_3, and the solvent was dried off *in vacuo*. The resulting polymer was dissolved in DCM and purified by reprecipitating in diethyl ether (3x). The white fiber-like gel final product was dried in a high vacuum (107 mg, 72% yield).

^{1}H NMR (400 MHz), $CDCl_3$, δ: 8.34 (s, 1H), 7.05 (s, 1H), 7.10 (s, 1H), 6.00 (s, 1H), 5.71 (s, 1H), 4.98 (s, 1H), 4.43-4.33 (m, 3H), 3.76-3.33 (m, 10H), 3.43-3.36 (m, 3H), 3.18 (s, 4H), 1.48 (s, 9H), 1.27 (s, 2H), 1.16 (s, 2H). FT-IR (neat): 3525.1, 3432.2, 3020.2, 2937.6, 1720.1, 1698.3, 1403.5, 1364.2, 1356.4, 1236.9, 1182.5 cm^{-1}.

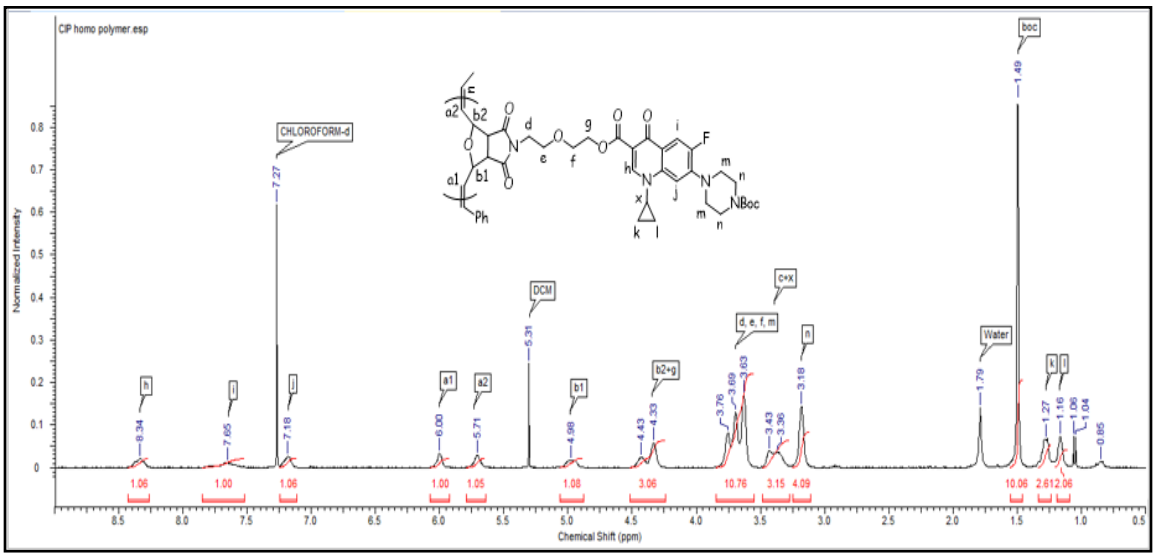

Figure 3.5. ^{1}H NMR of **CIP** homo polymer

Scheme 3.8. Synthesis of di block copolymer (**CIP-TPP block co-poly**)

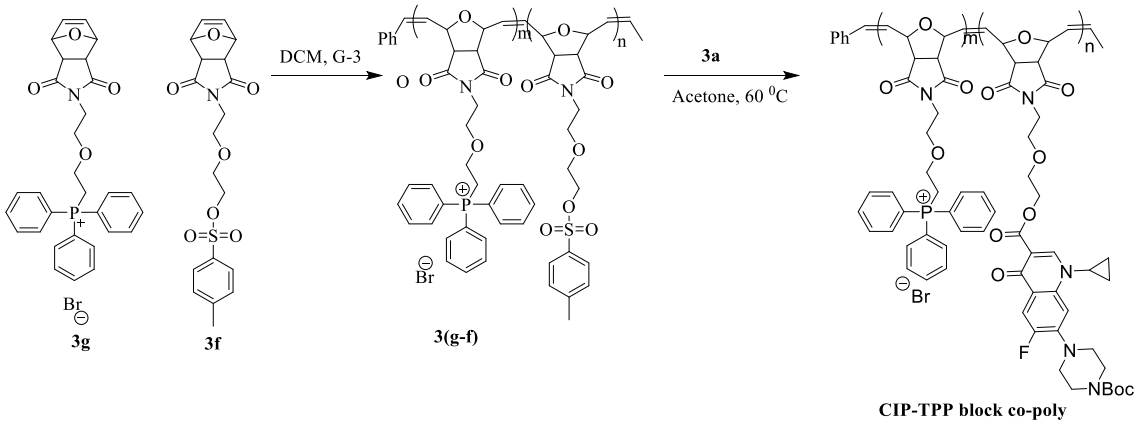

CIP-TPP block copolymer: The block copolymer was synthesized following the same procedure as CIP poly synthesis (Scheme 3.7). At first, monomer **3g** was polymerized using the ROMP procedure, and later monomer **3f** was added to the reaction mixture to make a di-block copolymer of **3(g-f)**. The post-polymerization of intermediate polymer, **3(g-f)** to **CIP-TPP** block copolymer was achieved following the same procedure as

discussed in Scheme 3.7. More precisely, compound **3g** (20.0 mg, 0.03 mmol), compound **3f** (12.2 mg, 0.03 mmol), and Grubb's third-generation catalyst (0.02 mg, 1 mole%) produced a white fiber-like product (22.0 mg, 68% yield).

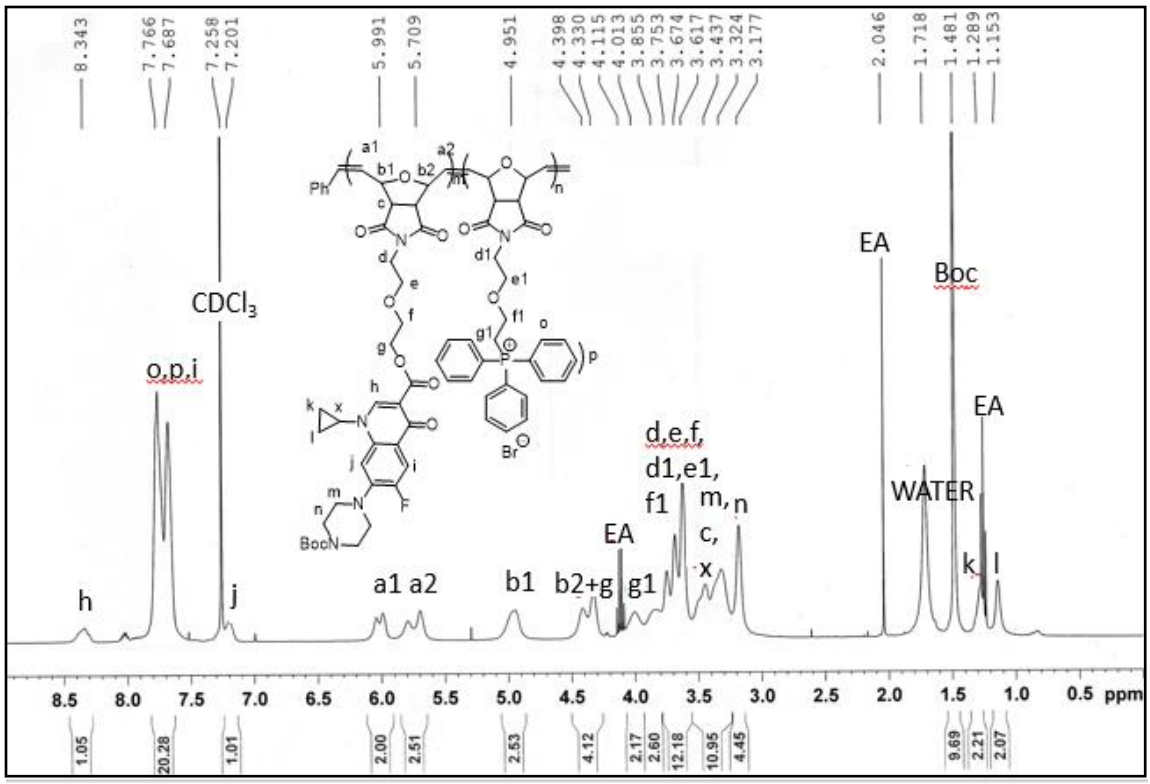

Figure 3.6. ^{1}H NMR of **CIP-TPP** block copolymer

The post-polymerization was carried out by addition of compound **3a** (51.6 mg, 0.12 mmol), intermediate di-block copolymer **3(g-f)** (107 mg, 0.10 mmol), and K_2CO_3 (66.0 mg, 0.48 mmol) in the presence of acetone as a solvent. The white fiber-like final product was purified by reprecipitating in diethyl ether and ethyl acetate, respectively. The final product was dried in a high vacuum (76.7 mg and 68% yield).

1H NMR (400 MHz), CDCl3, δ: 8.34 (s, 1H), 7.76 9-7.68 (br m, 20H), 7.20 (s, 1H), 5.99 (br s, 2H), 5.70 (m, 2H), 4.95 (br s, 2H), 4.40-4.33 (m, 4H), 4.11 (br s, 2H), 4.10-3.61 (m,

16H), 3.43-3.32 (m, 10H), 3.17 (s, 4H), 1.48 (s, 9H), 1.29 (s, 2H), 1.15 (s, 2H). FT-IR (neat): 3682.7, 3601.0, 3499.3, 2936.2, 2912.7, 2866.3, 2831.4, 2756.1, 1780.4, 1742.5, 1594.3, 1592.4, 1468.3, 1382.5, 1253.3, 1211.4, 1136.3, 1122.8, 1056.3 cm^{-1}.

3.6.3. Polymer characterization and block ratio calculation

As mentioned earlier, direct polymerization of **CIP-1** failed, and Cipro was attached after the post-polymerization reaction. The structure of the final polymer was determined by thorough analysis of ^{1}H-NMR. A comparative NMR is presented in Figure

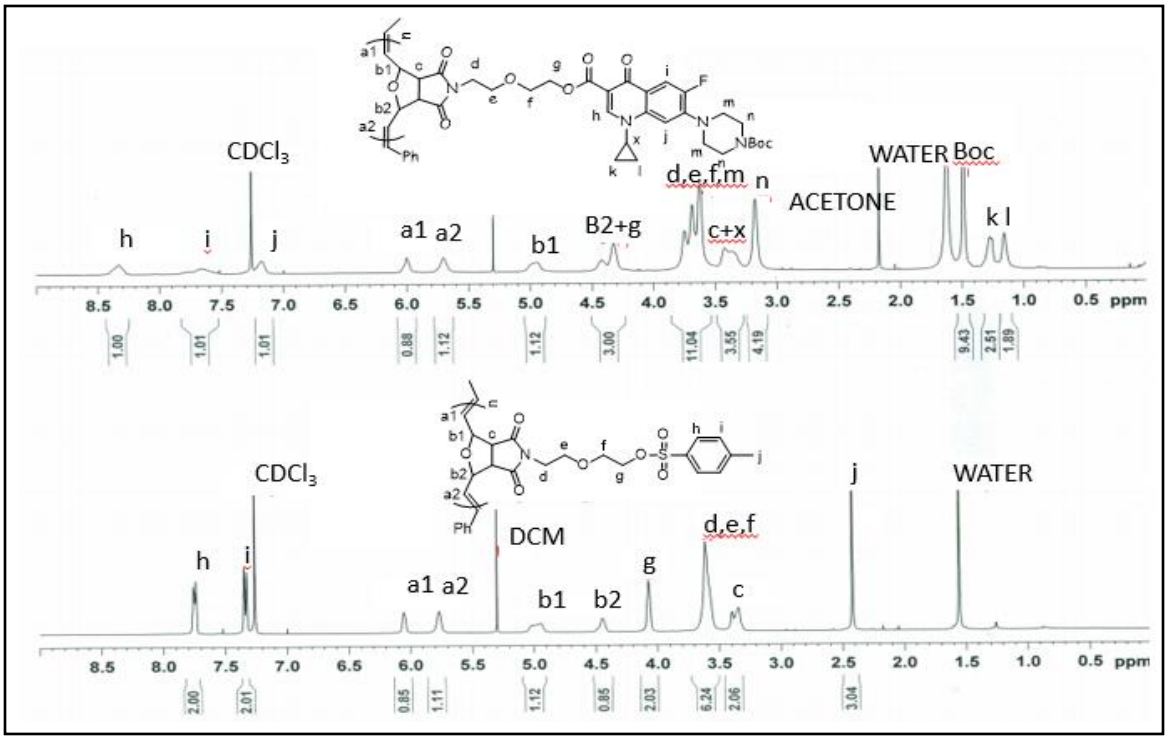

Figure 3.7. ^{1}H NMR comparison of **Tosyl** and **CI**P homo polymer.

3.7 for representation. The NMR showed the disappearance of methyl peaks from polymer **3f** (peak j) at 2.5 ppm and the appearance of characteristic peaks from Boc-protected Cipro (k, l). Another confirmation of Cipro attachment after the post-polymerization reaction can be considered as the disappearance of tosyl-aromatic peaks from compound **3f** at 7.7~7.27

ppm and the appearance of Cipro aromatic peaks at 8.4 ppm (h) and 7.6 ppm (i). The block ratio between two monomers (Cipro and TPP) was calculated using final ^{1}H NMR spectra (Figure 3.7). The Boc group was considered as 9 protons and triphenylphosphine as 15 protons. The ratio between these two protons was reported as the block ratio of CIP-TPP di-block copolymer.

3.6.4 Boc deprotection of antimicrobial polymers

Scheme 3.9. Boc deprotection of Cipro homo polymer (**CIP poly**)

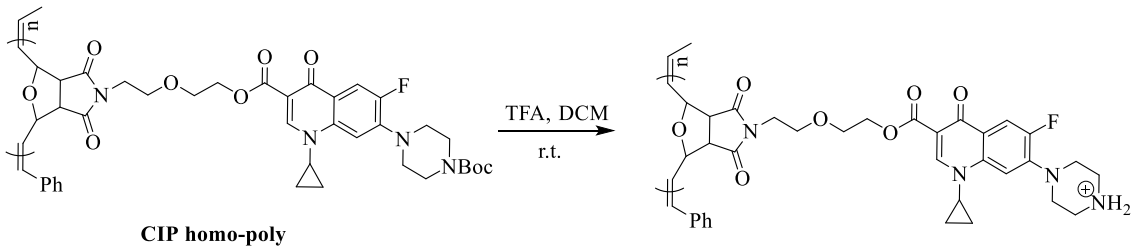

CIP homo-poly

The Boc deprotection of synthesized polymers was carried out by following the literature. Basically, Boc-protected polymer and trifluoroacetic acid (TFA) (1:5 equivalent by volume) were dissolved in DCM and stirred at r.t. overnight. The solvent was distilled off in *vacuo*, and the resultant polymer was dissolved in DMF. Upon being reprecipitated in diethyl ether (2x) and ethyl acetate (1x), a white fiber-like deprotected final polymer was dried in a high vacuum.

Boc deprotection of CIP homo polymer: following the general procedure discussed above, the final deprotected polymer was a white fiber (72% yield).

^{1}H NMR (400 MHz), DMSO-d_6, δ: 9.20 (br s, 2H), 8.31 (s, 1H), 7.56-7.35 (m, 2H), 5.85-5.66 (m, 2H), 4.83 (br s, 1H), 4.21 (br s, 3H), 3.66-3.33 (m, 10H), 1.20 (s, 2H), 1.08 (s, 2H). FT-IR (neat): 3613.2, 3540.4, 3033.2, 2954.8, 1740.3, 1654.9, 1432.2,

1368.4, 1254.7, 1136.1 cm^{-1}.

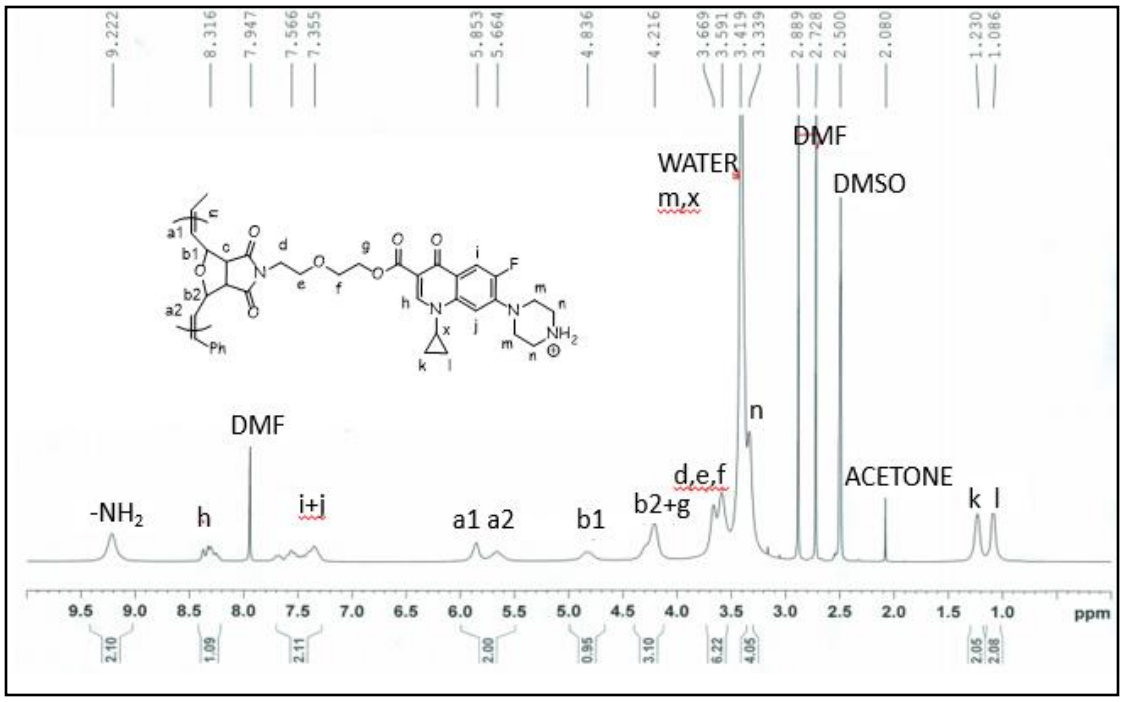

Figure 3.8. ^{1}H NMR of Boc deprotected **CIP homo** polymer.

Boc deprotection of CIP-TPP di-block copolymer: following the general procedure discussed above, the final deprotected polymer was a white fiber (68% yield). ^{1}H NMR (400 MHz), DMSO-d_6, δ: 9.4 br s, 1H), 8.34 (m, 1H), 7.93-7.36 (m, 10H), 7.44-7.34 (m, 2H), 5.99-5.69 (m, 4H), 4.83 (br s, 2H), 4.33-4.23 (m, 4H), 3.92 (br s, 2H), 3.53-3.32 (m, 14H),1.25 (s, 2H), 1.08 (s, 2H). FT-IR (neat): 3517.3, 3412.5, 3235.2, 2948.2, 2936.7, 2799.2, 2785.4, 1754.3, 16.92.5, 1543.4, 1479.5, 1441.8, 13.85.6, 1326.5, 1211.3, 1056.3 cm^{-1}.

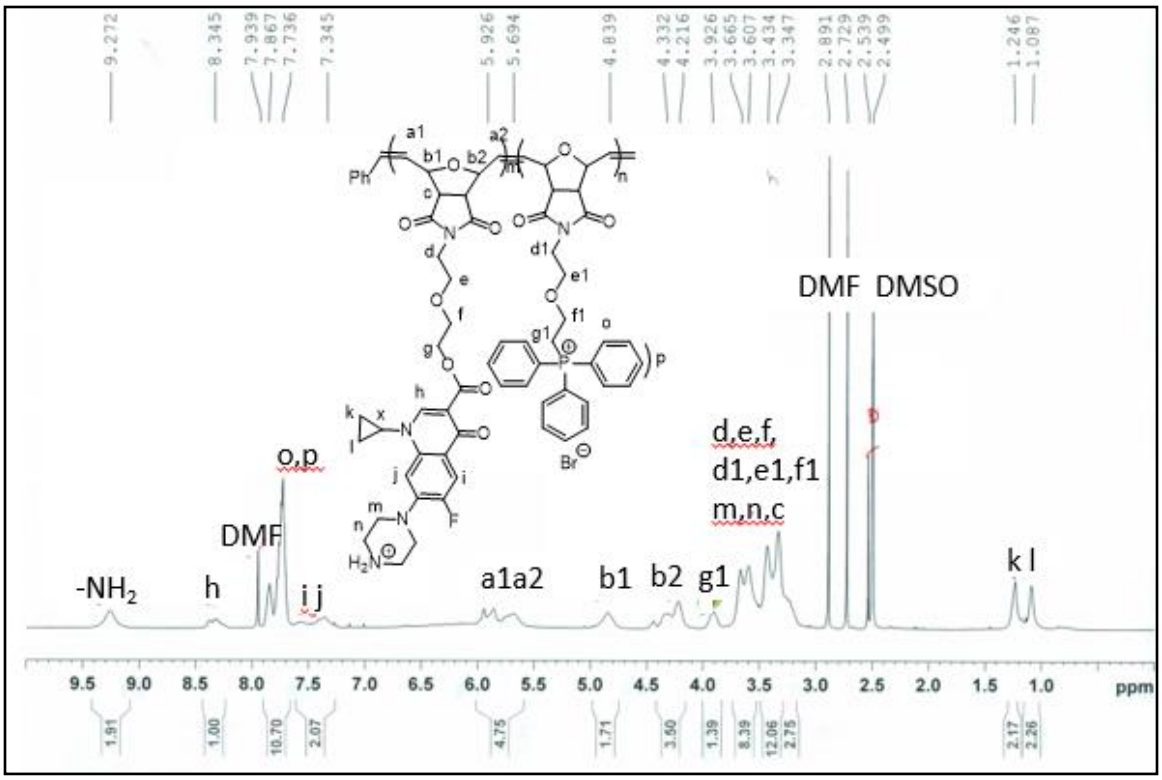

Figure 3.9. [1]H NMR of Boc deprotected **CIP-TPP di-block copolymer** polymer.

3.7. References

1. Kriti, S. (2012). Fluoroquinolones: Chemistry & Action—A Review. Ind Glob J Pharm Sci, 2:43-53.

2. Kumar, A., and Schweizer, H.P. (2005). Bacterial Resistance to Antibiotics: Active Efflux and Reduced Uptake. Adv Drug Deliv Rev, 57 (10):1486-513. Epub 2005/06/09. doi:10.1016/j.addr.2005.04.004. PubMed PMID: 15939505.

3. Marshall, A.J., and Piddock, L.J. (1994). Interaction of Divalent Cations, Quinolones and Bacteria. J Antimicrob Chemother, 34 (4):465-83. Epub 1994/10/01. PubMed PMID: 7868402.

4. Lambert, P.A. (2002). Cellular Impermeability and Uptake of Biocides and Antibiotics in Gram-Positive bacteria and Mycobacteria. Symp Ser Soc Appl Microbiol, (31):46S-54S. Epub 2002/12/17. PubMed PMID: 12481828.

5. Sutthasupa, S., Shiotsuki, M., Masuda, T., and Sanda, F. (2009). Alternating Ring-Opening Metathesis Copolymerization of Amino Acid-Derived Norbornene Monomers Carrying Nonprotected Carboxy and Amino Groups Based on Acid-Based Interaction. J Am Chem Soc, 131 (30):10546-51. Epub 2009/09/03. doi:10.1021/ja903248c. PubMed PMID: 19722629.

6. Sutthasupa, S., and Sanda, F. (2009). ROMP of Norbornene Monomers Carrying Nonprotected Amino Groups with Ruthenium Catalyst, 42:1519-25.

7. Berlanga, M., Montero, M.T., Hernandez-Borrell, J., and Vinas, M. (2004). Influence of the Cell Wall on Ciprofloxacin Susceptibility in Selected Wild-Type Gram-Negative and Gram-Positive Bacteria. Int J Antimicrob Agents, 23 (6):627-30. Epub 2004/06/15. doi:10.1016/j.ijantimicag.2003.12.015. PubMed PMID: 15194135.

8. Chapman, J.S., and Georgopapadakou, N.H. (1988). Routes of Quinolone Permeation in Escherichia Coli. Antimicrob Agents Chemother, 32 (4):438-42. Epub 1988/04/01. PubMed PMID: 3132091; PubMed Central PMCID: PMCPMC172197.

9. Lienkamp, K., Madkour, A.E., Musante, A., Nelson, C.F., Nusslein, K., and Tew, G.N. (2008). Antimicrobial Polymers Prepared by ROMP with Unprecedented Selectivity: A Molecular Construction Kit Approach. J Am Chem Soc, 130 (30):9836-43. Epub 2008/07/03. doi:10.1021/ja801662y. PubMed PMID: 18593128; PubMed Central PMCID: PMCPMC4106262.

10. Chen, M., Ren, Z.H., Wang, Y.Y., and Guan, Z.H. (2015). Palladium-Catalyzed Oxidative Carbonylation of Aromatic C-H bonds of N-alkylanilines with CO and Alcohols for the Synthesis of O-Aminobenzoates. J Org Chem, 80 (2):1258-63. Epub 2015/01/07. doi:10.1021/jo502581p. PubMed PMID: 25560397.

11. Liu, D., Canales, E., and Corey, E.J. (2007). Chiral Oxazaborolidine-Aluminum Bromide Complexes Are Unusually Powerful and Effective Catalysts for Enantioselective Diels-Alder Reactions. J Am Chem Soc, 129 (6):1498-9. Epub 2007/02/08. doi:10.1021/ja068637r. PubMed PMID: 17283985.

12. Wu, C.Y., Brik, A., Wang, S.K., Chen, Y.H., and Wong, C.H. (2005). Tetrabutylammonium Fluoride-Mediated Rapid Alkylation Reaction in Microtiter Plates for the Discovery of Enzyme Inhibitors in Situ. Chembiochem, 6 (12):2176-80. Epub 2005/11/05. doi:10.1002/cbic.200500295. PubMed PMID: 16270365.

13. Kabalka, G.W., Rajender, M.V., Varma, S.,Prem, Srivastava, C., Furn, and Knapp, F. (1986). The Tosylation of Alcohols. J Org Chem, 51:2386-8.

CHAPTER IV

FUNCTIONAL GROUP MODULATED CONJUGATED POLYMER FOR CELLULAR IMAGING AND GENE DELIVERY

Manuscript is in progress

4.1. Abstract

Cellular entry pathways depend on the surface charge and physical properties of external materials. A rigid aromatic backbone structure and positively charged side chain make guanidine-containing conjugated polymers (CPs) best suited as the delivery vehicle. Guanidine-containing CPs are excellent gene carriers because of their intrinsic fluorescent and surface charge properties. A small modification of guanine-containing CPs could lead to the inactivation of the polymer or a change in its biological properties. Interestingly, modification of the guanidine group with amines and alcohols showed impressive cell-penetrating properties, and that makes these polymers suitable for carrying external agents through the cell membranes. Modification of guanidine moiety in CPs with more hydrophobic and/or hydrophilic compounds led us to overcome the solubility issue along with the change in physical properties essential for cellular imaging and gene delivery. In this research, a series of guanidine-modified CPs was prepared and their transfection efficiency through the cell membranes has been evaluated using various methods, including confocal imaging. Modulated polymers were then tested as a gene delivery agent, and a 20% siRNA knockdown was achieved in normal human bronchial epithelial (NHBE) cells without causing cytotoxicity. The NHBE (known as primary) cells are difficult to transfect and the gold-standard transporter lipofectamine was toxic for this cell line. In this Chapter, we discuss details of the modification chemistry, modification-dependent cellular behaviors, and a knockdown of a target protein in primary cells.

4.2. Introduction

CPs are macromolecules with highly delocalized π-conjugated backbones and amphiphilic side chains[1-3]. CPs have been widely used for specific biological

applications because of their unique properties such as large absorption extinction coefficients, amplified quenching, high quantum yields, and tunable absorption and emission maxima[3, 4]. Incorporation of guanidine moiety as a side chain of CPs has attracted attention in numerous biological applications due to the valuable hydrogen bond-based catalysts[5]. Guanidinum is a part of the side chain of arginine and remains charged over a wide pH range, which is reflected in the high pKa value (12.48) of its protonated counterpart[6]. There are many guanidine-containing peptides available because of their ease of modification and straight-forward synthetic strategy. Guanidinum groups have proven to be a valuable addition to polymers, not only because of their cationic properties, but also for their mimic of cell-penetrating peptides (CPPs)[7], molecular recognition[8], and antimicrobial agent[9].

The chemical modification of the guanidine group is often considered to destroy its functionality. Nitrogen atoms of Boc-guanidine bearing electron-withdrawing substituents act as a reactive nucleophile[10]. The fairly acidic N-H protons in Boc-guanidine can be further functionalized with a variety of electrophiles to make diverse functional material[11]. There have only been a few methods reported so far for guanidine modification, including the reaction between guanidine with alcohols under the Mitsunobu reaction condition[12] and alkylation of guanidine with electrophiles such as alkyl halides under basic conditions[10]. Recently Kessler et al.[11] modified the guanidine group of Cilengitide ligand with *N*-methylation, *N*-alkylation, and *N*-acylation and successfully demonstrated the increased selectivity of Cilengitide ligands. Takemoto et al.[12] reported a convenient and direct modification of guanidine using a palladium- or iridium-catalyst. Moreover, in Chapter 2, we presented a synthesis of unique

antimicrobial polyamidinourea using guanidine modification chemistry. The direct modification of the guanidine head group has received much less attention, and we found no report on modification of guanidine moiety in polymers.

Despite the importance of guanidinum moiety in biological applications, it has some limitations in terms of its use in cellular imaging and gene or drug delivery. More precisely, guanidine-containing CPs have limited solubility in organic solvents. We hypothesized that modification of guanidinum moiety with more hydrophobic and/or hydrophilic compounds in CPs might improve the solubility and enhance the physical properties. Hence, we studied guanidine modification chemistry and developed a direct method for the guanidine head group modification in CPs. We anticipated that replacing the amino substituent with the strongly basic components would affect the physical properties and, in particular, the ionization and charge distribution. We also anticipated that changing physical properties, ionization, and charge distribution would enhance cellular transfection and imaging and reduce cytotoxicity, which is essential for gene delivery. We have followed the catalyst-free post-polymerization technique to incorporate a variety of hydrophilic and the hydrophobic functional group in guanidine-containing CPs. The modification reaction proceeds via generation of isocyanate in situ reaction conditions. With this technique, we have shown that a structural diverse polymer can be synthesized without observing tedious polymerization steps. To test the hypothesis, we first modified the guanidine head group with diisopropylamine (DIPA), and a dramatic change in solubility as well as physical properties of DIPA-modified CP were observed. Later we broadened our synthetic scheme to further head group modification with various functional compounds. We incorporated more hydrophobic

and hydrophilic groups such as piperidine, morpholine and aminoethoxyethanol and determined their physical and photo physical properties. The modulated CPs were able to integrate via ^{1}H NMR without any difficulty, and overall yields were high.

The cellular and subcellular transfection of the modified polymers were evaluated by using confocal imaging. Guanidine-modified CPs had shown better cellular uptake and no cytotoxicity up to 40 μM concentration in HeLa cells. Selectively, one polymer was chosen for gene delivery for the normal human epithelial cell (NHBE), known as the primary cell line. Where gold-standard lipofectamine has failed to transfect NHBE cell, we achieved a 20% siRNA knockdown and proven our hypothesis for a unique gene delivery vehicle.

4.3. Result and Discussion

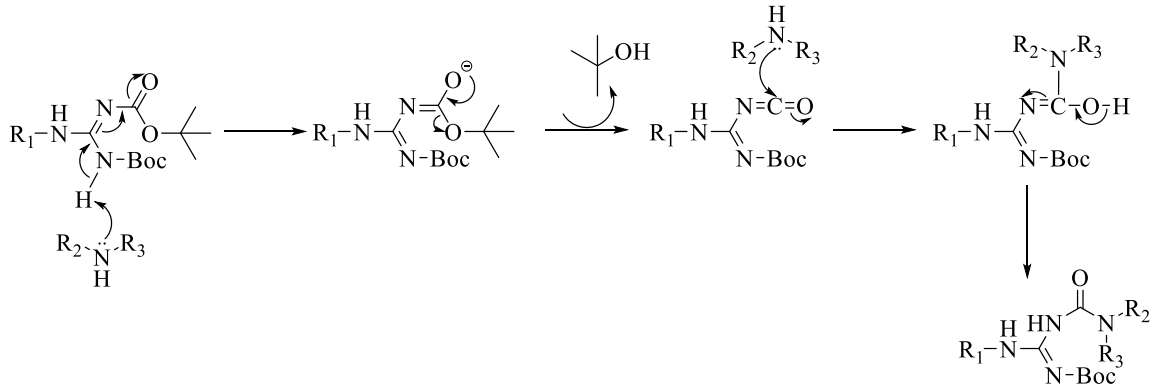

Figure 4.1. Plausible mechanism of guanidine head group modification[13]

Modified CP synthesis: As mentioned above, the primary goal of this research was to make a modulated CP with a post-modification technique. Thus, we have chosen guanidine-containing CP as a model polymer and modified its head group with various functional compounds such as amines and alcohols. In Chapter 2, we discussed modification of Boc-protected guanidine moiety and demonstrated the synthesis of

antimicrobial polyamidinourea using catalyst-free direct modification chemistry. Synthesized CPs are designated as follows: guanidine homo **(PG-H)**, DIPA modified **(PG-D)**, morpholine modified **(PG-M)**, piperidine modified **(PG-P)**, and Aminoethoxyethanol modified **(PG-A)**. To synthesize various guanidine-modulated CPs, we started with DIPA to make more hydrophobic polymer. The reaction condition was similar to conventional the Sonogashira coupling reaction to synthesis PPE polymer, except the temperature because 80^0C was the minimum requirement to deprotonate the amide proton in Boc-guanidine and to incorporate DIPA. The modification reaction proceeds via generation of isocyanate in situ. Figure 4.1 shows the possible reaction mechanism. Unlike **PG-H**, DIPA has two isopropyl groups with secondary amine. We anticipated that **PG-D** would show less charge on the surface and better solubility in organic solvent compared to **PG-H**. Because the conjugated backbone between **PG-H** and **PG-D** were similar, we did not observe any change in photo-physical properties between these two polymers (Table 4.1). But we clearly observed a distinct difference in solubility and photo-physical behavior after the Boc deprotection. **PG-H** was partially soluble in DMF and DMSO. However, **PG-D** was completely soluble in DMF and DMSO. We also recorded changes in UV absorbance and UV emission in water after the Boc deprotection. **PG-H** showed λ_{max} = 408 nm (95%water) and Fluoro λ_{max} = 476 nm (95% water), whereas **PG-D** showed λ_{max} = 417 nm (95%water) and Fluoro λ_{max} = 540 nm (95% water) (Figures 4.12 and 4.13). Being inspired by this work, we chose morpholine as a more hydrophilic compound and modified **PG-H** with morpholine using the post-polymerization technique. In this approach, **PG-H** were heated with excess morpholine in the presence of tetrahydrofuran (THF) as a solvent at 80^0C overnight under N_2 conditions. As expected, no change in photo-physical properties

were observed with **PG-M**. But change was noted after the Boc deprotection. Improved solubility and physical properties of **PG-M** were recorded and compared with **PG-H**. We then moved on to piperidine and aminoethoxyethanol to modify the guanidine head group and synthesize more hydrophobic and hydrophilic polymer **PG-P** and **PG-A,** respectively, by following the post-polymerization technique. After deprotection of the Boc group, its photo-physical data were recorded in DMSO and water. In water, UV absorbance and emission were changed due to the modification with the hydrophilic and hydrophobic moieties (Figure 4.14-4.16).

Table 4.1. Comparison of average physical and photo-physical properties of polymers **(PG-H, PG-D, PG-M, PG-P and PG-A)**

Polymer	n[a]	Mn (g/mol)[b]	PDI[c]	Yield (%)[d]	$\lambda_{max\text{-}abs}$ (nm)[e]	$\lambda_{max\text{-}emission}$ (nm)[e,f]	QY[g]	Hydrodynanic diameter, nm[h]
PG-H	20	13500	1.30	65	434	490	8.30	274
PG-D	14	13000	1.70	62	418	490	8.14	298
PG-M	14	12300	1.50	76	435	488	8.20	283
PG-P	14	12400	1.90	53	435	490	8.37	291
PG-A	15	13700	1.40	79	434	494	19.8	162

[a] Degree of polymerization. [b] Determined by gel permeation chromatography in THF. [c] PDI (polydispersity index) = *Mw/Mn*. [d] Percent yield per repeating unit after repeated purification by precipitation. [e] Measured in DMSO after Boc deprotection. [f] Measured in DMSO after Boc deprotection. [g] Quantum yield in DMSO after Boc deprotection. [h] Hydrodynamic diameter measured in PBS (0.2 μM) after Boc deprotection.

Polymer characterization: All Boc-protected polymers are soluble in regular organic solvents, such as DCM and tetrahydrofuran THF, and exhibit high molecular weights and acceptable experimental yields, as listed in Table 4.1. After Boc deprotection the polymer solubility was reduced, resulting in polymers soluble only in DMF and DMSO. The experimental yields of **PG-P** were low due to the removal by precipitation of low-MW fragments during the polymer purification process. The Proton NMR spectra of all

polymers were consistent with their predicted average structure. Our analysis of predicted polymer structures examined the ethoxy protons on the side chain of monomers **A** and **B** (b ~4.23 ppm) and the guanidinum NH protons characteristic of monomer **A** (g ~ 12.4 ppm and f ~ 8.2 ppm, respectively). As compared with **PG-H**, rest of the modified polymers have shown only one Boc peak at 1.42 ppm, another confirmation of guanidine head group modification. All proton peaks were integrated relative to the ethylene oxide proton peak (b) and were in good agreement with the integration values predicted by the theoretical head group modification analysis. Example spectra of **PG-H** and **PG-D** are presented in Figure 4.2.

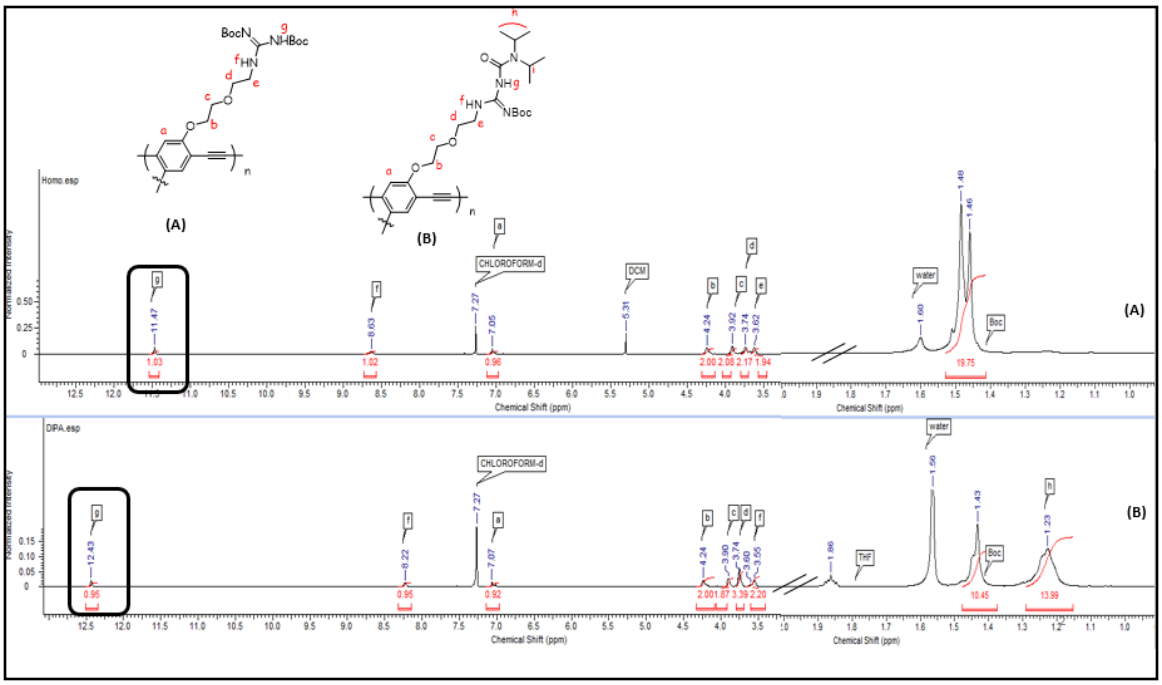

Figure 4.2. ^{1}H NMR Comparison of guanidine head group modified polymer **PG-H** and **PG-D**

Toxicity assay: The biocompatibility of the guanidine-modified CPs was evaluated with the HeLa cell line for their use in gene delivery vehicle. Toxicity measurements were carried out by Prakash Manandhar in my lab as a collaborator for this project. HeLA cells

were selected for cytotoxic studies because they are durable and prolific and can be grown easily in a 5% serum-supplemented standard DMEM medium with no specific growth component requirement. The viability percentage of the cells was plotted against the CPs' concentration at 48 hours (Figure 4.3). The concentration of CP up to 40 μM was not cytotoxic.

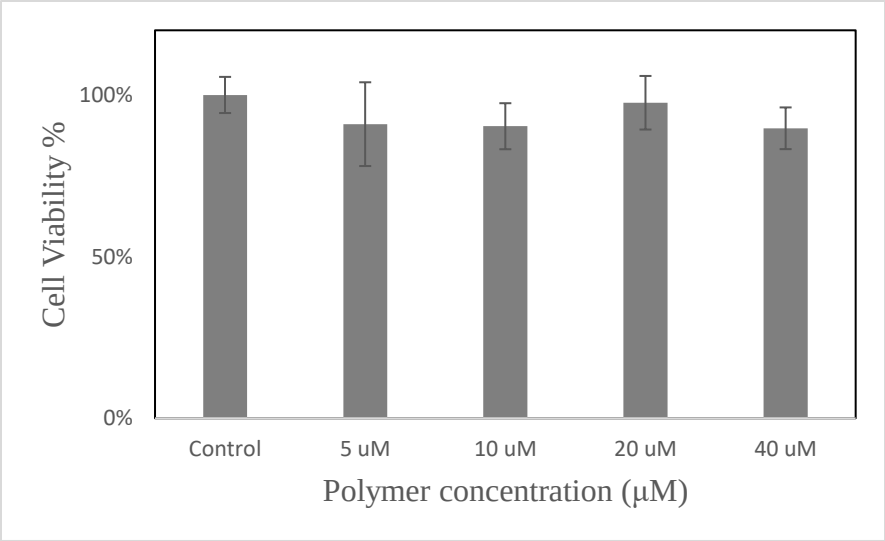

Figure 4.3. Cell viability evaluation by MTT assay of **PG-H**. **PG-H** caused no viability inhibition.

Cellular imaging: We evaluated the suitability of the modulated CPs as biological markers through live cell imaging. Figure 4.4 shows the confocal images of HeLa cells after incubation with the guanidine-modified series of polymers for 1 hour in a culture medium at 10 μM. The cell nuclei were stained with 4', 6-diamidino-2-phenylindole (DAPI). These images were taken upon excitation at 488 nm (2.5 mW laser power) with a 650 nm long pass barrier filter. A higher fluorescence intensity is observed in Figure **PG-A** than for the rest of the polymers. Thus, **PG-A** showed a higher quantum yield. The blue

and green channels were used; based on the composite images, polymers were able to penetrate the cell line, and some of them are co-stained with the nuclei.

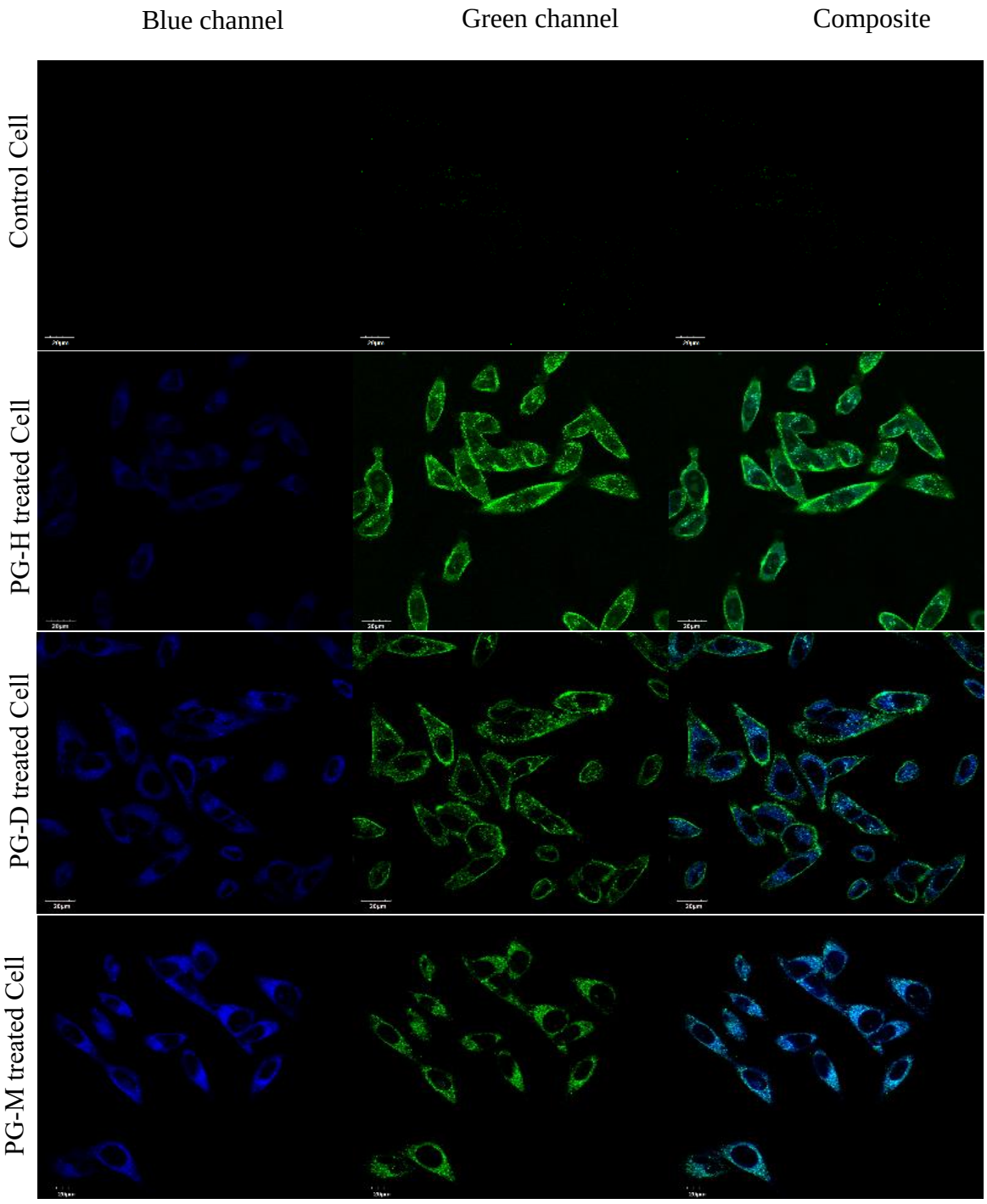

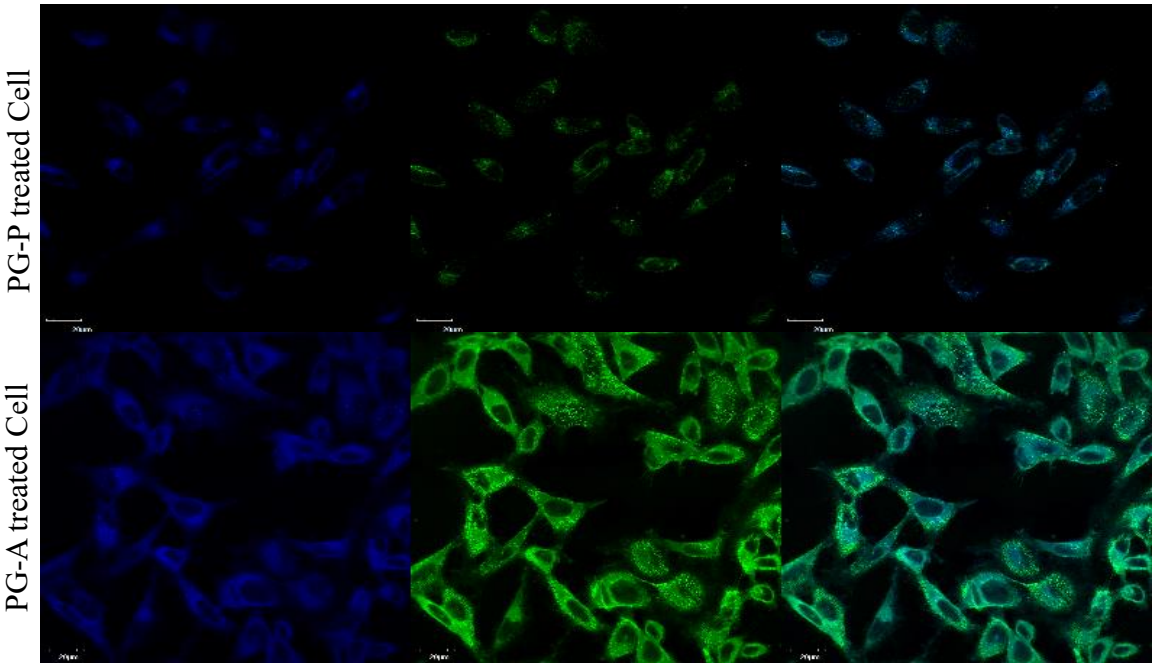

Figure 4.4. Confocal images of HeLA cells incubated with Guanidine series of polymers (10 μM for 1 h).

siRNA knockdown: Normal Human bronchial epithelial (NHBE) cells have a different cellular membrane structure from HeLA cells and are difficult to transfect. Even gold-standard transfection reagent lipofectamine was toxic to this cell line, and thus gene delivery thorough NHBE cells was limited. **PG-A** was tested for siRNA delivery through NHBE cells, and a maximum of 20% gene knockdown was achieved without killing the cells. Figure 4.5 shows the siRNA knockdown data. This measurement was carried out by Rajib Kumar Datta in Dr. Unwalla lab as a collaborator of this project.

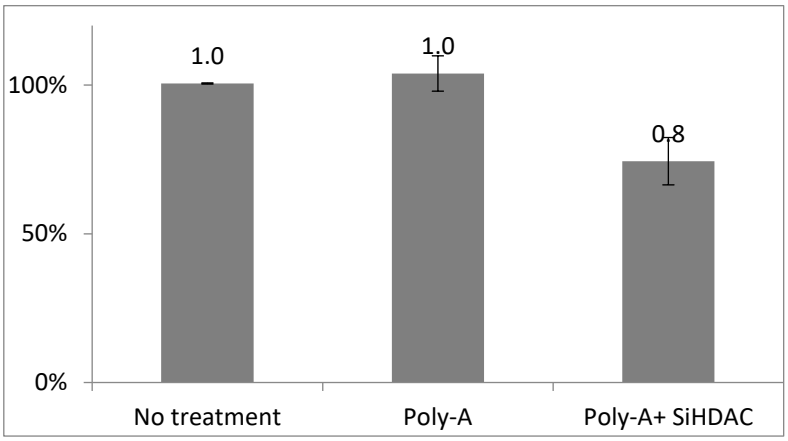

Figure 4.5. siRNA knockdown by **PG-A** in NHBE cell.

4.4. Conclusion

We have described the design, synthesis, and cellular behavior of a new class of guanidine-modified CPs. In this Chapter, we demonstrated successful synthesis of guanidine-containing CP and head group modification of guanidine moiety in CPs with various functional compounds. We also demonstrated that structurally diverse CPs can be made using post-modification of guanidine moiety in CP. We proved that modified polymers are well suited for gene or drug delivery because of their improved physical properties.

4.5. Outlook

Guanidine modification in small molecules has been reported, but we found no studies in the case of polymers. This could be a new research field. A library of versatile functional polymers can be made by following the post-modification method. At the same time, a specific functional group can be attached with an existing guanidine CP to better target a specific material.

4.6. Experimental Section

4.6.1. Monomer Synthesis

Synthesis of guanidinum-containing aryl halide monomer A

Synthesis of guanidinum-containing aryl halide monomer **A** discussed in Chapter 2 Scheme 2.1.

Synthesis of Monomer B

Scheme 4.1. Synthesis of Guanidinum-containing acetylene monomer **B**

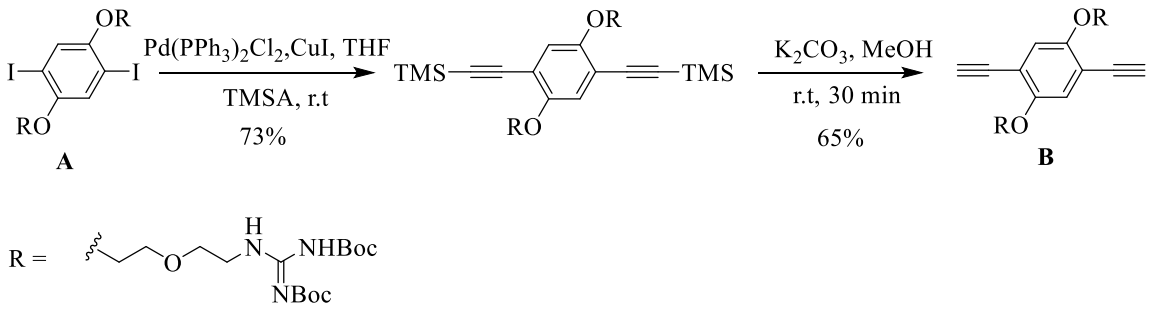

In an RBF charged with compound **A** (2.00 g, 1.96 mmol), trimethylsilylacetylene (0.77 g, 7.84 mmol), $PdCl_2(PPh_3)_2$ (137.6 mg, 0.20 mmol), and CuI (18.6 mg, 0.10 mmol). The RBF was evacuated and filled with N_2. A solution of THF and DIPA was mixed in a 4:1 ratio (v/v) and degassed with N_2 for 10 minutes, and 50 mL was transferred to the RBF via a cannula. The reaction was stirred at r.t for 3 hours under an N_2 balloon. The yellow reaction mixture was filtered to remove insoluble particles and THF distilled out *in vacuo*. The reaction mixture was dissolved in DCM and washed with 1M NH_4Cl (2x) followed by brine (1x). Column chromatography under 30% ethyl acetate in hexane yielded a final product of a white solid (1.22 g, 65% yield).

^{1}H NMR (400 MHz), $CDCl_3$, δ: 11.46 (s, 1H), 8.67 (s, 1H), 7.21 (s, 1H), 4.1 (t, *J* = 4.4 Hz, 2H), 3.88 (t, *J* = 4.8 Hz, 2.H), 3.78 (t, *J* = 4.8 Hz, 2H), 3.66 (q, *J* = 5.2 Hz, 2H), 1.50 (s, 9H), 1.45 (s, 9H), 0.10 (s, 18H).

In an RBF, trimethylsilyl-protected compound (1.00 g, 1.04 mmol) and potassium carbonate (0.36 g, 2.60 mmol) were dissolved in methanol (40 mL). The RBF was then stirred at r.t. for 20 minutes. Upon confirmation by TLC, the solvent was dried *in vacuo*. The reaction mixture was then purified in short-path column chromatography under 35% ethyl acetate in hexane and yielded a final product of a yellowish solid (0.51 g, 60% yield).

^{1}H NMR (400 MHz), $CDCl_3$, δ: 11.45 (s, 1H), 8.67 (s, 1.00H), 6.98 (s, 1H), 4.15 (t, *J* = 4.4 Hz, 2H), 3.86 (t, *J* = 4.8 Hz, 2H), 3.75 (t, *J* = 4.8 Hz, 2H), 3.65 (q, *J* = 5.2 Hz, 2H), 3.35 (s, 1H), 1.50 (s, 9H), 1.45 (s, 9H). ^{13}C NMR (400 MHz), $CDCl_3$, δ: 156.4, 154.2, 153.1, 118.3, 113.8, 83.2, 83.1, 79.6, 79.4, 70.0, 69.8, 69.4, 40.9, 28.4, 28.2. FT-IR (neat): 3330.9, 3281.4, 2975.3, 2930.5, 1720.2, 1636.1, 1613.1, 1568.2, 1495.8, 1410.3, 1319.7, 1222.7, 1129.0, 1049.9 $cm^{-1.}$

4.6.2. General procedure for guanidine homo polymer (PG-H)

Scheme 4.2 represents the synthetic procedure. A Schlenk flask was filled with monomer **A** (50.0 mg, 0.04 mmol), **B** (40.0 mg, 0.04 mmol), $PdCl_2(PPh_3)_2$ (3.43 mg, 0.005 mmol), and CuI (0.47 mg, 0.003 mmol). The Schlenk flask was evacuated and filled with N_2. A solution of THF and DIPA was mixed in a 4:1 ratio (v/v) and degassed with N_2, and 2.00 mL (volume) was transferred to the Schlenk flask via a cannula. The reaction was stirred at r.t for 16 hours. The solution was then filtered through a glass wool pipette filter process and transferred dropwise to methanol, resulting in precipitation. The supernatant was

decanted, the precipitate was redissolved in DCM (0.50 mL), and the purification method was repeated using methanol. The overall yield was 65% (26.9 mg). The resulting polymer in DCM was characterized by gel permeation chromatography (GPC), and its absorption/emission profiles were measured. The final polymer was allowed to dry under a high vacuum for 16 hours before ^{1}H NMR characterization.

Scheme 4.2. Synthesis of **PG-H** under the Sonogashira coupling condition

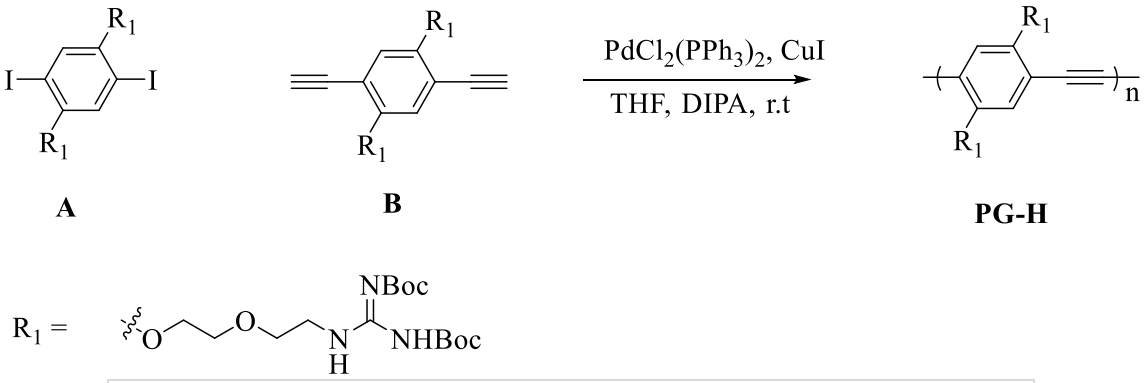

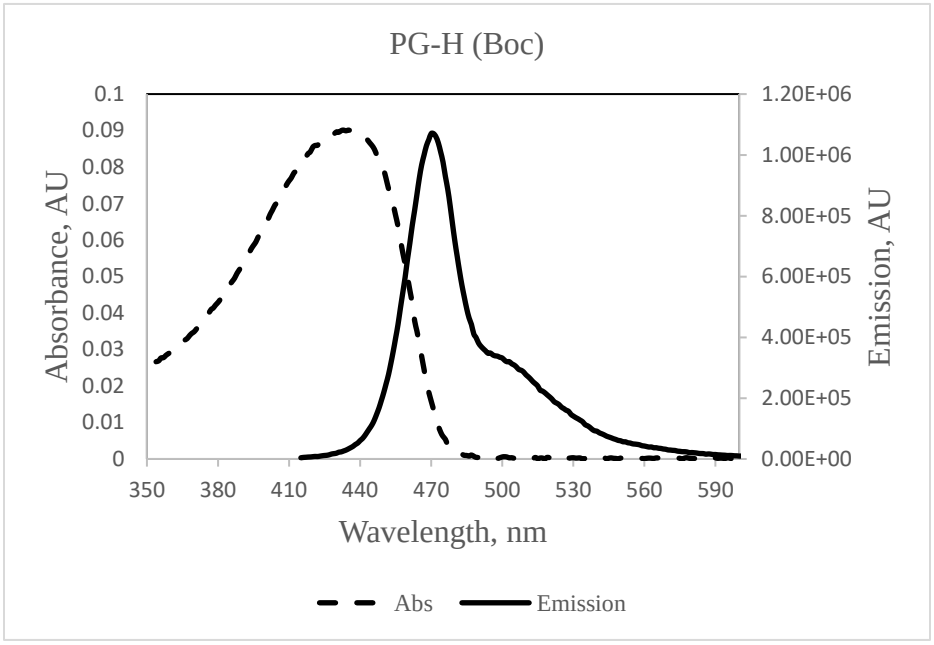

Figure 4.6. UV absorbance and emission of Boc protected Guanidine Homo polymer (**PG-H**)

^{1}H NMR (400 MHz), $CDCl_3$, δ: 11.46 (s, 1H), 8.62 (s, 1H), 7.05 (s, 1H), 4.24 (s, 2H), 3.91 (s, 2H), 3.74 (s, 2H), 3.62 (s, 2H), 1.48 (s, 9H), 1.45 (s, 9H). FT-IR (neat): 3329.4, 3131.7, 2975.3, 2931.3, 1720.1, 1635.2, 1614.0, 1567.7, 1503.9, 1411.8, 1364.5, 1319.8, 1280.5, 1249.7, 1131.0, 1048.8 $cm^{-1.}$ GPC: *Mn* = 13500 g/mol, *Mw* = 18000 g/mol, PDI = 1.30, UV-Vis (THF) λ_{max} = 442 nm, Fluo λ_{max} = 469 nm.

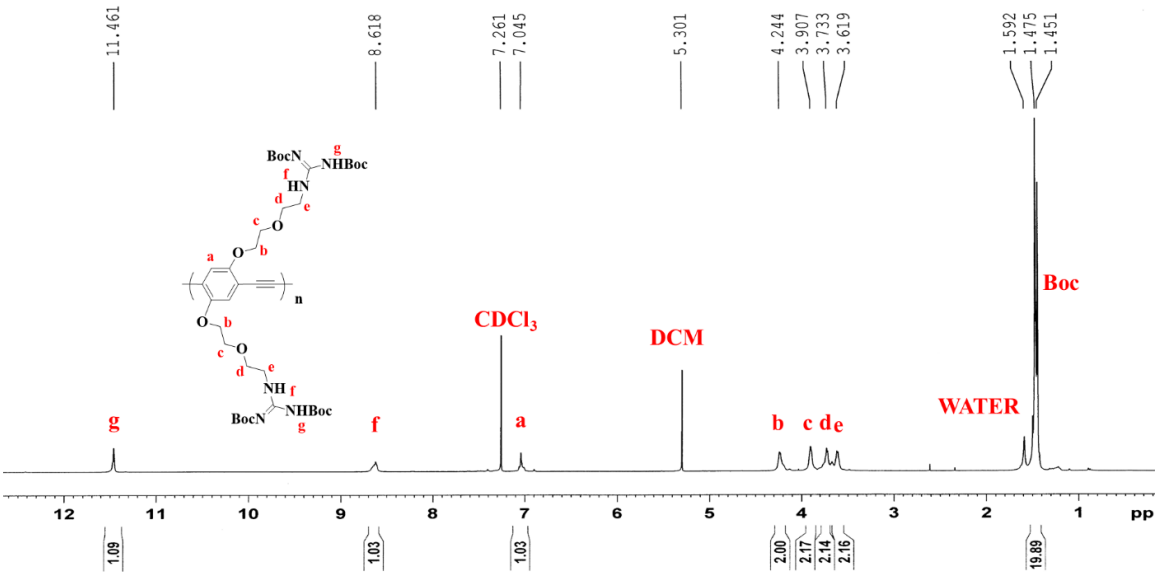

Figure 4.7. ^{1}H NMR Guanidine Homo polymer (**PG-H**)

PG-D (DIPA-modified CP)**:** Using the general polymerization procedure described above, the polymerization of monomers **A** (50.0 mg, 0.04 mmol) and **B** (40.0 mg, 0.04 mmol) in the presence of $PdCl_2(PPh_3)_2$ (3.43 mg, 0.005 mmol), CuI (0.47 mg, 0.003 mmol), THF, and DIPA (4:1) (v/v) were heated at 80^0C for 16 hours. The overall yield was 62% (26.9 mg). The resulting polymer in DCM was characterized by GPC, and its absorption/emission profiles were measured. The final polymer was allowed to dry under a high vacuum for 16 hours before ^{1}H NMR characterization.

Scheme 4.3. Synthesis of **PG-D** under the Sonogashira coupling condition

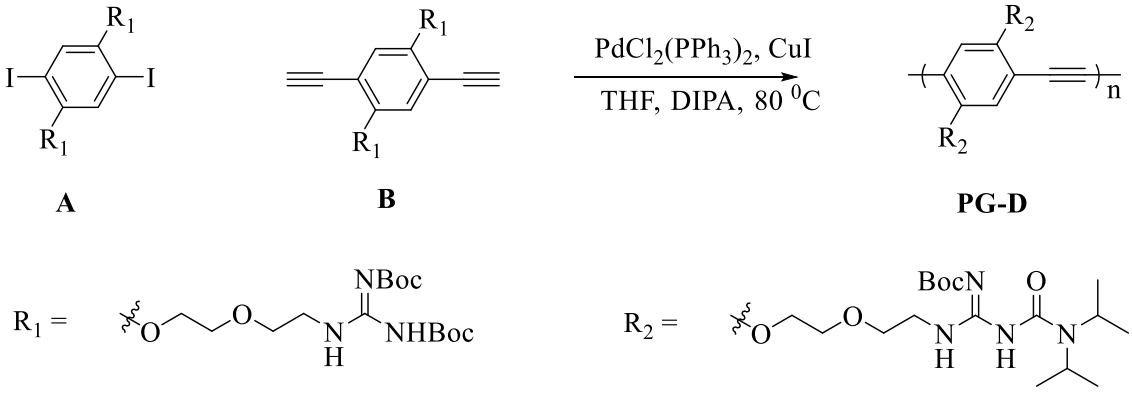

^{1}H NMR (400 MHz), $CDCl_3$, δ: 12.42 (s, 1H), 8.21 (s, 1H), 7.05 (s, 1H), 4.23 (s, 2H), 3.90 (s, 2H), 3.75 (s, 4H), 3.60 (s, 1H), 3.54 (s, 2H), 1.42 (s, 9H), 1.23 (s, 12H) FT-IR (neat): 3338.6, 3139.9, 2964.5, 2828.5, 2763.8, 2712.9, 2454.9, 2398.4, 1714.2, 1666.8, 1628.9, 1574.1, 1432.9, 1395.8, 1337.0. GPC: Mn = 13200 g/mol, Mw = 22400 g/mol, PDI = 1.70, UV-Vis (THF) λ_{max} = 434 nm, Fluo λ_{max} = 472 nm.

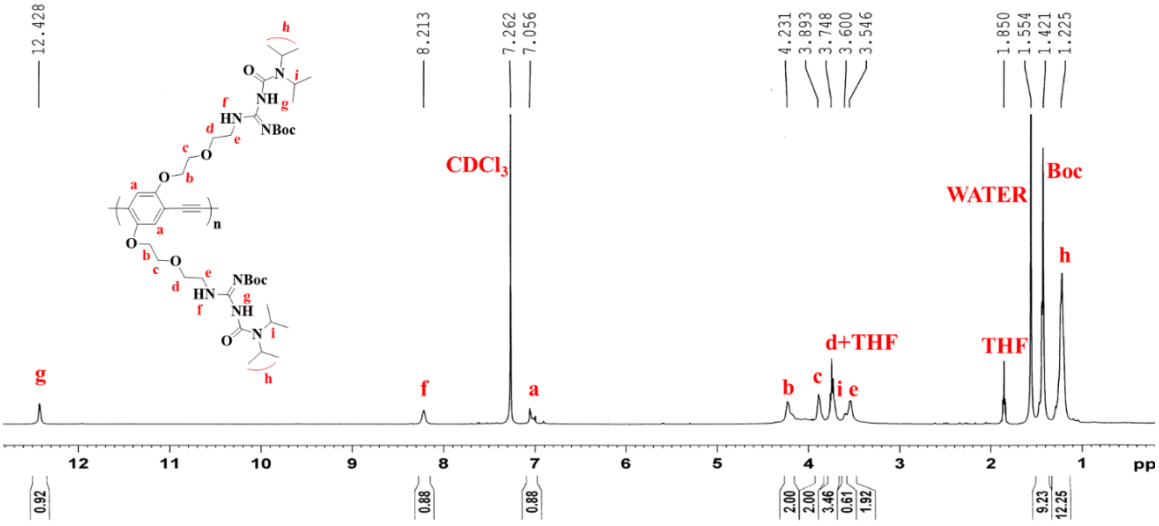

Figure 4.8. ^{1}H NMR Guanidine DIPA (**PG-D**)

PG-M (Morpholine-modified CP)**:** A Schlenk flask was charged with **PG-H** (10.0 mg, 0.012 mmol) and morpholine (2.57 mg, 0.03 mmol). The Schlenk flask was evacuated and filled with N_2. Degassed THF (1.5 mL) was transferred to the Schlenk flask via a cannula. The reaction was stirred at 80^0C for 16 hours. A viscous polymer solution purified by a glass wool filtration followed re-precipitation in diethyl ether and then in methanol. The final polymer was a yellow gel (7.72 mg with 76% yield).

Scheme 4.4. Synthesis of Guanidine head group modified polymers (**PG-M, PG-P, and PG-A**)

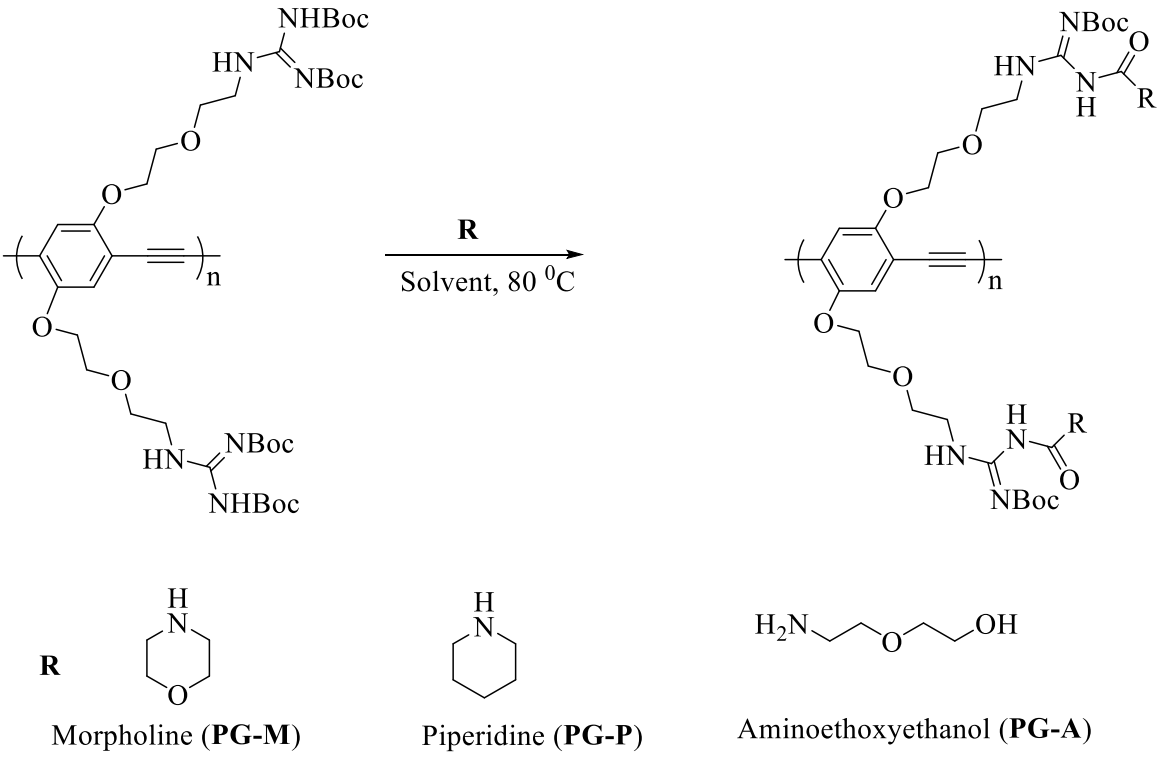

^{1}H NMR (400 MHz), $CDCl_3$, δ: 12.2 (s, 1H), 8.3 (s, 1H), 7.04 (s, 1H), 4.22 (s, 2H), 3.90 (s, 2H), 3.74 (s, 4H), 3.60 (s, 4H), 3.52 (s, 4H), 1.42 (s, 9H). FT-IR (neat): 3331.3, 2925.8, 2857.0, 1716.2, 1669.7, 1629.8, 1585.9, 1562.7, 1507.5, 1475.2, 1454.3, 1409.6, 1366.4,

1348.9, GPC: Mn = 12400 g/mol, Mw = 18600 g/mol, PDI = 1.50. UV-Vis (THF) λ_{max} = 428 nm, Fluo λ_{max} = 469 nm.

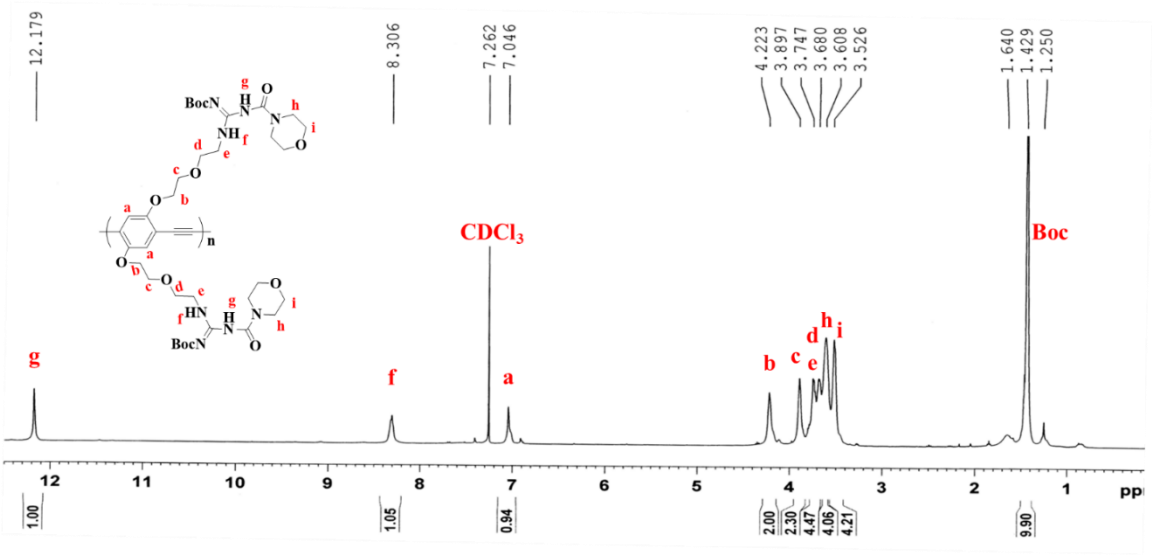

Figure 4.9. ^{1}H NMR Guanidine Morpholine (**PG-M**)

PG-P (Piperidine-modified CP)**:** A Schlenk flask was charged with **PG-H** (10.00 mg, 0.012 mmol) and piperidine (2.51 mg, 0.03 mmol). The Schlenk flask was evacuated and filled with N_2. Degassed THF (1.5 mL) was transferred to the Schlenk flask via a cannula. The reaction was stirred at 80^0C for 16 hours. A viscous polymer solution purified by glass wool filtration followed re-precipitating in diethyl ether and then in methanol. The final polymer was a yellow gel (5.36 mg with 53% yield).

^{1}H NMR (400 MHz), $CDCl_3$, δ: 12.30 (s, 1H), 8.22 (s, 1H), 7.05 (s, 1H), 4.22 (s, 2H), 3.90 (s, 2H), 3.74 (s, 2H), 3.65 (s, 2H), 3.59 (s, 1H), 3.53 (s, 2H), 3.47 (s, 2H) 1.42 (s, 9H). FT-IR (neat): 3332.9, 2929.9, 2853.7, 1714.7, 1666.8, 1630.8, 1583.8, 1560.5, 1475.5, 1423.6, 1365.9, 1253.2. GPC: Mn = 14600 g/mol, Mw = 27800 g/mol, PDI = 1.90. UV-Vis (THF) λ_{max} = 436 nm, Fluo λ_{max} = 461 nm.

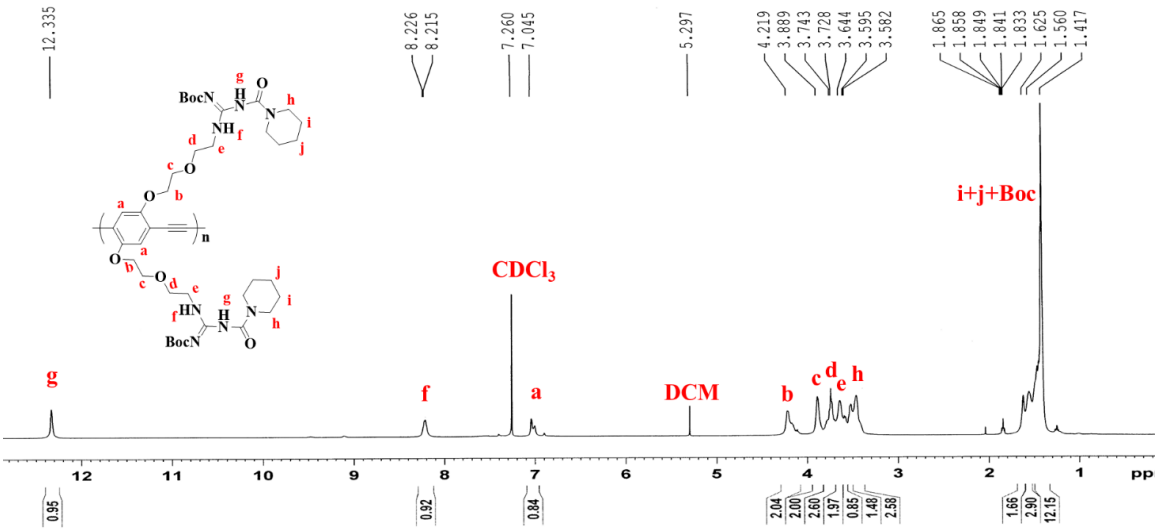

Figure 4.10. ^{1}H NMR Guanidine Piperidine (**PG-P**).

PG-A (Aminoethoxyethanol-modified CP)**:** A Schlenk flask was charged with **PG-H** (10.0 mg, 0.012 mmol) and aminoethoxyethanol (3.10 mg, 0.03 mmol). The Schlenk flask was evacuated and filled with N_2. Degassed THF (1.5 mL) was transferred to the Schlenk flask via a cannula. The reaction was stirred at 80^0C for 16 hours. A viscous polymer solution purified by glass wool filtration followed re-precipitating in diethyl ether and then in methanol. The final polymer was a yellow gel (8.20 mg with 79% yield).

^{1}H NMR (400 MHz), $CDCl_3$, δ: 12.05 (s, 1H), 8.27 (s, 1H), 7.04 (s, 1H), 6.03 (s, 1H), 4.22 (s, 2H), 3.90 (s, 2H), 3.72 (s, 5H), 3.53 (s, 8H), 3.36 (s, 2H), 1.42 (s, 7H). FT-IR (neat): 3323.5, 2929.8, 2870.9, 1716.7, 1633.2, 1597.8, 1507.7, 1453.7, 1411.0, 1347.9, 1311.7, 1277.2, 1227.2. GPC: Mn = 13800 g/mol, Mw = 19600 g/mol, PDI = 1.40. UV-Vis (THF) λ_{max} = 435 nm, Fluo λ_{max} = 465 nm.

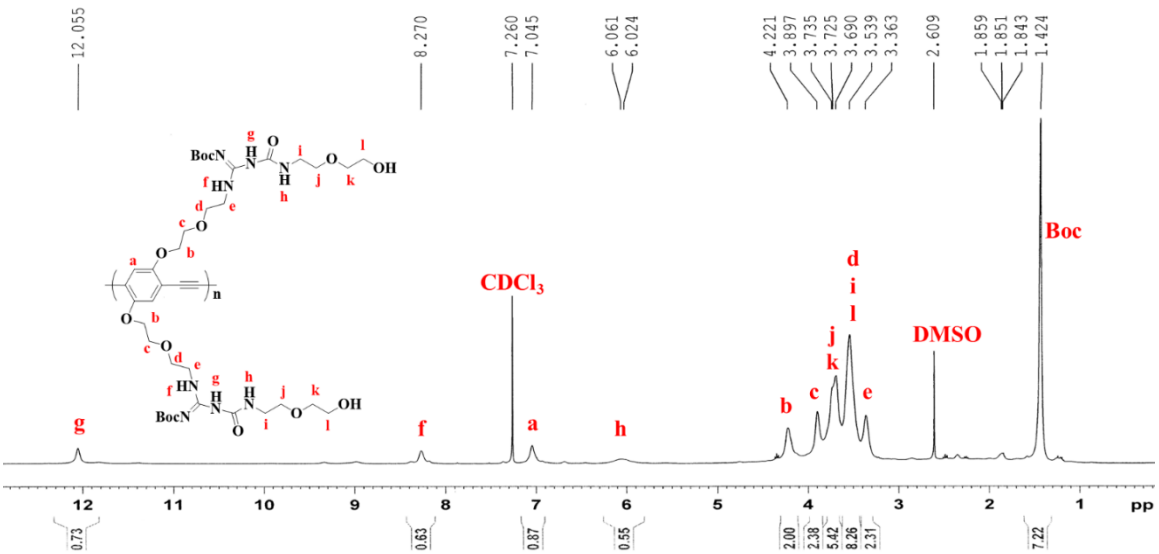

Figure 4.11. ^{1}H NMR Guanidine Aminoethoxyethanol (**PG-A**)

4.6.3. General procedure for Boc deprotection of modified CPs

In a vial, Boc-protected polymer was dissolved in DCM (1.00 mL) and TFA (1.00 mL) and stirred at r.t for 48 hours. Precipitation in DCM confirmed the complete Boc deprotection and solvent evaporated *in vacuo*. TFA was removed by azeotrope distillation and deprotected polymer purified by re-precipitating in EA(2x). After drying in a high vacuum, Boc deprotection was confirmed by ^{1}H NMR.

PG-H: Following the general procedure described above, the final deprotected polymer was a yellow gel (74.6 % yield).

^{1}H NMR (400 MHz, DMSO-d_6, δ): 8.13 (s, 1H), 7.92 (s, 2H), 7.27 (s, 2H), 6.87 (s, 1H), 5.77 (s, 1H), 5.03 (s, 1H), 4.30 (s, 2H), 3.98 (s, 2H), 3.59 (s, 4H), 3.50 (m, 6H), 2.98

(m,10H), 2.87 (s, 1H), 2.01 (m, 6H). FT-IR (neat): 3360.36, 2160.37, 1736.79, 1681.18 cm^{-1}. UV-Vis (DMSO) λ_{max} = 434 nm, Fluo λ_{max} = 490 nm, QY = 8.30.

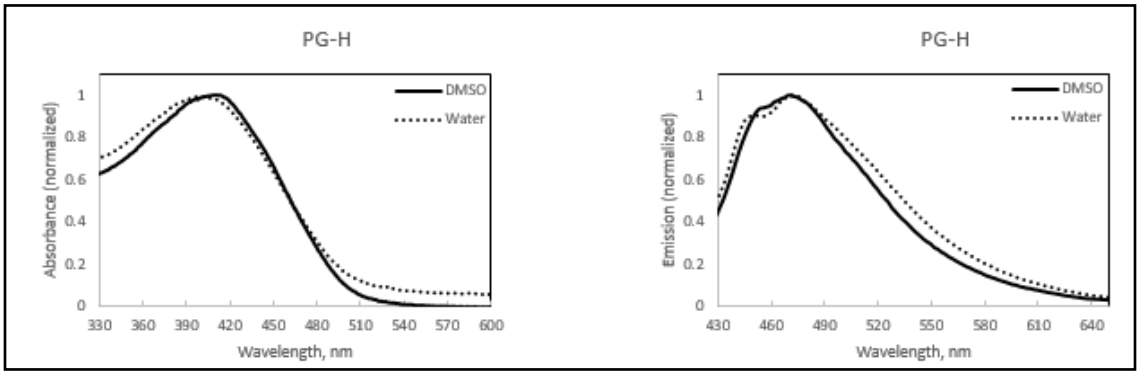

Figure 4.12. Absorption and emission spectra of **PG-H** in DMSO (left) and 95% water (right).

PG-D: Following the general procedure described above, the final deprotected polymer was a yellow gel (72.5 % yield).

^{1}H NMR (400 MHz, DMSO-d_6, δ): 9.73 (s, 1H), 9.27 (s, 1H), 8.65 (s, 2H), 7.5 (s, 2H), 4.62 (s, 2H), 4.4 (s, 2H), 4.03 (s, 2H), 3.76 (s, 4H), 3.56 (s, 2H), 3.50 (m, 6H), 1.17 (m, 13H). FT-IR (neat): 3512.0, 2994.8, 2992.6, 2159.87, 1733.97, 1679.4 $cm^{-1.}$ UV-Vis (DMSO) λ_{max} = 418 nm, Fluo λ_{max} = 490 nm, QY = 8.14.

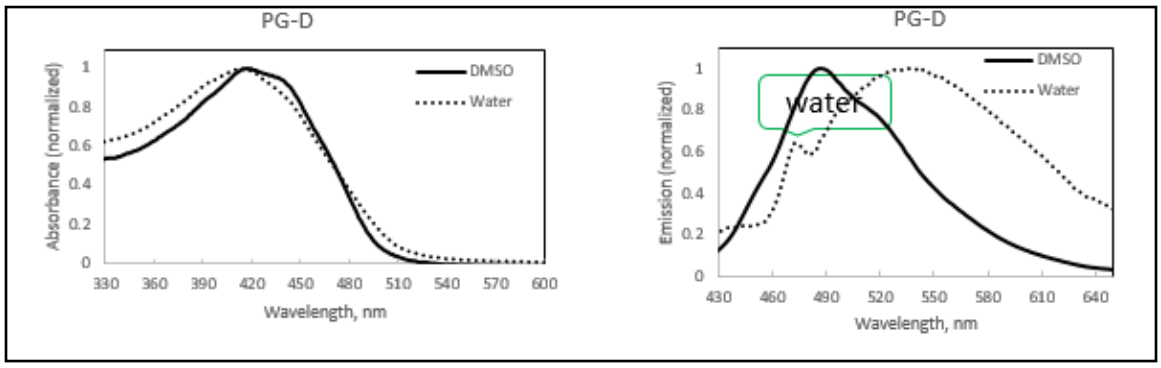

Figure 4.13. Absorption and emission spectra of **PG-D** in DMSO (left) and 95% water (right).

PG-M: Following the general procedure described above, the final deprotected polymer was a yellow gel (62 % yield).

^{1}H NMR (400 MHz, DMSO-d_6, δ): 10.2 (s, 1H), 9.20 (s, 2H), 8.60 (br s, 2H), 7.55 (s, 3H), 4.38 (br s, 4H), 4.10 (s, 2H), 3.80 (br s, 4H), 3.53 (br m, 11H), 3.59 (s, 4H). FT-IR (neat): 3280.78, 2872.4, 1670.82, 1440.13, 1303.92, 1251.30, 1198.86 cm^{-1}. UV-Vis (DMSO) λ_{max} = 435 nm, Fluo λ_{max} = 488 nm, QY = 8.20.

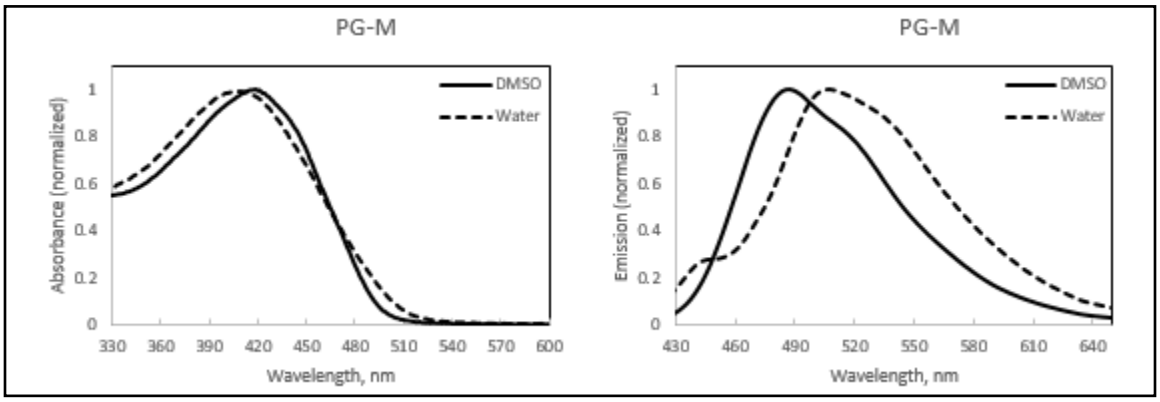

Figure 4.14. Absorption and emission spectra of **PG-M** in DMSO (left) and 95% water (right).

PG-P: Following the general procedure described above, the final deprotected polymer was a yellow gel (66.4 % yield).

^{1}H NMR (400 MHz, DMSO-d_6, δ): 10.03 (s, 1H), 9.25 (s, 1H), 8.60 (s, 2H), 7.53 (s, 2H), 4.38 (s, 1H), 4.03 (s, 1H), 3.81 (s, 2H). FT-IR (neat): 3305.85, 2940.75, 1667,98, 1444.67, 1252.02, 1198.52 cm-^{1}. UV-Vis (DMSO) λ_{max} = 435 nm, Fluo λ_{max} = 490 nm, QY = 8.37.

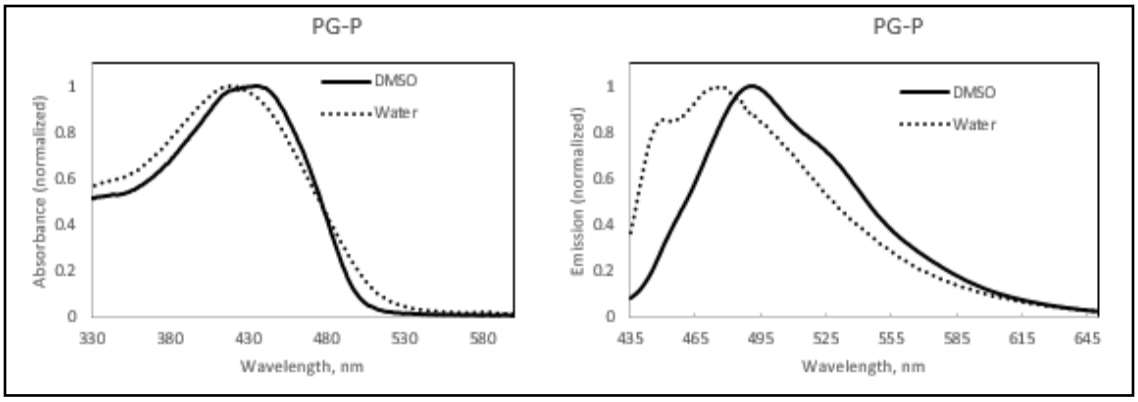

Figure 4.15. Absorption and emission spectra of **PG-P** in DMSO (left) and 95% water (right).

PG-A: Following the general procedure described above, the final deprotected polymer was a yellow gel (79% yield).

^{1}H NMR (400 MHz, DMSO-d_6, δ): 10.03 (s, 1H), 9.25 (s, 1H), 8.60 (s, 2H), 7.53 (s, 2H), 4.38 (s, 1H), 4.03 (s, 1H), 3.81 (s, 2H). FT-IR (neat): 3267.35, 2872.85, 1788.01, 1670.04, 1547.08, 1447.00, 1346.70, 1199.44. UV-Vis (DMSO) λ_{max} = 434 nm, Fluo λ_{max} = 494 nm, QY = 19.81.

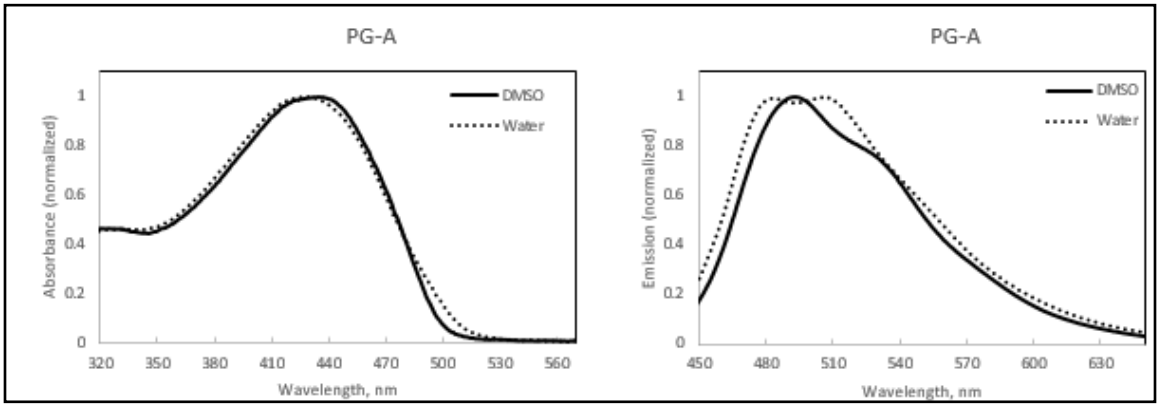

Figure 4.16. Absorption and emission spectra of **PG-A** in DMSO (left) and 95% water (right).

Scheme 4.5. Synthetic route toward precursor compound **3**

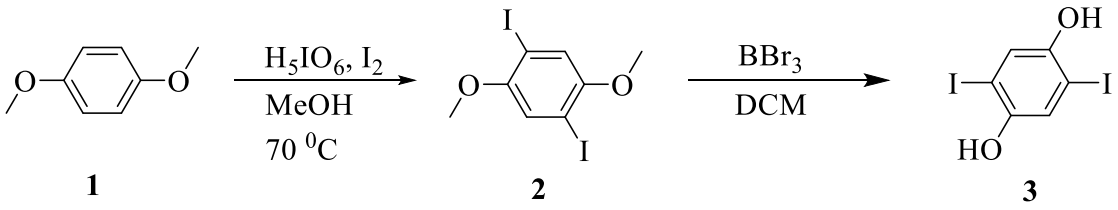

*Compound **2*** was synthesized according to the literature [1]. More specifically, H_5IO_6 (29.2 g, 130 mmol) and 200 mL methanol were added to an RBF and stirred for 10 minutes to make a solution. Later, I_2 (63.8 g, 250 mmol) was added to the RBF and made into a solution through stirring. Compound **1** (27.0 g, 190 mmol) was added to the RBF and left a reflux condition stirred in the flask overnight. Next day the reaction mixture was quenched into $Na_2S_2O_5$, and the resultant precipitate was filtered through vacuum filtration. The powder product on the filter paper was washed with water, methanol, and DCM. The organic layer was distilled off and filtered again to get the expected product **2** (63.0 g, 85% yield).

Compound 3 (Scheme 2.5)**:** Compound **3** was synthesized according to the literature[1]. Basically, compound **2** (33.1 g, 79.8 mmol) was dissolved in DCM (300 mL) degassed with a stream of N_2 for 15 minutes, and the mixture was placed in an ice/water bath. BBr_3 (100 g, 399 mmol) was added, and the reaction mixture was allowed to stir at r.t. overnight. The reaction was quenched with a DCM/methanol mixture and concentrated *in vacuo*. The resulting solid was washed with DCM on a Buchner funnel. Compound **3** was obtained as

a light beige solid (26.7 g, 87 %). ^{1}H NMR (400 MHz, DMSO-d_6): δ 9.80 (s, 2H), 7.14 (s, 2H)

Scheme 4.6. Synthetic route toward precursor compound **5**

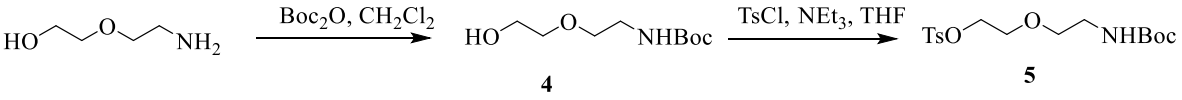

Compound 4 (Scheme 4.6): Compound **4** was synthesized according to the literature[15]. More specifically, aminoethoxyethanol (20.0 g, 95.1 mmol) was dissolved in DCM (300 mL) in an RBF. Di-tert-butyl decarbonate (Boc_2O) (39.4 g, 90.4 mmol) was dissolved in DCM (200 mL) and placed in an additional funnel. The solution was added dropwise during stirring, and the reaction was allowed to stir at r.t. overnight. The reaction was quenched with H_2O; the two layers were separated, and the organic layer was washed with H_2O and brine, dried over Na_2SO_4, and concentrated *in vacu*o to yield compound **4** as a colorless oil (34.6 g, 93%). ^{1}H NMR (400 MHz, $CDCl_3$): δ (br s, 1H), 1.43 (s, 9H)

Compound **5** was synthesized according to the literature[16]. More specifically, compound **4** (33.9 g, 165 mmol), tosyl chloride (31.5 g, 165 mmol), triethylamine (46.1 mL, 330 mmol), and DCM (500 mL) were reacted according to the procedure for the preparation of compound **5** above. Following extraction, the crude mixture was recrystallized from the THF/ether solvent system to yield compound **5** as a white solid (41.7 g, 70%).

^{1}H NMR (400 MHz, $CDCl_3$): δ 7.82 (d, 2H, *J* = 8.34 Hz), 7.36 (d, 2H, *J* = 8.08 Hz), 4.81 (br s, 1H), 4.18-4.16 (m, 2H), 3.65-3.63 (m, 2H), 3.46 (t, 2H, *J* = 5.31 Hz), 3.25 (q, 2H, *J* = 4.97 Hz), 2.46 (s, 3H), 1.46 (s, 9H)

Scheme 4.7. Synthetic route toward precursor compound **7**

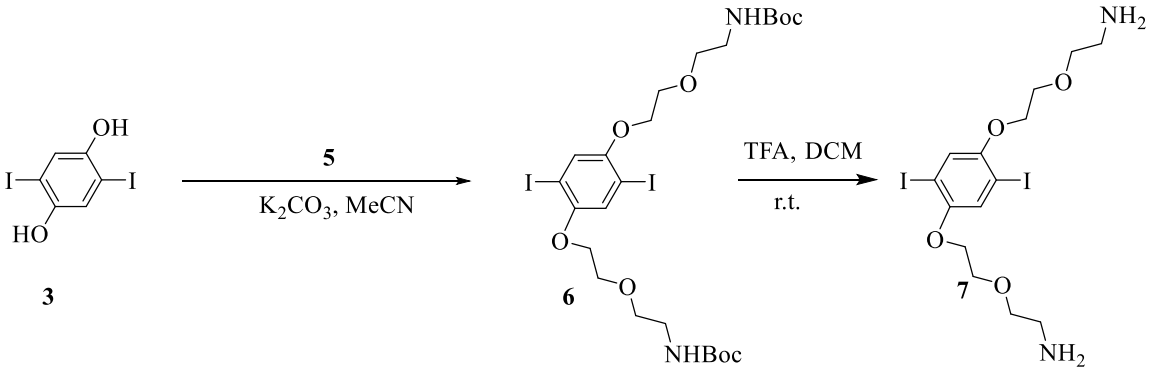

Compound 6 (Scheme 4.7): Following the synthetic procedure for compound **5**, the reaction of compound **3** (8.00 g, 22.1 mmol), compound **5** (17.5 g, 46.6 mmol), and potassium carbonate (12.2 g, 88.4 mmol) produced a crude product, which was purified by recrystallization from ethyl acetate to yield compound **6** as a beige crystalline solid (9.4 g, 58%).

^{1}H NMR (400 MHz, $CDCl_3$): δ 7.30 (s, 1H), 5.06 (br s, 1H), 4.13 (t, 2H, *J* = 4.55 Hz), 3.87 (t, 2H, *J* = 4.80 Hz), 3.69 (t, 2H, *J* = 5.05 (Hz), 3.40-3.39 (m, 2H), 1.48 (s, 9H)

Compound 7 (Scheme 4.7): Compound **7** was synthesized according to the literature[14]. More precisely, in an RBF, compound **6** (4.52 g, 6.14 mmol) was dissolved in DCM (100 mL). Trifluoroacetic acid (TFA) (3.50 g, 30.7 mmol) was added to the RBF and stirred at r.t. overnight. The reaction mixture was concentrated *in vacuo* and dissolved in ethyl

acetate. Triethylamine was added to make the pH 7 and resulted in precipitation. The precipitate was collected through vacuum filtration and dried over a high vacuum to yield compound **7** as a beige crystalline solid (2.90 g, 90%). ^{1}H NMR (400 MHz, DMSO-d_6): δ 7.87 (s, 2H), 7.38 (s, 1H), 4.13 (t, 2H, *J* = 4.55 Hz), 3.80 (t, 2H, *J* = 4.80 Hz), 3.72 (t, 2H, *J* = 5.05 (Hz), 3.10 (m, 2H).

4.7. References

1. Moon, J.H., Mendez, E., Kim, Y., and Kaur, A. (2011). Conjugated Polymer Nanoparticles for Small Interfering RNA Delivery. Chem Commun (Camb), 47 (29):8370-2. Epub 2011/06/23. doi:10.1039/c1cc10991j. PubMed PMID: 21695337.

2. Feng, Y., Duan, X., Liu, L., and Wang, S. (201). Lipid-Modified Conjugated Polymer Nanoparticles for Cell Imaging and Transfection. J Mater Chem, 20:1312-6.

3. Chen, S.Y., and Fan, L.J. (2014). Fluorescent Color Tuning of Conjugated Polymer Materials: Mechanisms and Methods. Progress in Chemistry, 26:1801-10.

4. Howes, P., Green, M., Levitt, J., Suhling, K., and Hughes, M. (2010). Phospholipid Encapsulated Semiconducting Polymer Nanoparticles: Their Use in Cell Imaging and Protein Attachment. J Am Chem Soc, 132 (11):3989-96. Epub 2010/02/24. doi:10.1021/ja1002179. PubMed PMID: 20175539.

5. Alegre-Requena, J., and Lopez, M.E. (2014). Guanidine Motif in Biologically Active Peptides. Aust J Chem, 67:965-71.

6. Tabujew, I., Freidel, C., Krieg, B., Helm, M., Koynov, K., Mullen, K., et al. (2014). The Guanidinium Group as a Key Part of Water-Soluble Polymer Carriers for siRNA Complexation and Protection against Degradation. Macromol Rapid Commun, 35 (13):1191-7. Epub 2014/04/05. doi:10.1002/marc.201400120. PubMed PMID: 24700561.

7. McKinlay, C.J., Waymouth, R.M., and Wender, P.A. (2016). Cell-Penetrating, Guanidinium-Rich Oligophosphoesters: Effective and Versatile Molecular Transporters for Drug and Probe Delivery. J Am Chem Soc, 138 (10):3510-7. Epub 2016/02/24. doi:10.1021/jacs.5b13452. PubMed PMID: 26900771, PubMed Central PMCID: PMCPMC5351964.

8. Kuchelmeister, H.Y., and Schmuck, C. (2011). Nucleotide Recognition in Water by a Guanidinium-Based Artificial Tweezer Receptor. Chemistry, 17 (19):5311-8. Epub 2011/04/05. doi:10.1002/chem.201003393. PubMed PMID: 21462273.

9. Gabriel, G.J., Madkour, A.E., Dabkowski, J.M., Nelson, C.F., Nusslein, K., and Tew, G.N. (2008). Synthetic Mimic of Antimicrobial Peptide with Nonmembrane-Disrupting Antibacterial Properties. Biomacromolecules, 9 (11):2980-3. Epub 2008/10/15. doi:10.1021/bm800855t. PubMed PMID: 18850741, PubMed Central PMCID: PMCPMC2646885.

10. Powell, D.A., Ramsden, P.D., and Batey, R.A. (2003). Phase-Transfer-Catalyzed Alkylation of Guanidines by Alkyl Halides under Biphasic Conditions: A Convenient Protocol for the Synthesis of Highly Functionalized Guanidines. J Org Chem, 68 (6):2300-9. Epub 2003/03/15. doi:10.1021/jo0265535. PubMed PMID: 12636395.

11. Kapp, T.G., Fottner, M., Maltsev, O.V., and Kessler, H. (2016). Small Cause, Great Impact: Modification of the Guanidine Group in the RGD Motif Controls Integrin Subtype Selectivity. Angew Chem Int Ed Engl, 55 (4):1540-3. Epub 2015/12/15. doi:10.1002/anie.201508713. PubMed PMID: 26663700.

12. Miyabe, H., Yoshida, K., Reddy, V.K, and Takemoto, Y. (2009). Palladium- or Iridium-Catalyzed Allylic Substitution of Guanidines: Convenient and Direct Modification of Guanidines. J Org Chem, 74 (1):305-11. Epub 2008/12/05. doi:10.1021/jo802271d. PubMed PMID: 19053613.

13. Yellol, G.S., Chung, T.W., and Sun, C.M. (2010). Novel Cyclization of Bis-Boc-Guanidines: Expeditive traceless synthesis of 1,3,5-oxadiazinones under microwave conditions. Chem Commun (Camb). 2010,46(48):9170-2. Epub 2010/11/03. doi:10.1039/c0cc03519j. PubMed PMID: 21042632.

14. Drake, M., and Lebl, M.A. (1994). Convenient Preparation of Monosubstituted N,N′-di(Boc)-Protected Guanidines. Synthesis, 6:579-82.

15. Kohmoto, S., Mori, E., and Kishikawa, K. (2007). Room-Temperature Discotic Nematic Liquid Crystals over a Wide Temperature Range: Alkali-Metal-Ion-Induced Phase Transition from Discotic Nematic to Columnar Phases. J Am Chem Soc, 129 (44):13364-5. Epub 2007/10/18. doi:10.1021/ja073962f. PubMed PMID: 17939661.

16. Mendez, E., and Moon, J.H. (2013). Side Chain and Backbone Structure-Dependent Subcellular Localization and Toxicity of Conjugated Polymer Nanoparticles. Chem Commun (Camb), 49 (54):6048-50. Epub 2013/06/01. doi:10.1039/c3cc43015d. PubMed PMID: 23722239, PubMed Central PMCID: PMCPMC3725290.

CHAPTER V

GENERAL CONCLUSIONS

Antimicrobial polymers have been gaining in prominence because of their low tendency to cause drug-resistant pathogens. Synthetic polymers have emerged as promising antimicrobial candidates in combating resistant bacteria over the last few years. Understanding bacterial cell walls, cytoplasmic membranes, and outer membranes, we designed a smart design of monomers and polymers and a great development on synthesis of antimicrobial polymers called polyaminorea has been achieved. The majority of polyamidinourea is composed of cationic and is hydrophobic in nature, and their bactericidal properties regarding the physical membrane disruption of the bacteria cell wall was evaluated using various methods. More precisely, we presented in Chapter 2 a novel method for synthesis of polyamidinoure containing antimicrobial polymer and their biological properties. In Chapter 3, we focused on Cipro-containing homo and block copolymer synthesis using ring-opening metathesis polymerization (ROMP).

We discussed synthesis of guanidine-modified conjugated polymers (CPs) in Chapter 4, as well as the novel method to develop a series of CPs by the post-polymerization technique. We tested synthesized CPs in the development of a CP-based gene or drug delivery system.

VITA

MD SALAUDDIN AHMED

mahme010@fiu.edu

EDUCATIONAL QUALIFICATION

2012–2018 Ph.D. Candidate (expected graduation April 2018)

Florida International University, Miami, FL, USA

Dissertation Title: Synthesis of Antimicrobial Polymers to Overcome Antimicrobial Resistance

Advisor: Joong Ho Moon, Ph.D.

2012–2016 Masters in Chemistry en route Ph.D.

Florida International University, Miami, FL, USA

2010–2012 Masters in Applied Chemistry and Chemical Engineering

University of Dhaka, Dhaka, Bangladesh

2005–2010 BSc in Applied Chemistry and Chemical Engineering

University of Dhaka, Dhaka, Bangladesh

ACADEMIC WORKS AND PUBLICATIONS:

- Ahmed, Md Salauddin.; Annamalai, A.; Xuerong, Le.; Seddek, A.; Teng, P.; Tse-Dinh, YC.; Moon, J. H., Synthesis of Antimicrobial Poly(guanylurea)s. *Bio Conjugate Chem.* 2018. DOI: 10.1021/acs.bioconjchem.8b00057. Published online: Mar 12, 2018.

- Chen, F.; Manandhar, P.; Ahmed, Md Salauddin.; Chang, S.; Panday, N.; Zhang, H.; Moon, J. H., He, J. Extracellular Potential mapping of live cells interacting with positively charged conjugated polymers reveals dynamic membrane features including pores. *Nanoscience* 2018 (Manuscript is in review).

- Ahmed, Md Salauddin.; Dutta, R.; Unwalla, H. J.; Moon, J. H., Modified guanidine-containing conjugated polymer for efficient siRNA delivery to well-differentiated human primary bronchial cells. (Manuscript is *in progress,* expected submission April 2018).

- Ahmed, Md Salauddin.; Moon, J. H., Synthesis of Fluorescent Phenyleneethynylene Trimer-Containing Polymer. Poster presentation, Division of Polymeric Materials Science and Engineering, Spring 2017 Meeting, Apr 2–6, 2017, San Francisco, CA.

PATENT:

- Moon, J. H., Ahmed, Md Salauddin. Modulated Guanidine-Containing Polymers or Nanoparticles. US provisional Patent # US 62/598,578, Dec 14, 2017.

- Moon, J. H., Ahmed, Md Salauddin. Antimicrobial Poly(guanylurea)s. US provisional Patent Application# US 15/911, 299, Mar 05, 2018.